The world of the complex Ginzburg-Landau equation

Igor S. Aranson

Materials Science Division, Argonne National Laboratory, Argonne, Illinois 60439

Lorenz Kramer

Physikalisches Institut, University of Bayreuth, D-95440 Bayreuth, Germany

(Published 4 February 2002)

The cubic complex Ginzburg-Landau equation is one of the most-studied nonlinear equations in the physics community. It describes a vast variety of phenomena from nonlinear waves to second-order phase transitions, from superconductivity, superfluidity, and Bose-Einstein condensation to liquid crystals and strings in field theory. The authors give an overview of various phenomena described by the complex Ginzburg-Landau equation in one, two, and three dimensions from the point of view of condensed-matter physicists. Their aim is to study the relevant solutions in order to gain insight into nonequilibrium phenomena in spatially extended systems.

CONTENTS

I. PRELIMINARY REMARKS

A. The equation

The cubic complex Ginzburg-Landau equation (CGLE) is one of the most-studied nonlinear equations in the physics community. It describes on a qualitative, and often even on a quantitative, level a vast variety of phenomena from nonlinear waves to second-order phase transitions, from superconductivity, superfluidity, and Bose-Einstein condensation to liquid crystals and strings in field theory (Kuramoto, 1984; Cross and Hohenberg, 1993; Newell *et al.*, 1993; Bohr *et al.*, 1998; Dangelmayr and Kramer, 1998; Pismen, 1999).

Our goal is to give an overview of various phenomena described by the CGLE from the point of view of condensed-matter physicists. Our approach is to study the relevant solutions to gain insight into nonequilibrium phenomena in spatially extended systems. More elementary and detailed introductions to the concepts underlying the equation can be found in Manneville (1990), van Saarloos (1995), van Hecke *et al.* (1994), Nicolis (1995), and Walgraaf (1997).

The equation is given by

$$\partial_t A = A + (1+ib)\Delta A - (1+ic)|A|^2 A, \tag{1}$$

where A is a complex function of (scaled) time t and space $\vec{x}$ (often in reduced dimension $D=1$ or 2) and the real parameters b and c characterize linear and nonlinear dispersion. The equation arises in physics in particular as a "modulational" (or "envelope" or "amplitude") equation. It provides a reduced, universal description of weakly nonlinear spatio-temporal phenomena in extended (in $\vec{x}$) continuous media whose linear dispersion is of a very general type (see below) and that are invariant under a global change of gauge [multiplication of A by $\exp(i\Phi)$]. This symmetry typically arises when A is the (slowly varying) amplitude of a phenomenon that is periodic in at least one variable (space and/or time) as a consequence of translational invariance of the system.

The assumptions of slow variation and weak nonlinearity are valid in particular near the instability of a homogeneous (in $\vec{x}$) basic state, and Eq. (1) can be viewed as a (generalized) normal form of the resulting primary bifurcation. In analogy with phase transitions, A is often called an order parameter.

To see more clearly the analogy with the order-parameter concept, we write the equation in the unscaled form,[1] as derived, for example, from the underlying set of basic (i.e., hydrodynamic) equations for a definite physical situation,

$$\tau(\partial_{\tilde{t}}\tilde{A} - \vec{v}_g\cdot\tilde{\nabla}\tilde{A}) = \epsilon(1+ia)\tilde{A} + \xi^2(1+ib)\tilde{\Delta}\tilde{A} - g(1+ic)|\tilde{A}|^2\tilde{A}. \tag{2}$$

Equation (1) is obtained from Eq. (2) by the transformations $\tilde{A} = (\epsilon/g)^{1/2} A \exp[-i(\epsilon a/\tau)\tilde{t}]$, $\tilde{t} = (\tau/\epsilon)t$, and $\vec{\tilde{x}} - \vec{v}_g\tilde{t} = (\xi/\epsilon^{1/2})\vec{x}$. The case $\epsilon>0$ and $g>0$ was assumed. Otherwise the signs in front of the first and/or last term on the right-hand side of Eq. (1) have to be reversed. The physical quantities $\mathbf{u}(\tilde{t},\tilde{r})$ (temperature, velocities, densities, electric field, etc.) are given in the form

$$\mathbf{u} = \tilde{A}\, e^{i(\vec{q}_c\cdot\vec{x} - \omega_c t)}\mathbf{U}_l(\vec{z}) + \text{c.c.} + \text{h.o.t.} \tag{3}$$

(c.c.=complex conjugate, h.o.t.=higher-order terms). If the phenomena occur in (thin) layers, on surfaces, or in (narrow) channels, then $\mathbf{U}_l$, derived from the linear problem, describes the spatial dependence of the physical quantities in the transverse $\vec{z}$ direction(s). $\mathbf{U}_l$ is a linear eigenvector and $\omega_c, \vec{q}_c$ the corresponding eigenvalues. In the case of periodically driven systems, $\mathbf{U}_l$ would include a periodic time dependence.

In order to identify the character of the various terms in the linear part of Eq. (2), one may also consider the dispersion relation obtained from Eqs. (2) and (3) for small harmonic perturbations of the basic state $A=0$,

$$\tau\lambda = -i\tau\omega_c + i\vec{v}_g\cdot(\vec{q}-\vec{q}_c) + \epsilon(1+ia) - \xi^2(1+ib)(\vec{q}-\vec{q}_c)^2. \tag{4}$$

Here $\vec{q}$ is the wave vector in the physical system and $\lambda = \sigma - i\omega$ is the complex growth rate of the perturbation. τ is a characteristic time, ξ the coherence length, $\vec{v}_g$ a linear group velocity, and $\epsilon a/\tau$ a correction to the Hopf frequency ω_c. ϵ measures in a dimensionless scale the distance from the threshold of the instability, i.e., $\epsilon = (R-R_c)/R_c$, with R the control parameter that carries the system through the threshold at R_c. Note that there is an arbitrary overall factor in Eqs. (2) and (4) which is fixed by the ultimately arbitrary choice of the definition of ϵ. The value of the nonlinear coefficient g in Eq. (2) depends on the choice of the normalization of the linear eigenvector $\mathbf{U}_l$.

Now we can proceed to summarize the conditions for validity of the CGLE. The following four points are to some extent interrelated.

(a) Correct choice of order-parameter space, i.e., a single complex scalar: First of all, this necessitates that ω_c and/or $\vec{q}_c$ be nonzero, because otherwise one would expect a real order parameter, as in simple phase transitions. An exception is the transition to superconductivity and superfluidity, in which the order parameter is complex for quantum-mechanical reasons (see below).

[1] An exception might be a simple rescaling and rotation of the coordinate system; see below.

Moreover, if $q_c=0$, one may run into problems with conservation laws which frequently exclude a homogeneous change of the system. In this case of long-wavelength instabilities, somewhat different order-parameter equations often arise (see, for example, Nepomnyashchii, 1995a). Second, a discrete degeneracy (or near degeneracy) of neutral modes is excluded, which may arise by symmetry (see below for an example) or by accident. If the eigenvectors of the different modes were different, one would need several order parameters and a set of coupled equations. If the eigenvectors coincide (or nearly coincide), which may happen at (or near) a codimension-2 point, one can again use one equation, which would now contain higher space or time derivatives.

(b) Validity of the dispersion relation (4): Since there is no real contribution linear in $\vec{q}-\vec{q}_c$ and since ξ^2 is a positive quantity, the real growth rate σ has a minimum at $\vec{q}_c$. In more than one dimension this excludes an important class of systems, namely, isotropic ones with $q_c \neq 0$ like Rayleigh-Bénard convection in simple 2D fluid layers. There one has a continuous degeneracy of neutral linear modes. The neglect of terms of higher order in ϵ and in $\vec{q}-\vec{q}_c$ is usually justified near the bifurcation.

(c) Symmetries: translation invariance in $\vec{x}$ and t. Actually the CGLE incorporates translational invariance with respect to space and/or time on two levels. One is expressed by the global gauge invariance, which in the CGLE can be absorbed in a shift of $\vec{x}$ and/or time t. Note that this invariance excludes terms that are quadratic in A. The other is expressed by the autonomy of the CGLE (no explicit dependence on space and time). The two invariances reflect the fact that the fast and slow space and time scales are not coupled in this description. This is an approximation that cannot be overcome by going to higher order in the expansion in terms of amplitude and gradients. The coupling effects are in fact nonanalytic in ϵ (nonadiabatic effects; see, for example, Pomeau, 1984; Kramer and Zimmermann, 1985; Bensimon *et al.*, 1988).

(d) Validity of the (lowest-order) weakly nonlinear approximation: We shall deal mostly with the case of a supercritical (forward or normal) bifurcation where $g>0$; higher-order nonlinearities in Eq. (1) can then be neglected sufficiently near threshold. If the nonlinear term in Eq. (1) has the opposite sign, which corresponds to a subcritical (backward or inverse) bifurcation, higher-order nonlinear terms are usually essential. However, even in this case, there exist for sufficiently large values of $|c|$ relevant solutions that bifurcate supercritically, which will be discussed in Sec. VI.A.1.

From the linear theory we can now distinguish three classes of primary bifurcations in which Eq. (1) arises:

(i) $\omega_c=0, \vec{q}_c\neq 0$: for such *stationary periodic instabilities* λ is real, and in fact all the imaginary coefficients (including the group velocity $\vec{v}_g$) vanish. Generically, reflection symmetry is needed (see below). Equation (1) then reduces to the "real" Ginzburg-Landau equation,

$$\partial_t A = A + \Delta A - |A|^2 A, \tag{5}$$

which one might also call the "complex nonlinear diffusion equation" in analogy with the nonlinear Schrödinger equation (see below). Examples that display such an instability are Rayleigh-Bénard convection in simple and complex fluids, Taylor-Couette flow, electroconvection in liquid crystals, and many others. In more than one dimension there is the restriction mentioned under (b). Thus in isotropic 2D systems the dispersion relation is changed and the Laplacian in Eq. (5) has to be replaced by a different differential operator. The corresponding equation derived by Newell and Whitehead (1969) and by Segel (1969) was in fact the first amplitude equation that included spatial degrees of freedom. It is applicable only for situations with nearly parallel rolls, which is in isotropic systems an important restriction.

In more than one dimension, therefore, the system must be anisotropic, which is the case in particular for convective instabilities in liquid crystals (Kramer and Pesch, 1995), but also holds for Rayleigh-Bénard convection in an inclined layer (Daniels *et al.*, 2000) or in a conducting fluid in the presence of a magnetic field with an axial component (Eltayeb, 1971). The Taylor-Couette instability in the small-gap limit can also be viewed as an anisotropic quasi-2D system. In two dimensions Eq. (5) was first considered in the context of electrohydrodynamic convection in a planarly aligned nematic liquid-crystal layer (Pesch and Kramer, 1986; Bodenschatz, Zimmermam, and Kramer, 1988; Kramer and Pesch, 1995; for a review see Buka and Kramer, 1996). The Laplacian in Eq. (2) is obtained after a linear coordinate transformation.

(ii) $\omega_c\neq 0, \vec{q}_c=0$: The prime example of such *oscillatory uniform instabilities* are oscillatory chemical reactions (see, for example, de Wit, 1999). In lasers (or passive nonlinear optical systems) this type may also arise (Newell and Moloney, 1992). In hydrodynamic systems such instabilities are often suppressed by mass conservation (see, however, Börzsönyi *et al.*, 2000). Isotropy does not cause any problems here, and the Laplacian applies directly. In the presence of reflection symmetry the group velocity term in Eq. (2) is absent. The spatial patterns obtained from A directly reflect those of the physical system. The imaginary parts proportional to b and c pertain to linear and nonlinear frequency changes (renormalization) of the oscillations, respectively. In most systems the nonlinear frequency change is negative (frequency decreases with amplitude), so that $c<0$ with our choice of signs. Coefficients for the CGLE have been determined, for example, from experiments on the Belousov-Zhabotinsky reaction (Hynne *et al.*, 1993; Kramer *et al.*, 1995).

(iii) $\omega_c\neq 0, \vec{q}_c\neq 0$: This *oscillatory periodic instability* occurs in hydrodynamic and optical systems. The best-studied example is Rayleigh-Bénard convection in binary mixtures, although here the bifurcation is mostly subcritical in the accessible parameter range (Schöpf and Zimmermann, 1990; Lücke *et al.*, 1992). Also, in two dimensions the system is isotropic, so that the simple complex GLE (2) is not applicable. Other 1D examples are the oscillatory instability in Rayleigh-Bénard con-

vection in low-Prandtl-number fluids, which in two dimensions occurs as a secondary instability of stationary rolls. In a 1D geometry with just one longitudinal roll it can be treated as a primary bifurcation (Janiaud *et al.*, 1992). Other examples include the wall instability in rotating Rayleigh-Bénard convection (Tu and Cross, 1992; van Hecke and van Saarloos, 1997; Yuanming and Ecke, 1999) and hydrothermal waves, where the coefficients of the CGLE were determined from experiment (Burguette *et al.*, 1999). In two dimensions the prime example is the electrohydrodynamic instability in nematic liquid crystals in thin and clean cells (otherwise one has the more common stationary rolls; Treiber and Kramer, 1998). Actually in such an anisotropic 2D system one is led to a generalization of Eq. (1) in which the term $ib\Delta A$ is replaced by a more general bilinear form $i(b_1\partial_x^2+b_2\partial_y^2)$; see Sec. VI.D.

Most of the oscillatory periodic systems just mentioned have reflection symmetry, and one then has to allow for the possibility of counterpropagating waves, which makes a description in terms of two coupled CGLE's necessary (see Cross and Hohenberg, 1993). The degeneracy between left- and right-traveling waves can be lifted by breaking the reflection symmetry by applying additional fields or an additional flow. In this situation one roll system is favored over the other and, if the effect is strong enough, a single CGLE can be used. By breaking reflection symmetry in stationary periodic instabilities [case (i)], one causes the rolls generically to start to travel, and one indeed, arrives at an oscillatory periodic instability [case (iii)]. This has been studied experimentally by applying a through flow in thermal convection (Pocheau and Croquette, 1984) or in the Taylor-Couette system (Babcock, Ahlers, and Cannell, 1991; Tsameret and Steinberg, 1994;) or by nonsymmetric surface alignment in the electroconvection of nematics (pretilt or hybrid alignment; see, for example, Krekhov and Kramer, 1996).

Since the drift introduces a frequency, for sufficiently strongly broken reflection symmetry the distinction between cases (i) and (iii) is lost, as is obvious in open-flow systems (Leweke and Provansal, 1994, 1995; Roussopoulos and Monkewitz, 1996). Actually, with broken reflection symmetry also case (ii) transforms generically into (iii), i.e., the homogeheous Hopf bifurcation is in general preempted by a periodic one (Rovinksy and Menzinger, 1992, 1993).

The CGLE may also be viewed as a dissipative extension of the conservative nonlinear Schrödinger equation,

$$i\partial_t A=\Delta A\pm|A|^2A, \tag{6}$$

which describes weakly nonlinear wave phenomena (Newell, 1974). The prime examples are waves on deep water (Dias and Kharif, 1999) and nonlinear optics (Newell and Moloney, 1992). The conservative limit of Eq. (1) is obtained in Eq. (2) by letting $\vec{v}_g$, ϵ,ξ, $g\to 0$ with $\xi^2 b$, gc remaining nonzero, so that b, $c\to\infty$; one then rescales space and the amplitude.

B. Historical remarks

Four key concepts come together in the CGLE philosophy:

- *Weak nonlinearity*, which amounts to an expansion in terms of the order parameter $|\tilde{A}|$. This concept goes back to Landau's theory of second-order phase transitions (Landau, 1937a). Landau also employed this type of expansion in his attempt to explain the transition to turbulence (Landau, 1944). In the context of stationary, pattern-forming, hydrodynamic instabilities, the weakly nonlinear expansion leading to a solvability condition at third order was introduced by Gorkov (1957) and Malkus and Veronis (1958). In the 1957 work of Abrikosov (for a review see Abrikosov, 1988), he presents the theory of the mixed state of type-II superconductors in a magnetic field based on the Ginzburg-Landau theory of superconductivity. The mixed state is a periodic array of flux lines (or vortices) corresponding to topological defects (see below). Abrikosov introduced a weakly nonlinear expansion to describe this state, which is valid near the upper critical field.
- *Slow relaxation time dependence* was first used by Landau in the above-mentioned 1944 paper on turbulence. In the context of pattern-forming instabilities this concept goes back to Stuart (1960).
- *Slow nonrelaxation time dependence* with nonlinear frequency renormalization in the complex-amplitude formulation was introduced by Stuart in 1960 using multiscale analysis. Of course perturbation theory for periodic orbits (in particular, conservative Hamiltonian systems) is a classical subject that was treated by Bogoliubov, Krylov, and Mitropolskii in 1937 (for a review, see Bogoliubov and Mitropolskii, 1961).
- *Slow spatial dependence* was included by Landau (1937b) in the context of x-ray scattering by crystals in the neighborhood of the Curie point. However, the concept became known with the success of the (stationary) phenomenological Ginzburg-Landau theory of superconductivity (Ginzburg and Landau, 1950).

The stationary Ginzburg-Landau theory for superconductivity has a particular resemblance to the modulational theories of pattern-forming systems because the order parameter is complex, although for a very different reason. Superconductivity being a macroscopic quantum state, an order parameter is required that has the symmetries of a wave function. In spite of the different origin there are many analogies. However, in superconductors the time dependence is rendered nonvariational primarily through the coupling to the electric field due to local gauge invariance (see, for example, Abrikosov, 1988), a mechanism that has no analog in pattern-forming systems.

The time-dependent Ginzburg-Landau theory for superconductors was presented (phenomenologically) only in 1968 by Schmid (and derived from microscopic theory

shortly afterwards by Gorkov and Eliashberg, 1968), when the first modulational theory was derived in the context of Rayleigh-Bénard convection by Newell and Whitehead (1969) and Segel (1969). Equation (5) with an additional noise term has been studied intensively as a model of phase transitions in equilibrium systems; see, for example, Hohenberg and Halperin (1977).

The full CGLE was introduced phenomenologically by Newell and Whitehead (1971). It was derived by Stewartson and Stuart (1971) and DiPrima, Eckhaus, and Segel (1971) in the context of the destabilization of plane shear flow, where its applicability is limited by the fact that a strongly subcritical bifurcation is involved. In the context of chemical systems the CGLE was introduced by Kuramoto and Tsuzuki (1976).

There is an extensive mathematical literature on the CGLE, which we shall only touch upon; see, for example, Doering *et al.* (1987, 1988); van Harten (1991); Schneider (1994); Doelman (1995); Mielke and Schneider (1996); Levermore and Stark (1997); Melbourne (1998); Mielke (1998).

C. Simple model–vast variety of effects

Clearly the CGLE (1) may be viewed as a very general normal-form type of equation for a large class of bifurcations and nonlinear wave phenomena in spatially extended systems, so a detailed investigation of its properties is well justified. The equation interpolates between the two opposing limits of the conservative nonlinear Schrödinger equation and the purely relaxative GLE. The world of the CGLE lies between these limits where new phenomena and scenarios arise, such as sink and source solutions (spirals in two dimensions and filaments in three dimensions), various core and wave instabilities, nonlinear convective versus absolute instability, interaction screening and competition between sources, various types of spatio-temporal chaos, and glassy states.

II. GENERAL CONSIDERATIONS

In this section we shall study general properties of Eq. (1) that are relevant in all dimensions.

A. Variational case

For the case of $b=c$ it is useful to transform into a rotating frame $A\to A\exp(ibt)$. Then Eq. (1) changes to

$$\partial_t A=(1+ib)(A+\Delta A-|A|^2A). \tag{7}$$

Equation (7) can be obtained by variation of the functional

$$\mathcal{V}=\int U d^Dr, \quad U=-|A|^2+\frac{1}{2}|A|^4+|\nabla A|^2, \tag{8}$$

leading to $\partial_t A=-(1+ib)\,\delta\mathcal{V}/\delta A^*$ and

$$\partial_t\mathcal{V}=-\frac{2}{1+b^2}\int|\partial_t A|^2d^Dr. \tag{9}$$

One sees that for all noninfinite b the value of $\mathcal{V}$ decreases, so the functional (8) plays the role of a global Lyapunov functional or generalized free energy ($\mathcal{V}$ is bounded from below). The system then relaxes towards local minima of the functional. In particular, the stationary solutions $A(\vec{r})$ of the GLE ($b=0$) correspond in the more general case to Ae^{-ibt} with corresponding stability properties.

In the limit $b\to\infty$ of the nonlinear Schrödinger approximation, the functional becomes a Hamiltonian, which is conserved. More generally, the nonlinear Schrödinger equation is obtained from the CGLE by taking the limit $b,c\to\infty$ without further restrictions. After rescaling one obtains Eq. (6). One sees that the equation comes in two variants, the focusing (+ sign) and defocusing (− sign) cases (the notation comes from nonlinear optics). In one dimension it is completely integrable (Zakharov and Shabat, 1971). In the focusing case it has a two-parameter family of "bright" solitons (irrespective of space translations and gauge transformation). In $D>1$, solutions typically exhibit finite-time singularities (collapse; Zakharov, 1984; for a recent review see Robinson, 1997). In the defocusing case one has in one dimension a three-parameter family of "dark solitons" that connect asymptotically to plane waves and vortices in two and three dimensions. We shall not discuss the equation here since there is a vast literature on it (see, for example, the Proceedings of the Conference on the Nonlinear Schrödinger Equation, 1994). It is useful to treat the CGLE in the limit of large b and c from the point of view of a perturbed nonlinear Schrödinger equation.

B. The amplitude-phase representation

It is often useful to represent the complex function A by its real amplitude and phase in the form $A=R\exp(i\theta)$. Then Eq. (1) becomes

$$\begin{aligned}\partial_t R&=[\Delta-(\nabla\theta)^2]R-b(2\nabla\theta\cdot\nabla R+R\Delta\theta)\\&\quad+(1-R^2)R,\\ R\partial_t\theta&=b[\Delta-(\nabla\theta)^2]R+2\nabla\theta\cdot\nabla R+R\Delta\theta-cR^3.\end{aligned} \tag{10}$$

For $b=0$ this corresponds to a class of reaction-diffusion equations called $\lambda-\omega$ systems, which are generally of the form

$$\begin{aligned}\partial_t R&=[\Delta-(\nabla\theta)^2]R+R\lambda(R),\\ R\partial_t\theta&=2\nabla\theta\cdot\nabla R+R\Delta\theta+R\omega(R).\end{aligned} \tag{11}$$

Such equations have been extensively studied in the past by applied mathematicians (see Hagan, 1982 and references therein). Clearly one can combine Eqs. (10) in such a way that the right-hand sides are those of a $\lambda-\omega$ system.

C. Transformations, coherent structures, similarity

The obvious symmetries of the CGLE are time and space translations, spatial reflections and rotation, and

global gauge (or phase) symmetry $A \to A e^{i\phi}$. The transformation $A, b, c \to A^*, -b, -c$ leaves the equation invariant so that only a half plane within the b,c parameter space has to be considered.

Other transformations hold only for particular classes of solutions. To see this it is useful to consider the following transformation:

$$A(\vec{x},t) = e^{i(\vec{Q}\cdot\vec{x}-\omega t)} B(\vec{x}-\vec{v}t,t), \tag{12}$$

leading to

$$\partial_t B = [\sigma + \vec{w}\cdot\nabla + (1+ib)\Delta - (1+ic)|B|^2]B, \tag{13}$$

with $\sigma = 1 + i\omega - (1+ib)Q^2$, $\vec{w} = \vec{v} - i(1+ib)\vec{Q}$. Most known solutions are either of the coherent-structure type, where B depends only on its first argument (i.e., with properly chosen ω it is time independent in a moving frame), or are disordered in the sense of spatio-temporal chaos. Coherent structures can be localized or extended. The outer wave vector $\vec{Q}$ could be absorbed in B (in which case ω would be replaced by $\omega - Qv$). It may be useful to introduce $\vec{Q}$ when the gradient of the phase of B, integrated over the system, is zero (or at least small).

With a little bit of algebra one can now derive a useful similarity transformation that connects coherent structures along the lines $(b-c)/(1+bc) = \text{const}$ in parameter space. Defining

$$\vec{r} = \beta\vec{r}', \quad |B| = \gamma|B'|, \tag{14}$$

we can write the transformation relations between unprimed and primed quantities as

$$\beta^{-2} = \frac{1}{1+b^2}\left(1 + bb' + (b-b')(\omega - Qv) + \frac{1}{4}(b-b')^2 v^2\right),$$

$$\omega' = b' + \beta^2 \frac{1+b'^2}{1+b^2}(\omega - b), \quad v' = \beta\frac{1+b'^2}{1+b^2}v,$$

$$Q' = \beta\left(Q - \frac{1}{2}\frac{b-b'}{1+b^2}v\right), \tag{15}$$

$$\frac{b-c}{1+bc} = \frac{b'-c'}{1+b'c'}, \quad \gamma\beta = \left[\frac{1+bc}{1+b'c'}\frac{1+c'^2}{1+c^2}\right]^{1/2}. \tag{16}$$

The relations (15) are independent of the nonlinear part of Eq. (1) and therefore survive generalizations. Solutions with $\vec{v}=0$ remain stationary (for $b<\infty$), and that transformation was given by Hagan (1982). Clearly one can very generally transform to $b=0$, where the CGLE represents a $\lambda-\omega$ system. Note that for $v\neq 0$ one cannot have $Q=0$ and $Q'=0$. The similarity line $b=c$ (vanishing group velocity; see below) includes the real case.

Note that the stability limits of coherent states are in general not expected to conform with the similarity transform. By taking the limit $b\to\infty$ in Eqs. (16), one finds $c'=c$. Then the 1 in the factor $1+ib$ can be dropped and changes in b can be absorbed in a rescaling of length. The similarity transformation then connects solutions with arbitrary velocity, which is a manifestation of a type of Galilean invariance (van Saarloos and Hohenberg, 1992). Thus in this limit solutions appear as continuous families moving at arbitrary velocity.

Similarly, when $c\to\infty$, b tends to a constant. Then, in addition to the 1 in the factor $1+ic$, the linear growth term can be dropped, and changes in c can be absorbed in a rescaling of B as well as length and time. The similarity transformation then turns into a scaling transformation. Thus in this limit solutions appear as continuous families of rescaled functions.

For b and $c\to\infty$ one has both transformations together, so solutions appear generically as two-parameter families. Indeed, one is then left with the nonlinear Schrödinger equation.

D. Plane-wave solutions and their stability

The simplest coherent structures are the plane-wave solutions

$$A = \sqrt{1-Q^2}\exp\{i[\mathbf{Q}\cdot\mathbf{r} - \omega_p(Q)t + \phi]\},$$
$$F^2 = 1-Q^2, \quad \omega_p(Q) = c(1-Q^2) + bQ^2, \tag{17}$$

where ϕ is an arbitrary constant phase. These structures exist for $Q^2<1$. To test their stability one considers the complex growth rate λ of the modulational modes. One seeks the perturbed solution in the form

$$A = [F + \delta a_+ \exp(\lambda t + i\mathbf{k}\cdot\mathbf{r}) + \delta a_- \exp(\lambda^* t - i\mathbf{k}\cdot\mathbf{r})] \times \exp[i(\mathbf{Q}\cdot\mathbf{r} - \omega t)], \tag{18}$$

where $\mathbf{k}$ is a modulation wave vector and $\delta a_\pm$ are the amplitudes of the small perturbations. One easily finds the expression for the growth rate λ (Stuart and DiPrima, 1980):

$$\lambda^2 + 2(F^2 + 2ib\mathbf{Q}\cdot\mathbf{k} + k^2)\lambda + (1+b^2)[k^4 - 4(\mathbf{Q}\cdot\mathbf{k})^4] + 2F^2[(1+bc)k^2 + 2i(b-c)\mathbf{Q}\cdot\mathbf{k}] = 0. \tag{19}$$

By expanding this equation for small k one finds

$$\lambda = -iV_g k - D_2 k^2 + i\Omega_g k^3 - D_4 k^4 + O(k^5), \tag{20}$$

with

$$V_g = 2(b-c)Q_k,$$
$$D_2 = 1 + bc - \frac{2(1+c^2)Q_k^2}{1-Q^2},$$
$$\Omega_g = \frac{2[b(1-Q^2) - 2cQ_k^2](1+c^2)Q_k}{(1-Q^2)^2},$$
$$D_4 = \frac{1+c^2}{2(1-Q^2)^3}[b^2(1-Q^2)^2 - 12bc(1-Q^2)Q_k^2 + 4(1+5c^2)Q_k^4], \tag{21}$$

where $Q_k = \mathbf{Q}\cdot\hat{\mathbf{k}}$ is the component of $\mathbf{Q}$ parallel to $\mathbf{k}$. The quantities V_g, D_2, Ω_g, and D_4 for $\mathbf{k}\|\mathbf{Q}$ will be denoted by $V_{g\|}$, $D_{2\|}$, $\Omega_{g\|}$, and $D_{4\|}$. Similarly, for $\mathbf{k}\perp\mathbf{Q}$

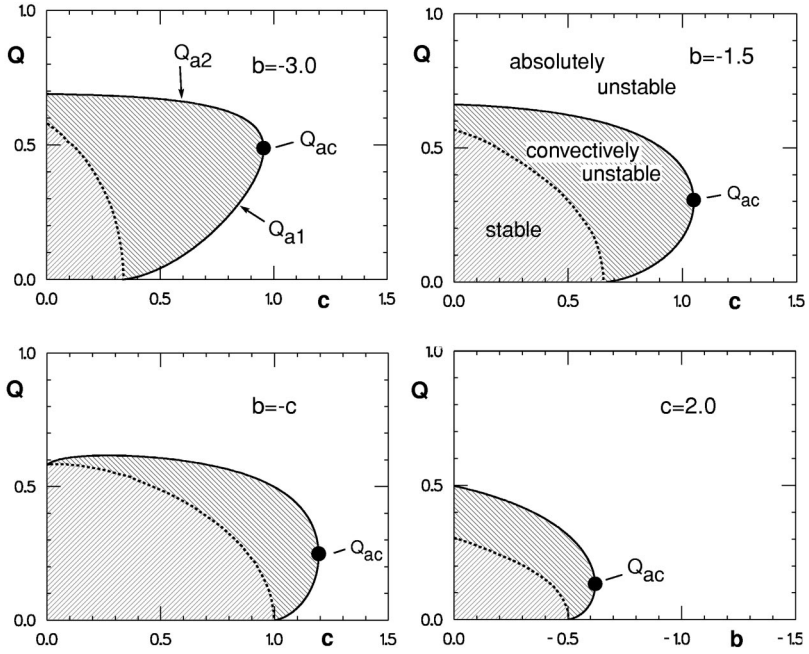

FIG. 1. Absolute stability limits $Q_{a1,2}$ for four cuts in the b,c plane. Also included are the convective (=Eckhaus) stability limits that separate the stable (light-shaded) from the convectively unstable (dark-shaded) regions.

one may use the notation $V_{g\perp}$, $D_{2\perp}$, $\Omega_{g\perp}$, and $D_{4\perp}$. Clearly the longitudinal perturbations with $\mathbf{k}\|\mathbf{Q}$ are the most dangerous ones. The solutions (17) are long-wave stable as long as the phase diffusion constant $D_{2\|}$ is positive. Thus one has a stable range of wave vectors with $Q^2<Q_E^2=(1+bc)/(3+2c^2+bc)$ enclosing the homogeneous ($Q=0$) state as long as the Benjamin-Feir-Newell criterion, $1+bc>0$, holds. This criterion conforms with the similarity transform (16). The condition $D_{2\|}>0$ is the (generalized) Eckhaus criterion. For $b=c$ it reduces to the classical Eckhaus criterion, $Q^2<Q_E^2=1/3$ for stationary bifurcations. We shall call the quadrants in the b,c plane with $bc>0$ the "defocusing quadrants." Otherwise we shall speak of the "focusing quadrants."

From Eqs. (19) and (20) one sees that for $b-c\neq 0$ and $Q\neq 0$ the destabilizing modes have a group velocity $V_g=\nabla_Q\Omega=2(b-c)\mathbf{Q}$, so the Eckhaus instability is then of a convective nature and does not necessarily lead to destabilization of the pattern (see the next subsection).

The Eckhaus instability signals bifurcations to quasiperiodic solutions (including the solitary limit), which are of the form of Eq. (13) with periodic function $B(\vec{x}-\vec{V}t)$. This instability becomes supercritical before the Benjamin-Feir-Newell criterion is reached (Janiaud *et al.*, 1992) and remains so in the unstable range. The bifurcation is captured most easily in the long-wave limit by phase equations (see below). A general analysis of the bifurcating solutions has recently been made (Brusch *et al.*, 2000); see Sec. III.C.

It is well known that the Eckhaus instability in the CGLE is not of the long-wave type in all cases. Clearly, a necessary condition for this to be the case is that $D_{4\|}$ be positive where $D_{2\|}$ changes sign.

From the above expressions one deduces that this condition is not met for $|b|>b_4(c)$, where

$$b_4=[2|c|(1-c^2)-\sqrt{4c^2(1-c^2)^2-(1-3c^2)(1+5c^2)}]/(1-3c^2),\quad bc>0. \tag{22}$$

Thus the range is in the defocusing quadrant, far away from the Benjamin-Feir-Newell stability limit. We are at present not aware of effects in which this phenomenon is of relevance.

E. Absolute versus convective instability of plane waves

For a nonzero group velocity $V_g=\nabla_Q\Omega=2(b-c)\mathbf{Q}$ the Eckhaus criterion can be taken only as a test for convective instability. In this case a localized 1D initial perturbation $S_0(x)$ of the asymptotic plane wave, although amplified in time, drifts away and does not necessarily amplify at a fixed position (Landau and Lifshitz, 1959). For absolute instability localized perturbations have to amplify at fixed position. The time evolution of a localized perturbation is in the linear range given by

$$S(x,t)=\int_{-\infty}^{\infty} dk/(2\pi)\hat{S}_0(k)\exp[ikx+\lambda(k)t], \tag{23}$$

where $\hat{S}_0(k)$ is the Fourier transform of $S_0(x)$.[2] The integral can be deformed into the complex k plane. In the limit $t\to\infty$ the integral is dominated by the largest saddle point k_0 of $\lambda(k)$ (the steepest-descent method; see, for example, Morse and Feshbach, 1953), and the test for absolute instability is

$$\mathrm{Re}[\lambda(k_0)]>0 \quad \text{with} \quad \partial_k\lambda(k_0)=0. \tag{24}$$

[2]It can be strictly shown that the destabilization occurs at first for purely longitudinal perturbations $\mathbf{Q}\|\mathbf{k}$.

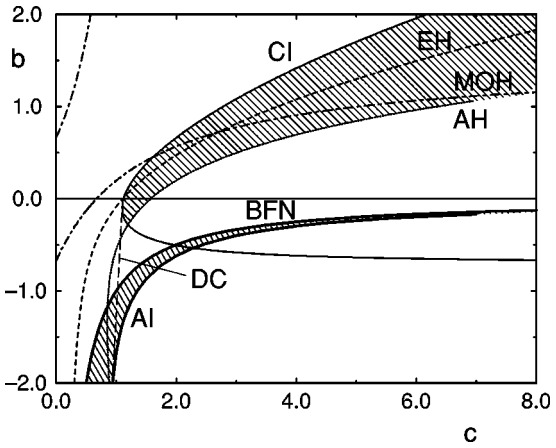

FIG. 2. Phase diagram of the 1D CGLE: BFN, Benjamin-Feir-Newell instability line up to which one has convectively stable plane-wave solutions; AI, absolute instability line up to which one has convectively unstable plane-wave solutions; DC, boundary of existence of DC towards small $|c|$. The other lines pertain to standing Nozaki-Bekki hole solutions: CI, core instability line; EH, convective (Eckhaus) instability of the emitted plane waves; AH, absolute instability of the emitted plane waves; MOH, boundary between monotonic and oscillatory interaction.

The long-wavelength expansion (20) indicates that at the Eckhaus instability, where D_2 becomes negative, the system remains stable in the above sense. When D_2 vanishes and $Q \neq 0$ the main contribution comes from the term linear in k that can then suppress instability.

In the following, results of the analysis are shown in the b-c plane (Aranson *et al.*, 1992; Weber *et al.*, 1992). In Fig. 1 the scenario is demonstrated for four cuts in the b,c,Q space. The stable region (light shading) is limited by the Eckhaus curve, which terminates at $Q=0$ on the curve. To the right of it there exists a convectively unstable wave-number band $0<Q_{a1}<|Q|<Q_{a2}$ (dark shading). Q_{a1} goes to zero on the Benjamin-Feir-Newell curve as $(1+bc)^{3/2}$, which can be seen from the long-wavelength expansion (20) with the fourth-order term included. Moving away from the Benjamin-Feir-Newell line (into the unstable regime), Q_{a1} increases and Q_{a2} decreases until they come together in a saddle-node-type process at a value Q_{ac}. Beyond Q_{ac} there are no convectively unstable plane waves. The saddle nodes Q_{ac} are shown in the b,c plane in Fig. 2 (curve AI). Thus convectively unstable waves exist up to this curve. The Benjamin-Feir-Newell criterion curve, up to which convectively unstable waves exist, is also included. The other curves include the Eckhaus instability and the absolute stability limit for waves with wave number selected by the stationary-hole solutions (see Sec. III.B).

Equation (24) by itself gives only a necessary condition for absolute stability. However, it is also sufficient, as long as one of the two roots $k_{1,2}$ of the dispersion relation, which collide at the saddle point when $\mathrm{Re}[\lambda]$ is decreased from positive values to zero (say k_1), is the root that produced the convective instability, and if k_2 does not cross the real k axis before k_1 does, when $\mathrm{Re}[\lambda]$ is increased from zero. (Note that k_1 has to cross the axis when $\mathrm{Re}[\lambda]$ is increased. Note also that, because of the symmetry $\lambda, k \rightleftharpoons \lambda^*, -k^*$ one has parallel processes with the opposite sign of $\mathrm{Im}[\lambda]$.) For a discussion of the underlying "pinching condition" see, for example, Brevdo and Bridges (1996). In the parameter range considered here the sufficient condition is fulfilled.

Clearly the absolute stability boundary can be reached only if reflection at the boundaries of the system is sufficiently weak, so in general one should expect the system to lose stability before the exact limit is reached. In many realistic situations in the CGLE the interaction of the emitted waves with the boundaries leads to sinks (shocks), analogously to the situation in which different waves collide. These shocks are strong perturbations of the plane-wave solutions but they absorb the incoming perturbations. Thus here, even for periodic boundary conditions, the absolute stability limit is relevant. Moreover, in infinite systems, states with a cellular structure made up of sources surrounded by sinks can exist in the convectively unstable regime. However, the convectively unstable states are very susceptible to noise, which is exponentially amplified in space. The amplification rate goes to zero at the convective stability limit and diverges at the absolute stability limit.

The concept of absolute stability is relevant in particular for the waves emitted by sources and possibly also for some characteristics of spatio-temporally chaotic states. When boundaries are considered one also has to allow for a linear group velocity term in the CGLE [see Eq. (2)]. Such a term does not change the convective stability threshold, but clearly the absolute stability limit is altered, and this is important particularly in the context of open-flow systems. The saddle-point condition in Eq. (24) ensures the existence of bounded solutions of the linear problem that satisfy nonperiodic boundary conditions (regardless of their precise form) at well-separated side walls (sometimes called "global modes"), because for that purpose one needs to superpose neighboring (extended) eigenmodes, which are available precisely at the saddle point. This is an alternative view of the absolute instability (Huerre and Monkowitz, 1990; Tobias and Knobloch, 1998; Tobias, Proctor, and Knobloch, 1998).

Often the condition (24) coincides with the condition that a front invades the unstable state in the upstream direction according to the linear front selection criterion (the marginal stability condition; see, for example, van Saarloos, 1988).

F. Collisions of plane waves and effect of localized disturbances

The nonlinear waves discussed above have very different properties from linear waves. In particular, when two waves collide they almost do not interpenetrate. Instead a "shock" (sink) is formed along a point (1D), line (2D), or surface (3D). When the frequency of the two waves differs, the shock moves with the average phase velocity, provided there are no phase slips in one dimension, or

its equivalent in higher dimensions (creation of vortex pairs in two dimension and inflation of vortex loops in three dimensions); for a review see Bohr *et al.* (1998). A stationary shock is formed most easily when a wave impinges on an absorbing boundary. Here we shall consider the general situation in which a plane wave is perturbed by a stationary, localized disturbance. This concept will be particularly useful in the context of the interaction of defects.

Sufficiently upstream (i.e., against the group velocity) from the disturbance the perturbation will be small and we can linearize around the plane-wave solution. In general we obtain exponential behavior with exponents $p=ik$ calculated from the dispersion relation (19) with $\lambda=0$. This gives

$$p\{(1+b^2)(4Q^2+p^2)p - 2F^2[(1+bc)p-2(b-c)Q]\}=0. \tag{25}$$

After separating out the translational mode $p=0$ we are left with a cubic polynomial. To discuss the roots p_1,p_2,p_3 choose the group velocity $V_{g\|}=2(b-c)Q\geqslant 0$ (otherwise all signs must be reversed). For $V_{g\|}=0$ we have $p_1=-p_3<0, p_2=0$ in the Eckhaus stable range. For $V_{g\|}>0$ we find that p_2 increases with increasing $|Q|$. Before $|Q|=1$ is reached p_2 and p_3 collide and become complex conjugate.

The existence of roots with a positive real part is an indication of the screening of disturbances in the upstream direction because one needs the solutions that grow exponentially to match to the disturbance. The screening length is given by $(\mathrm{Re}\, p_2)^{-1}$, the root with the smaller real part, so the screening is in general exponential. The length diverges for $V_g\to 0$ and then one has a crossover to a power law.

In the focusing quadrants the root collision always occurs before the Eckhaus instability is reached (except in the part of the defocusing quadrant away from the origin and restricted to $c^2>b^2$). We shall refer to the situation in which $p_{2,3}$ are real as the monotonic case and other situations as the oscillatory case, because this characterizes the nature of the asymptotic interaction of sources that emit waves (see Secs. III and IV). In Fig. 2 the transition from monotonic to oscillatory behavior for the waves emitted by standing hole solutions is also shown (curve MOH). A generalization to disturbances that move with velocity v is straightforward by replacing in Eq. (19) the growth rate λ by $-vp$.

G. Phase equations

The global phase invariance of the CGLE leads to the fact that, starting from a coherent state (in particular, a plane wave), one expects solutions in which the free phase ϕ becomes a slowly varying function, and one can construct appropriate equations for these solutions. (In the case of localized structures one then also has to allow for a variation of the velocity.) In the mathematical literature these phase equations are sometimes called "modulated modulation equations." There are several ways to proceed technically in their derivation, but the simplest is to first establish the linear part of the equation by a standard linear analysis and then construct nonlinearities by separate reasoning. It is helpful to include symmetry considerations to exclude terms from the beginning.

By starting from a plane-wave state (17) with wave number Q in the x direction one may perform a gradient expansion of ϕ leading in one dimension to

$$\partial_t\phi = V_{g\|}\partial_x\phi + D_{2\|}\partial_x^2\phi - \Omega_{g\|}\partial_x^3\phi - D_{4\|}\partial_x^4\phi + \text{h.o.t.} \tag{26}$$

Note the absence of a term proportional to ϕ which would violate translation invariance. The prefactors of the gradient terms have to be chosen according to Eq. (21) in order to reproduce the linear stability properties of the plane wave (with the wave number Q_k replaced by Q).

Nonlinearity can be included in Eq. (26) by substituting in the coefficients of Eq. (21) $Q\to Q+\partial_x\phi$. Expanding $V_{g\|}(Q)$ and $D_{2\|}(Q)$ one generates the leading nonlinear terms, so that Eq. (26) becomes (Janiaud *et al.*, 1992)

$$(\partial_t - V_{g\|}\partial_x)\phi = D_{2\|}\partial_x^2\phi - D_{4\|}\partial_x^4\phi - g_1(\partial_x\phi)^2 - \Omega_{g\|}\partial_x^3\phi - g_2\partial_x\phi\partial_x^2\phi + \text{h.o.t.} \tag{27}$$

with the linear parameters from Eq. (21) and

$$g_1 = -\frac{1}{2}\partial_Q V_{g\|} = (b-c),$$

$$g_2 = -\partial_Q D_{2\|} = \frac{4Q_0(1+c^2)}{1-Q_0^2}. \tag{28}$$

Because of translation invariance the lowest relevant nonlinearities are $(\partial_x\phi)^2$ and $\partial_x\phi\partial_x^2\phi$ (Kuramoto, 1984).

In the stationary case ($c=b$) one has $V_{g\|}=\Omega_{g\|}=g_1=0$. The remaining nonlinearity $\partial_x\phi\partial_x^2\phi$ does not saturate the linear instability and one recovers the results for the nonlinear Eckhaus instability (Kramer and Zimmermann, 1985). For $b\neq c$ and $Q=0$ the dominant nonlinearity is $(\partial_x\phi)^2$, which does saturate the linear instability. The resulting equation with $\Omega_{g\|}=g_2=0$,

$$\partial_t\phi - D_{2\|}\partial_x^2\phi + D_{4\|}\partial_x^4\phi + g_1(\partial_x\phi)^2 = 0, \tag{29}$$

describes the (supercritical) bifurcation at the Benjamin-Feir-Newell instability and is known as the Kuramoto-Sivashinsky equation. It has stationary periodic solutions, which are stable in a small wave-number range $0.77p_0<p<0.837p_0$, where $p_0=\sqrt{D_2/D_4}$ (Frisch *et al.*, 1986; Nepomnyashchii, 1995b). It also has spatiotemporally chaotic solutions, which are actually the relevant attractors, and it may represent the simplest partial differential equation displaying this phenomenon. Since it is a rather general equation for long-wavelength instabilities, independent of the present context of the CGLE, it has attracted much attention in recent years (see, for example, Bohr *et al.*, 1998).

In the general case $Q\neq 0$ both nonlinearities are important (as is the term proportional to Ω_g). The bifur-

cation to modulated waves, which are represented by periodic solutions of Eq. (26), can then be either forward or backward depending on the values of b,c. In fact, the Eckhaus bifurcation always becomes supercritical before the Benjamin-Feir-Newell instability is reached. Modulated solutions can be found analytically in the limit $D_{2\|}\to 0$, where Eq. (26) reduces to

$$\partial_t\phi - V_{g\|}\partial_x\phi + \partial_x^3\phi + (\partial_x\phi)^2 + O(\epsilon) = 0, \tag{30}$$

with $\epsilon = \sqrt{D_4 D_2}/|\Omega_g| \ll 1$. This limit is complementary to that leading to the Kuramoto-Sivashinsky equation and one is in fact left with a perturbed Korteweg–de Vries equation. This equation is (in one dimension) completely integrable. The perturbed case was studied by Janiaud *et al.* (1992) and by Bar and Nepomnyashchii (1995). They showed that a fairly broad band of the periodic solutions (much larger than in the Kuramoto-Sivashinsky equation) perpetuate the perturbation of the Korteweg–de Vries equation and is stable. Outside this limit, and in particular in the Kuramoto-Sivashinsky equation regime, one has in extended systems spatio-temporally chaotic solutions. It is believed that this chaotic state is a representation of the phase chaos observed in the CGLE, although this view has been challenged (see Sec. III.D). Sakaguchi (1992) introduced higher-order nonlinearities into the Kuramoto-Sivashinsky equation, which allowed him to capture the analog of the transition (or crossover) to amplitude chaos manifesting itself by finite-time singularities in $\partial_x\phi$.

Under some conditions, namely, when $D_{2\|}$ is positive and Q is small, the first nonlinearity in Eq. (27) is dominant and reduces to the Burgers equation,

$$\partial_t\phi - D_{2\|}\partial_x^2\phi + g_1(\partial_x\phi)^2 = 0, \tag{31}$$

which is completely integrable within the space of functions that do not cross zero, because it can be linearized by a Hopf-Cole transformation $\phi = (D_{2\|}/g_1)\ln W$. The equation allows one to describe analytically sink solutions, or shocks (see, for example, Kuramoto and Tsuzuki, 1976; Malomed, 1983), and is (in two dimensions) useful for the qualitative understanding of the interaction of spiral waves in the limit $b,c\to 0$ (see Biktashev, 1989; Aranson *et al.*, 1991a, 1991b).

Clearly generalization of the phase equations to higher dimensions is possible. Using the full form of Eq. (21) one can easily generalize the phase equation to two dimensions (for details see Kuramoto, 1984; Lega, 1991). The equation is most useful in the range where $D_{2\|}$ goes through zero and becomes negative. Generalizations can also be derived outside the range of applicability of the CGLE (far from threshold) and for more general nonlinear long-wavelength phenomena, where ϕ does not represent the phase of a periodic function (see, for example, Bar and Nepomnyashchii, 1995).

H. Topological defects

Zeros of the complex field A result in singularity of the phase $\theta = \arg A$. In two dimensions, point singularities correspond to quantized vortices with topological charge $n = 1/(2\pi)\oint_L \nabla\theta\,\mathbf{dl}$, where L is a contour encircling the zero of A. Although for $b\neq c$ they represent wave-emitting spirals, they are analogous to vortices in superconductors and superfluids and represent topological defects because a small variation of the field will not eliminate the phase circulation condition. Clearly, vortices with topological charge $n=\pm 1$ are topologically stable. The vortices with multiple topological charge can be split into single-charged vortices.[3] Two-dimensional point defects become line defects in three dimensions. One can then close such a line to a loop, which can shrink to zero. Some definitions of topological defects from the point of view of energy versus topology are given by Pismen (1999).

Topological arguments do not guarantee the existence of a stable, coherent solution of the field equations. In particular, the stability of the topological defect depends on the background state in which it is embedded. For example, spiral waves are stable in a certain parameter range, where they select the background state (see Sec. IV). Simultaneously charged sinks coexist with spirals and play a passive role. Defects can also become unstable against the spontaneous acceleration of their cores.

I. Effects of boundaries

Boundaries may play an important role in nonequilibrium systems. Even in large systems the boundary may provide restriction or even selection of the wave number. We shall not discuss this topic (see, Cross and Hohenberg, 1993) and shall consider situations in which such effects are not important.

III. DYNAMICS IN ONE DIMENSION

In this section we shall consider the properties of various 1D solutions of the CGLE. We shall discuss the stability and interaction of coherent structures and the transition to and characterization of spatio-temporal chaos.

A. Classification of coherent structures, counting arguments

The coherent structures introduced in the previous section can be characterized using simple counting arguments put forward by van Saarloos and Hohenberg (1992). It should be mentioned, however, that the counting arguments cannot account for all circumstances (for example, hidden symmetries) and may fail for certain class of solutions (see below). One-dimensional coherent structures can be written in the form

$$A(x,t) = e^{-i\omega_k t + i\phi(x-vt)}a(x-vt), \tag{32}$$

[3] In small samples vortices with multiple charge can be dynamically stable; for details see Geim *et al.* (1998) and Deo *et al.* (1997).

with the real functions ϕ,a satisfying a set of three ordinary differential equations:

$$\begin{aligned} a_x &= s; \\ s_x &= \psi^2 a - \gamma^{-1}[(1+b\omega_k)a + v(s+b\psi a) \\ &\quad -(1+bc)a^3]; \\ \psi_x &= -2s\psi/a + \gamma^{-1}[b-\omega_k + v(sb/a-\psi) \\ &\quad -(b-c)a^2]. \end{aligned} \tag{33}$$

Here $\gamma=1+b^2$, $a_x=da/dxf$, $s_x=ds/dx$, and $\psi=d\phi/dx$. These ordinary differential equations constitute a dynamical system with three degrees of freedom.

The similarity transform of Sec. II.C can be adapted to these equations by absorbing the external wave number in the phase ϕ, which leads to $\omega_k=\omega-Qv$, $\omega_k'=\omega'-Q'v'$, and

$$\begin{aligned} \omega_k' &= b' + \beta^2 \frac{\gamma'}{\gamma}\left[\omega_k - b + \frac{1}{2}\frac{b-b'}{\gamma}v\right], \\ \psi' &= \beta\left(\psi - \frac{1}{2}\frac{b-b'}{\gamma}v\right). \end{aligned} \tag{34}$$

The other relations (14)–(16) remain.

The counting arguments allow one to establish necessary conditions for the existence of localized coherent structures, which correspond to homoclinic or heteroclinic orbits of Eqs. (33). Consider, for example, the trajectory of Eqs. (33) flowing from fixed point N to fixed point L. If N has n_N unstable directions, there are n_N-1 free parameters characterizing the flow on the n_N-dimensional subspace spanned by the unstable eigenvectors. Together with the parameters ω_k and v this will yield n_N+1 free parameters. If L has n_L unstable directions, the requirement that the trajectory come in orthogonal to these yields n_L conditions. The multiplicity of this type of trajectory will therefore be $n=n_N-n_L+1$ and, depending on n, it will give either an n-parameter family ($n\geqslant 1$), a discrete set of structures ($n=0$), or no structure ($n<0$). In addition, one may have symmetry arguments that reduce the number of conditions.

The asymptotic states can correspond either to nonzero steady states (plane waves) or to the trivial state $a=0$. Accordingly, the localized coherent structures can be classified as *pulses, fronts*, *domain boundaries*, and *homoclons*. A pulse corresponds to the homoclinic orbit connecting to the trivial state $a=0$. Pulses come in discrete sets (van Saarloos and Hohenberg, 1992). For a full description of pulses see Akhmediev *et al.* (1995, 1996, 2001) and Afanasjev *et al.* (1996). Fronts are heteroclinic orbits connecting on one side to a plane-wave state and on the other side to the unstable trivial state. They come in a continuous family, but sufficiently rapidly decaying initial conditions evolve into a "selected" front that moves at velocity $v^*=2\sqrt{1+b^2}$ and generates a plane wave with wave number $Q^*=b/\sqrt{1+b^2}$ ("linear selection"). For a discussion, see van Saarloos and Hohenberg (1992) and Cross and Hohenberg (1993).

Domain boundaries are heteroclinic orbits connecting two different plane-wave states. The domain boundaries can be active (sources, often called holes) or passive (sinks or shocks), depending on whether in the comoving frame the group velocity is directed outward or inward, respectively. They will be discussed in the next subsection. Homoclons (or homoclinic holes, phasons) connect to the same plane-wave state on both sides. They are embedded in solutions representing periodic arrangements of homoclons, which represent quasiperiodic solutions satisfying ansatz (32) and correspond to the closed orbits of Eqs. (33). They will be discussed in Sec. III.C.2. There are also chaotic solutions of Eqs. (33), which correspond to nonperiodic arrangement of holes and shocks, or homoclons (see Secs. III.B.2 and III.C.2).

B. Sinks and sources, Nozaki-Bekki hole solutions

Sinks (shocks) conform with the counting arguments of van Saarloos and Hohenberg (1992): there is a two-parameter family of sinks. However, there are no exact analytic expressions for the sink solution connecting two traveling waves with arbitrary wave numbers. The exact sink solution found by Nozaki and Bekki (1984) corresponds to a special choice of wave numbers and is therefore not typical. For slightly different wave numbers a phase description of sinks is possible (Kuramoto, 1984).

However, the counting arguments (which are, strictly speaking, neither necessary nor sufficient and cannot account for specific circumstances, such as a hidden symmetry) fail for the source solution. According to the counting arguments there should be only a discrete number, including in particular the symmetric standing-hole solution that has a zero at the center and emits plane waves of a definite wave number (for given b,c). However, the standing hole is embedded in a continuous family of analytic moving sources, the Nozaki-Bekki hole solutions. They are characterized by a localized dip in $|A|$ that moves with constant speed v and emits plane waves with wave numbers $q_1\neq q_2$.

This is a special feature of the cubic CGLE, as demonstrated by the discovery that the moving holes do not survive a generic perturbation of the CGLE, e.g., a small quintic term (see below). Thus they are not structurally stable (Popp *et al.*, 1993, 1995; Stiller *et al.*, 1995a, 1995b). With a perturbation the holes either accelerate or decelerate depending on the sign of the perturbation, and other solutions appear (see also Doelman, 1995). Clearly, the 1D CGLE possesses a "hidden symmetry" and has retained some remnant of integrability from the nonlinear Schrödinger equation. Apparently this nongenericity has no consequences for other coherent structures.

The Nozaki-Bekki hole solutions are of the form (Nozaki and Bekki, 1984)

$$A_v^{NB} = [\hat{B}\,\partial_\zeta \varphi_v(\kappa\zeta) + \hat{A}\,v]\exp[i\varphi_v(\kappa\zeta) + i\hat{\alpha}v - i\Omega t], \tag{35}$$

where

$$\varphi_v(\kappa\zeta)=\hat{\kappa}^{-1}\ln\cosh(\kappa\zeta)$$

and $\zeta=x-vt$, v is the velocity of the hole, and $q_{1/2}$ are the asymptotic wave numbers. Symbols with a "hat" denote real constants depending only on b and c, for example, $\hat{\alpha}=1/2(b-c)$. The frequency Ω and κ^2 are linear functions of v^2. The emitted plane waves have wave numbers

$$q_{1/2}=\pm\beta+\alpha, \tag{36}$$

where $\beta=\kappa/\hat{\kappa}$ and $\alpha=v\hat{\alpha}$. One easily derives the relation

$$v=[\omega(q_2)-\omega(q_1)]/(q_2-q_1), \tag{37}$$

where $\omega(q)$ is the dispersion relation for the plane waves. This relation can be interpreted as phase conservation and is also valid for more general equations possessing phase invariance. For the cubic CGLE it reduces to $v=(b-c)(q_1+q_2)$, i.e., the hole moves simply with the mean of the group velocities of the asymptotic plane waves. The exact relations between the parameters can be derived by inserting ansatz (35) into the CGLE. The resulting algebraic equations (eight equations for eight parameters) turn out not to be independent, yielding a one-parameter family. κ^2 becomes zero at a maximal velocity $\pm v_{max}$, and here the hole solution merges with a plane wave with wave number $q_1=q_2=v_{\max}/2(b-c)$. In a large part of the b,c plane these bifurcations occur in the range of stable plane waves. This is the case outside a strip around the line $b=c$ given by $|b-c|>\delta$ with δ varying from 1/2 for large values of $|b|,|c|$ to 0.55 for small values. The region extends almost to the Benjamin-Feir-Newell curves. The bifurcation cannot be captured by linear perturbation around a plane wave, since the asymptotic wave numbers of holes differ. Presumably the bifurcation can be captured by the phase equation (27). For $b\to c$ only the standing hole survives (the velocities of the moving holes diverge in this limit).

The interest in the hole solutions comes particularly from the fact that they are dynamically stable in some range. The stability was first investigated by Sakaguchi (1991a) in direct simulations of the CGLE. The stability problem was then studied by Chaté and Manneville (1992) numerically for $v=0,v=0.2$, by Sasa and Iwamoto (1992) semianalytically for $v=0$, and by Popp *et al.* (1995), essentially analytically. As a result, hole solutions were found to be stable in a narrow region of the b-c plane, which is shown in Fig. 2 for the standing hole ($v=0$) (upper shaded region). From below, the region is bounded by the border of (absolute) stability of the emitted plane waves with wave number $q(b,c)$ [see Eq. (35)] corresponding to the continuous spectrum of the linearized problem (see curve AH in Fig. 2.) From the other side, the stable range is bounded by the instability of the core with respect to localized eigenmodes corresponding to a discrete spectrum of $\mathcal{L}_v$ (see curve CI in Fig. 2). For $c\to\infty$, one has

$$b_{CI}^2\to\frac{3}{4}c+O(\sqrt{c}) \quad \text{for } b>0, \tag{38}$$

$$b_{CI}\to-\frac{1}{\sqrt{2}}+O(1/c) \quad \text{for } b<0.$$

The result could be reproduced fully analytically by perturbing around the nonlinear Schrödinger equation limit, where the Nozaki-Bekki holes emerge as a subclass of the three-parameter family of dark solitons; it is supported by detailed numerical simulations and shows excellent agreement (Stiller, Popp, and Kramer, 1995). It differs from that obtained by Lega and Fauve (1997) and by Kapitula and Rubin (2000), Lega and Fauve (1997), and Lega (2001) who claim a larger stability domain in disagreement with simulations (Stiller, Popp, and Kramer, 1995).

The core instability turns out to be connected with a stationary bifurcation where the destabilizing mode passes through the neutral mode related to translations of the hole. This degeneracy is specific to the cubic CGLE and is thus structurally unstable (see below). When going through the stability limit, the standing hole transforms into a moving one. Indeed, the cores of moving holes were found to be more stable than those of standing ones (Chaté and Manneville, 1992).

1. Destruction of Nozaki-Bekki holes by small perturbations

Consider the following perturbed cubic CGLE:

$$\partial_t A=[1+(1+ib)\partial_x^2-(1+ic)|A|^2+d|A|^4]A, \tag{39}$$

where a quintic term with a small complex prefactor $d=d'+id''$ ($|d|\ll 1$) is included, which will be treated as a perturbation. There are, of course, other corrections to the cubic CGLE, but their perturbative effect is expected to be similar.

Simulations with small but finite d show that stable, moving holes are in general either accelerated and eventually destroyed or slowed down and stopped to the standing-hole solution, depending on the phase of d (Popp *et al.*, 1993, 1995; Stiller, Popp, Aranson, and Kramer, 1995; Stiller, Popp, and Kramer, 1995). In particular, for real $d=d'$ one has

$$\left[\frac{\partial_t v}{v}\right]_{<}^{>}0\Leftrightarrow d'\lessgtr 0. \tag{40}$$

One finds that the relations (37) connecting the core velocity and the emitted wave numbers are (almost) satisfied at each instant during the acceleration process. The acceleration thus occurs approximately along the Nozaki-Bekki hole family, and it can be described by taking $v=v(t)$ as a slowly varying variable while other degrees of freedom follow adiabatically. The semianalytic matching-perturbation approach gives the reduced acceleration, which agrees with the simulations (see Fig. 3).

Of special interest is the case in which the core-stability line is crossed while $d\neq 0$ (which corresponds to the typical situation with higher-order corrections to the

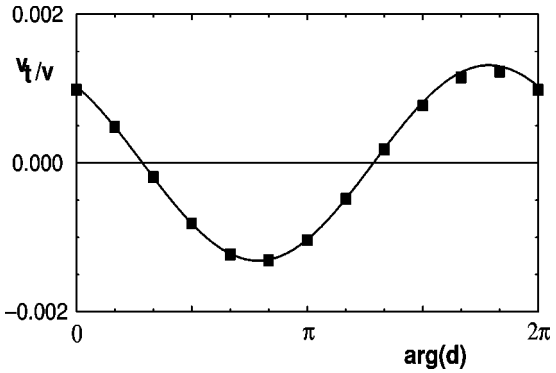

FIG. 3. Acceleration instability in the perturbed (cubic) CGLE: Solid line, the reduced acceleration $\partial_t v/v$ from theory [Eq. (43)]; ■, simulations for $b=0.5$, $c=2.0$, $|d|=0.002$, and varying phase $arg(d)$. From Stiller, Popp, and Kramer (1995) and Stiller, Popp, *et al.* (1995).

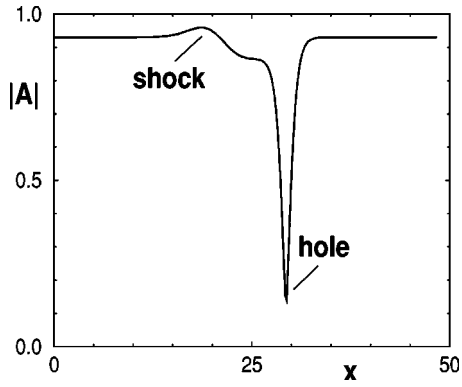

FIG. 5. Snapshot of the modulus $|A|=|A(x)|$ of a stable uniformly moving hole-shock pair in a simulation for $b=0.5$,$c=2.3$,$d'=+0.0025$. The solution is space periodic with period $P=48.4$.

CGLE). Then the two modes that cause the acceleration instability and the core instability (which is stationary for $d=0$) are coupled, which in the decelerating case leads to a Hopf bifurcation. As a result, slightly above the (supercritical) bifurcation, one has solutions with oscillating hole cores (Popp *et al.* 1993); see Fig. 4(d). The normal form for this bifurcation—valid for small $|d|,v,u$—is

$$\dot{u}=(\lambda-sv^2)u+d_1v, \tag{41}$$

$$\dot{v}=\mu u+d_2v, \tag{42}$$

which is easy to analyze. Here u and v are the amplitudes of the core-instability and acceleration-instability modes, respectively. s and μ are of order d^0 while $d_{1,2}$ must be of order d^1, since in the absence of a perturbation holes with nonzero velocity exist. λ can be identified with the growth rate of the core-instability mode at $d=0$. The nonlinear term in Eq. (41) takes care of the fact that moving holes are more stable than standing ones and at the same time saturates the instability ($s>0$).

Far away from the core-instability threshold where λ is strongly negative, u can be eliminated adiabatically from Eqs. (41), which for $v\to 0$ yield

$$\dot{v}=\left(d_2-d_1\frac{\mu}{\lambda}\right)v. \tag{43}$$

The term in parentheses can be identified with the growth rate of the acceleration instability. The parameters of Eq. (43) were calculated fully analytically by Stiller, Popp, and Kramer (1995) for $b,c\to\infty$, $bc>0$.

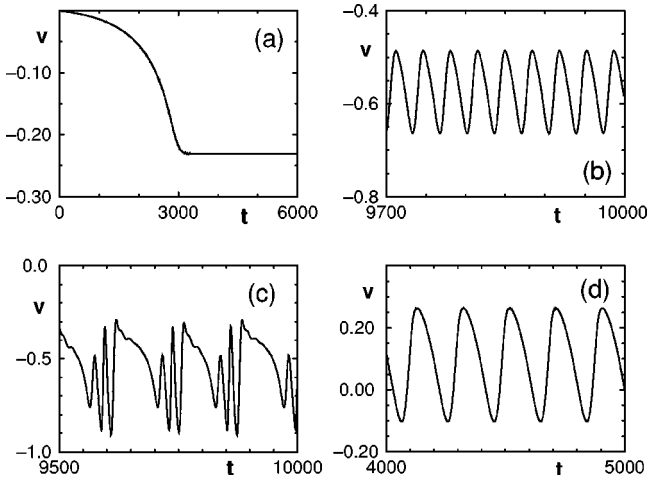

FIG. 4. Simulations showing the velocity of the hole center $v=v(t)$ of interacting hole-shock pairs (periodic boundary conditions). In (a), (b), and (c) the CGLE parameters were $b=0.5$, $c=2.3$, $d'=+0.0025$ (i.e., far away from the core instability line): (a) relaxation into a constantly moving solution for period $P=48.4$; (b) selected final state with (almost) harmonic oscillating velocity for period $P=37.0$; (c) selected final state with anharmonic oscillating velocity for period $P=40.0$; (d) CGLE parameters $b=0.21$,$c=1.3$,$d'=-0.005$ (near the core-instability line), $d''=0$; state with oscillating velocity (including change of direction) for period $P=50$.

2. Arrangements of holes and shocks

When there is more than one hole they have to be separated by shocks. The problem of several holes is analogous to that of interacting conservative particles, which is difficult to handle numerically. The solutions resulting from a periodic arrangement of holes and shocks are actually special cases of the quasiperiodic solutions—"homoclons" in the limit of large periodicity—to be discussed in the next subsection. In the situation discussed here the solutions depend sensitively on perturbations of the CGLE.

Such states are frequently observed in simulations with periodic boundary conditions [see, for example, Chaté and Manneville (1992); Popp *et al.* (1993); Stiller, Popp, Aranson, and Kramer (1995); Stiller, Popp, and Kramer (1995)]. Figure 5 shows the modulus $|A|=|A(x)|$ of a typical solution found in a simulation.[4] As shown in Fig. 4, one finds uniform as well as (almost)

[4]For $d=0$ one expects to observe conservative dynamics for holes and shocks, similar to interacting particles for zero friction.

harmonic and strongly anharmonic oscillating hole velocities. Slightly beyond the core instability line the direction of the velocity is changed in the oscillations [see Fig. 4(d)]. The solutions are seen to be very sensitive to d perturbations of the cubic CGLE.

The uniformly moving solutions can be well understood from the results of the last subsections. First, they are not expected to exist (and we indeed could not observe them in simulations) in the range of monotonic interaction, below curve MOH in Fig. 2,[5] since here the asymptotic hole-shock interaction is always attractive. In the oscillatory range, and away from the core instability line, uniformly moving periodically modulated solutions can then be identified as fixed points of a first-order ordinary differential equation for the hole velocity v, which can be derived by the matching-perturbation method (Popp *et al.*, 1995). In addition, solutions with oscillating hole velocities were found coexisting (stably) with uniformly moving solutions [see Figs. 4(b) and (c)]. They can (in a first approximation) be identified as stable limit cycles of a two-dimensional dynamical system with the hole velocity v and the hole-shock distance L as active variables. These oscillations are of a different nature than those found slightly beyond the core instability line [Fig. 4(d); see above].

By an analysis of the perturbed equations (33) Doelman (1995) has shown that the quintic perturbations create large families of traveling localized structures that do not exist in the cubic case.

3. Connection with experiments

Transient hole-type solutions were observed experimentally by Lega *et al.* (1992) and Flesselles *et al.* (1994) in the (secondary) oscillatory instability in Rayleigh-Bénard convection in an annular geometry. Here one is in a parameter range where holes are unstable in the cubic CGLE, so that small perturbations are irrelevant. Long-time stable stationary holes ("1D spirals") were observed by Perraud *et al.* (1993) in a quasi-1D chemical reaction system (the CIMA reaction) undergoing a Hopf bifurcation. The experiments were performed in the vicinity of the crossover (codimension-2 point) from the spatially homogeneous Hopf bifurcation to the spatially periodic, stationary Turing instability. Simulations of a reaction-diffusion system (Brusselator) with appropriately chosen parameters exhibited the hole solutions (and in addition more complicated localized solutions with the Turing pattern appearing in the core region). Strong experimental evidence for Nozaki-Bekki holes in hydrothermal nonlinear waves is given by Burguette *et al.* (1999).

Finally we mention experiments by Leweke and Provensal (1994), where the CGLE is used to describe results of open-flow experiments on the transitions in the wake of a bluff body in an annular geometry. Here the sensitive parameter range is reached and in the observed amplitude-turbulent state holes should play an important role.

C. Other coherent structures

Coherent states (32) with periodic functions a and $\psi = d\phi/dx$ (same period) have been of particular interest. In general, when the spatial average of ψ is nonzero, the complex amplitude A is quasiperiodic, i.e., A can be written in the form of Eq. (12) with B a periodic function of $\zeta = x - vt$. The associated wave number p will be called the "inner wave number," in contrast to the outer wave number Q, which is equal to the spatial average of ψ. These quasiperiodic solutions bifurcate from the traveling waves (17) in the Eckhaus unstable range $Q_E^2 < Q^2 < 1$ at the neutrally stable positions obtained from Eq. (19) with $\mathrm{Re}\,\lambda = 0$ and k replaced by $p\,(|p|<2)$. In fact, the long-wave Eckhaus instability is signaled in particular by bifurcations of the solitary (or homoclinic) limit solution $p \to 0$. In this limit the velocity v is at the bifurcation equal to the group velocity V_g [see Eq. (21)].

Well away from the Benjamin-Feir-Newell instability (on the stable side) the bifurcation is subcritical (as for the GLE). However, it becomes supercritical before the Benjamin-Feir-Newell line is reached (Janiaud *et al.*, 1992) and remains so in the unstable range. The bifurcation is captured analytically most easily in the long-wave limit by phase equations (see Sec. II.G). The supercritical nature of the bifurcation allows one to understand the existence of "phase chaos" that is found when the Benjamin-Feir-Newell line is crossed (see below).

1. The Ginzburg-Landau equation and nonlinear Schrödinger equation

For the GLE a full local and global bifurcation analysis is possible, and the quasiperiodic solutions can be expressed in terms of elliptic functions (Kramer and Zimmermann, 1985; Tuckerman and Barkley, 1990). Indeed, for $b = c = 0$ Eqs. (33) lead to the second-order system

$$a_{xx} = \partial_a U \quad \text{where} \quad U = \frac{1}{2}\left(-a^2 + \frac{1}{2}a^4 - h^2/a^2 \right), \tag{44}$$

with $h = a^2\psi$ an integration constant. This allows one to invoke the mechanical analog of a point particle (position a, time x) moving in the potential $-U(a)$. One sees that for $|h| < h_E = \sqrt{4/27} \approx 0.385$ the potential $-U$ has extrema at $a_{1,2}$ with $a_{1,2}^2\sqrt{1-a_{1,2}^2} = h$ corresponding to the plane-wave solutions (17) with $F_{1,2} = a_{1,2}, |Q_{1,2}| = \sqrt{1-a_{1,2}^2}$. The maximum corresponds to $|Q_1| < Q_E := 1/\sqrt{3}$. It is stable since it corresponds to a minimum of $\mathcal{V}$. The solution $|Q_2| > Q_E$ is unstable. In this way the Eckhaus instability is recovered. The bifurcations of the quasiperiodic solutions are subcritical and the solutions are all unstable. They represent the saddle points separating (stable) periodic solutions of different wave number and thus characterize the barriers against wavelength-changing processes involving phase slips.

[5]The boundary between monotonic and oscillatory interaction depends on the hole velocity (see Sec. II.F).

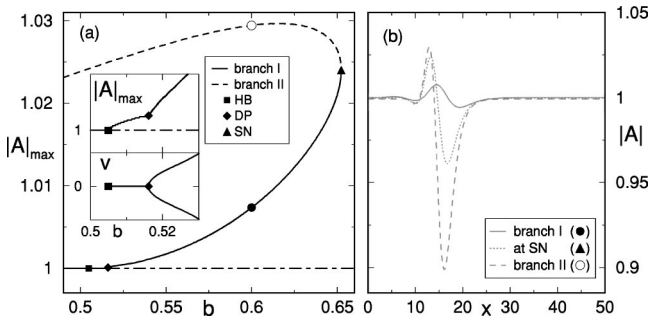

FIG. 6. Quasiperiodic solutions: (a) Example of the bifurcation diagram of the quasiperiodic solutions for $c=-2.0$,$p=2\pi/50$ (see text). The inset illustrates the drift pitchfork bifurcation ($v=0$ branch not shown beyond bifurcation). (b) Quasiperiodic solution profiles: ●, at lower branch; ○, at upper branch; ▲, at the saddle node (SN); HB, Hopf bifurcation; DP, drift pitchfork bifurcation. From Brusch *et al.* (2000).

As was mentioned in Sec. II, all stationary solutions and their stability properties of the 1D (defocusing) nonlinear Schrödinger equation coincide with those of the GLE. In addition, the nonlinear Schrödinger equation has more classes of coherent structures due to the additional Galilean and scaling invariance absent in GLE. We shall not pursue this question since the 1D nonlinear Schrödinger equation is a fully integrable system (Zakharov and Shabat, 1971) that has been studied in great detail (see, for example, Proceedings of the Conference on the Nonlinear Schrödinger Equation, 1994).

2. The complex Ginzburg-Landau equation

For the CGLE an analysis of the local bifurcation was first carried out in the limit of small p using the phase equation (27) (Janiaud *et al.*, 1992) and subsequently for arbitrary p (Hager, 1996). These analyses showed that the Eckhaus instability becomes supercritical slightly before the Benjamin-Feir-Newell curve is reached. The bifurcation has in the long-wave limit a rather intricate structure, since the limits $p\to 0$ and $Q\to Q_E$ do not interchange (this can already be seen in the GLE). When taking first the solitonic limit $p\to 0$ (while $Q>Q_E$) one finds that the Eckhaus instability becomes supercritical slightly later than in the other ("standard") case, which corresponds to harmonic bifurcating solutions. These features are captured nicely by the phase equation description.

Recently Brusch *et al.* (2000, 2001) carried out a systematic numerical bifurcation analysis based on Eqs. (33) for the case $Q=0$, where A is periodic (nevertheless we shall usually refer to these solutions as quasiperiodic solutions). It shows that the supercritically bifurcating quasiperiodic branch (the *shallow quasiperiodic solution*) terminates in a saddle-node bifurcation and merges there with an "upper" branch (the *deep quasiperiodic solution*); see Fig. 6. For $p\neq 0$ the bifurcating solution has velocity $v=0$ [in Eqs. (33) the bifurcation is of the Hopf type]. It is followed by a drift-pitchfork bifurcation generating a nonzero velocity. The separation between the two bifurcations tends to zero for vanishing p, so that the solitary solutions develop a drift from the beginning on (at second order in the amplitude).[6] These features can be reproduced by the Kuramoto-Sivashinsky equation, which exhibits only the shallow homoclons. By adding higher-order (nonlinear) terms (Sakaguchi, 1990) one can generate the other branch. Brusch *et al.* (2000) give evidence that the existence of the two branches provides a mechanism for the stabilization of phase chaos (see below).

Deep quasiperiodic solutions (in the solitary limit) were first studied by van Hecke (1998) and then by van Hecke and Howard (2001) in the context of spatio-temporal chaos in the intermittent regime (see the next subsection). Following this author we have adopted the name "homoclons" for the localized objects.

The stability properties of quasiperiodic solutions were also analyzed by Brusch *et al.* (2000). Both branches of quasiperiodic solutions have neutral modes corresponding to translation and phase symmetries. The eigenvalue associated with the saddle-node bifurcation is positive for deep homoclons and negative for shallow ones. Apart from these three purely real eigenvalues, the spectrum consists of complex-conjugate pairs.

For a not too small wave number p all the eigenvalues of the shallow branch are stable within a system of length $L=2\pi/p$, but when L increases, the quasiperiodic solutions may become unstable with respect to finite-wavelength instabilities (near the bifurcation they certainly do).

Shallow quasiperiodic solutions can be observed in simulations of the CGLE (away from the bifurcation from the plane waves), in particular for $Q\neq 0$ (Janiaud *et al.*, 1992; Montagne *et al.*, 1996, 1997; Torcini, 1996; Torcini, Frauenkron, and Grassberger, 1997).

More complex coherent structures, corresponding to nonperiodic arrangements of shallow homoclons, were also found numerically, reflecting the oscillatory nature of interaction between shallow homoclons for a certain rouge of parameters. This is suggested by the fact that in the supercritical regime the spatial exponents introduced in Sec. II.F are complex. Clearly chaotic solutions may be expected to exist in Eqs. (33).

Recently, quasiperiodic solutions have been observed experimentally in the form of modulations of spiral waves excited by core meandering (see Secs. IV.B.2 and IV.H.2) in an oscillatory reaction-diffusion system by Zhou and Ouyang (2000).

D. Spatio-temporal chaos

1. Phase chaos and the transition to defect chaos

When crossing the Benjamin-Feir-Newell line with initial conditions $A\approx 1$ (actually any nonzero, spatially

[6]For $Q\neq 0$ there is already drift after the first bifurcation, so the drift pitchfork gets unfolded (Brusch, private communication).

constant A is equivalent), one first encounters phase chaos, which persists approximately in the lower dashed region between Benjamin-Feir-Newell and absolute instability curves in Fig. 2. In this spatio-temporally chaotic state $|A|$ remains saturated (typically above about 0.7–0.9), so there is long-range phase coherence and the global phase difference (here equal to 0) is conserved. In this parameter range one also has stable, periodic solutions, but they obviously have a small domain of attraction which is not reached by typical initial conditions. Beyond this range phase slips occur and a state with a nonzero (average) rate of phase slips is established (defect or amplitude chaos). Since in phase chaos only the phase is dynamically active it can be described by phase equations [in the case of zero global phase the Kuramoto-Sivashinsky equation, otherwise Eq. (27)].

In the CGLE, phase chaos and the transition to defect chaos (see below) were first studied by Sakaguchi (1990) and subsequently systematically in a large parameter range by Shraiman *et al.* (1992) and, for selected parameters and in particular very large systems by Egolf and Greenside (1995). One of the interests driving these studies was the question of whether in phase chaos the rate of phase slips is really zero, so it could represent a separate phase (in the thermodynamic sense), or whether the rate is only very small. The recent studies by Brusch *et al.* (2000) on the quasiperiodic solutions with small modulation wave number p (see Sec. III.C.2) point to a mechanism that prevents phase slips in a well-defined parameter range.

In fact, phase chaos "lives" on a function space spanned by the forwardly bifurcating branches of the quasiperiodic solutions. Thus snapshots of phase chaos can be characterized (roughly) as a disordered array of shallow homoclons (or disordered quasiperiodic solutions); see Fig. 7. The dynamics can be described in terms of birth and death processes of homoclonal units. When these branches are terminated by the saddle-node bifurcation, phase-slip processes are bound to occur. Brusch *et al.* (2000) have substantiated this concept by extensive numerical tests with system sizes ranging from $L=100$ to $L=5000$ and integration times up to 5×10^6. For a given L (not too small) phase slips occurred only past the saddle node for the quasiperiodic solutions with inner wave number $p=2\pi/L$. Tracking of (rare) phase-slip events corroborated the picture. Thus the authors conjectured that the saddle-node line for $p\to0$ provides a strict lower boundary for the transition from phase to defect chaos.

One expects the existence of a continuous family of phase chaos with different background wave numbers Q. For $Q\neq0$ the state should arise when crossing the Eckhaus boundary for the plane wave with wave number Q, before the Benjamin-Feir-Newell limit. Such states were studied by Montagne *et al.* (1996, 1997), Torcini (1996), and Torcini *et al.* (1997). It was found that the parameter range exhibiting phase chaos decreases with increasing Q. Thus at fixed parameters b,c one has a band of phase-chaotic states that is bounded from above by some $Q_{\max}(b,c)$. Approaching the limit of phase chaos, $Q_{\max}$ decreases smoothly to zero, i.e., the phase-chaotic state with $Q=0$ is the last to lose stability, similar to the situation for the plane waves. As mentioned before, for not too small Q, one finds coexistence with quasiperiodic solutions and spatially disordered coherent states.

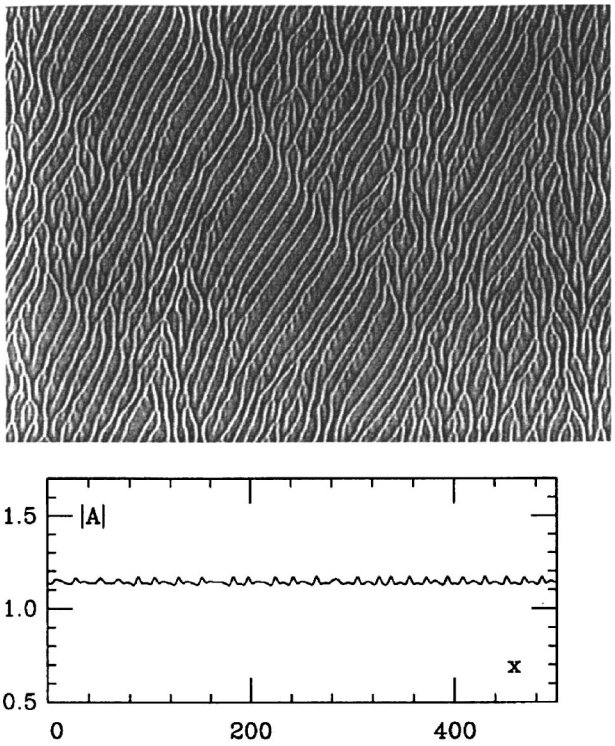

FIG. 7. Phase turbulence observed for $b=-1$ and $c=1.333$. Upper figure is a spatio-temporal plot of A; lower figure shows snapshot $|A|$. From Chaté (1994).

2. Defect chaos

The transition (or crossover) between phase and defect chaos is reversible only for $|b|$ larger than about 1.9 (near the lower edge of Fig. 2; Shraiman *et al.*, 1992). There, when approaching the transition from the side of defect chaos, the phase-slip rate goes smoothly to zero. On the other hand, for $|b|<1.9$, there is a region where phase and defect chaos coexist ("bichaos," the lower dashed region to the right of the line DC), and in fact defect chaos even persists into the Benjamin-Feir-Newell stable range (the limit towards small c is approximated by the dashed line DC in Fig. 2; Shraiman *et al.*, 1992; Chaté, 1994, 1995). There the defect chaos takes on the form of spatio-temporal intermittency.

A qualitative understanding of the parameter region where one has bistable defect chaos can be obtained as follows: In this region, starting from the (saturated) state with $|A|\approx1$ and forcing a large excursion of $|A|$ leading to a phase slip makes it easier for other phase slips to follow. This memory effect is suppressed with increasing

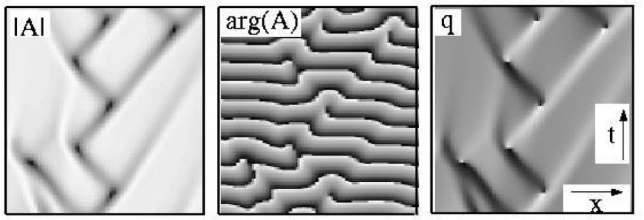

FIG. 8. Space-time plots (over a range of 60×50) of $|A|$ (black corresponds to $|A|=0$) showing chaotic states in the spatio-temporal intermittent regime, for coefficients $(b,c)=(0.6,-1.4)$. From van Hecke (1998).

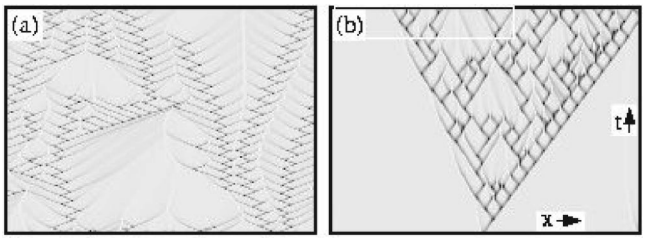

FIG. 9. Space-time plots (over a range of 512×1000) of $|A|$ showing (a) zigzagging holes near the transition to plane waves for $b=-0.6,c=1.2$; (b) evolution of a homoclons in a background state with wave number 0.05 for $b=-0.6,c=1.4$, space$\times$time $=512\times250$. From van Hecke (1998).

$|b|$, as can be seen from the increase of the velocity $v^*=2\sqrt{1+b^2}$ with $|b|$ of fronts that tend to restore a saturated state (see Sec. III.A).

From above (towards small values of $|b|$) the chaotic state joins up with the region of stable Nozaki-Bekki holes. The characteristics of these holes are influenced by small perturbations of the CGLE, and this in turn affects the precise boundary of spatio-temporal chaos (see Sec. III.D.4).

3. The intermittency regime

This regime, in which defect chaos coexists with stable plane waves, has been studied numerically in detail by Chaté (1994, 1995), and he has pointed out the relation with spatio-temporal intermittency. There, typical states consist of patches of plane waves, separated by various localized structures characterized by a depression of $|A|$. The localized structures can apparently be divided into two groups depending on the wave numbers q_l and q_r of the asymptotic waves they connect. On the one hand, one has slowly moving structures that can be related to Nozaki-Bekki holes, which in this regime either are core stable or have long lifetimes. They become typical as the range of stable Nozaki-Bekki holes is approached (Chaté, 1994, 1995).

However, on the other hand, the dominant local structures have velocities and asymptotic wave numbers over a larger range that are incompatible with the Nozaki-Bekki holes and that, according to van Hecke (1998), must be associated with the deep homoclons. Space-time plots of the amplitude $|A|$, the phase $[\arg(A)]$, and the local wave number $q:=\partial_x\arg(A)$ in such a regime are shown in Fig. 8 [the plot is a close-up view of a larger simulation as shown in Fig. 9(b)]. The wave numbers of the laminar patches are quite close to zero, while the cores of the local structures are characterized by a sharp phase gradient (peak in q) and dip of $|A|$. The holes propagate with a speed of 0.95 ± 0.1 and either their phase gradient spreads out and the hole decays, or the phase gradient steepens and the hole evolves to a phase slip. The phase slip then sends out one or two new localized objects which repeat the process. van Hecke (1998) provides evidence that the dynamics is continually evolving around the one-dimensional unstable manifold of homoclons with background wave number near zero. They provide the saddle points that separate dynamical processes leading to phase slips from those leading back to the (laminar) plane-wave state. When the parameters b and c are quenched in the direction of the transition to plane waves, these zigzag motions of the holes become very rapid [Fig. 9(a)].

A further consideration of homoclons and their role in spatio-temporal chaos is presented by van Hecke and Howard (2001). The simulations of the CGLE show that when an unstable hole invades a plane-wave state, defects are nucleated in a regular, periodic fashion, and new holes can then be born from these defects. Relations between the holes and defects obtained from a detailed numerical study of these periodic states are incorporated into a simple analytic description of isolated "edge" holes, which can be seen in Fig. 9.

Recently Ipsen and van Hecke (2001) found in long-time simulations that in a restricted parameter range composite zigzag patterns formed by periodically oscillating homoclinic holes represent the attractor.

4. The boundary of defect chaos towards Nozaki-Bekki holes

As the boundary of stability of Nozaki-Bekki holes is approached (curve AH in Fig. 2) one can increasingly observe Nozaki-Bekki-hole-like structures that emit waves and thereby organize ("laminarize") their neighborhood. In this regime the state becomes sensitive to small perturbations of the cubic CGLE, as discussed in Sec. III.B.

It is found that stable hole solutions suppress spatio-temporal chaos and as a consequence, for a decelerating ($d'<0$ if $d''=0$) perturbation, the (upper) boundary of spatio-temporal chaos is simply given by the stability boundary AH in Fig. 2 of the Nozaki-Bekki hole solutions, whereas for an accelerating perturbation spatio-temporal chaos is also observed further up (Popp *et al.*, 1993; Stiller, Popp, Aranson, and Kramer, 1995). For $d'<0$ random initial conditions lead to an irregular grid of standing holes, separated by shocks from each other [see Fig. 10(b)]. Such grids are the 1D analog of the "vortex glass" state found in two dimensions (see Sec. IV.G, and also Chaté, 1995).

Clearly, for accelerating $d'>0$, such a grid is unstable. In this case Nozaki-Bekki holes are created from random initial conditions, too. In their neighborhood they suppress small-scale variations of $|A|$ typical of ampli-

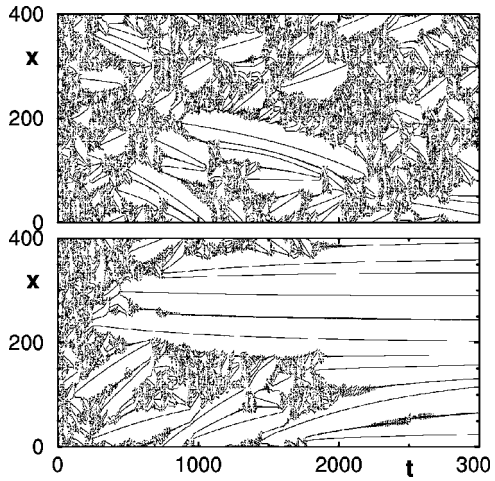

FIG. 10. Space-time plot of the zeros of the local phase gradient $\partial_x \phi = 0$ (with $A = |A| \exp[i\phi]$) for the perturbed cubic CGLE. The parameters are: upper figure, $b = 0.9, c = 5.55$ (i.e., slightly below the absolute instability line for the plane waves AH of Fig. 2), and $d' = 0.005$; lower figure, $d' = -0.005$, $d'' = 0$, with periodic boundary conditions and small-amplitude noise as initial conditions. Isolated lines can be identified as holes and shocks (alternating), which are spontaneously formed out of the chaotic state. In their neighborhood there are approximate plane waves. For decelerating d' the holes suppress the chaotic state after some transience (lower figure) and one is left with a 1D vortex glass, while in the accelerating case ($d' > 0$, upper figure) the chaotic state persists.

tude chaos over much of the chaotic regime. However, since they are accelerated they have only a finite lifetime [see Fig. 10(a)]. For parameters b, c below about curve EH in Fig. 2 (the coincidence with the Eckhaus limit is presumably fortuitous), destruction of the holes leads to the creation of new holes and shocks, yielding a chaotic scenario of subsequent acceleration, destruction, and creation processes.

IV. DYNAMICS IN TWO DIMENSIONS

A. Introduction

The 2D CGLE has a variety of coherent structures. In addition to the quasi-1D solutions derived from the coherent structures in one dimension discussed above, the CGLE possesses localized sources in two dimensions known as spiral waves. An isolated spiral solution is of the form

$$A(r,\theta,t) = F(r) \exp\{i[-\omega t + m\theta + \psi(r)]\}, \tag{45}$$

where r, θ are polar coordinates. The (nonzero) integer m is the topological charge, ω is the (rigid) rotation frequency of the spiral, $F(r) > 0$ is the amplitude, $\psi(r)$ is the phase of the spiral, $Q = \partial_r \psi$ for $r \to \infty$ is the asymptotic wave number selected by the spiral (Hagan,

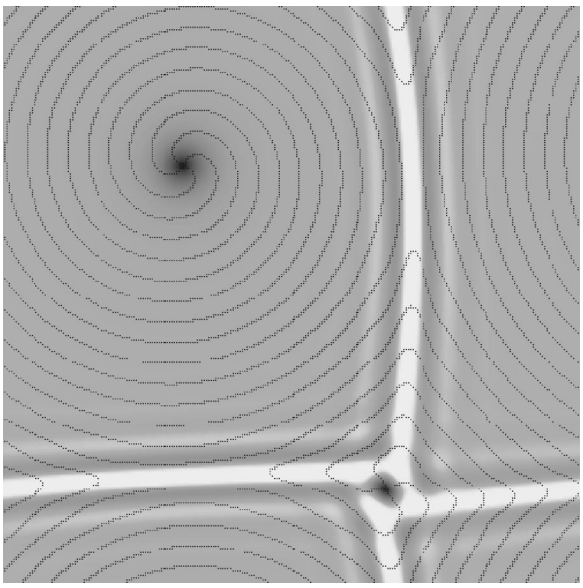

FIG. 11. Image of the amplitude $|A|$ and contour lines of the phase $\phi = \arg A = 0, \pi$ for a single-charged spiral solution in a domain with periodic boundary conditions. Note the edge vortex (sink) in the corner. Image is coded in the gray scale; the maximum of the field corresponds to black, the minimum to white.

1982), and $\omega = c + (b-c)Q^2$ is the spiral frequency.[7] Since spirals emit plane waves asymptotically [group velocity $V_g = 2(b-c)Q > 0$], they are a source of solutions. In addition to spirals there are sinks that absorb waves. The form of these sinks is determined by the configuration of surrounding sources. Sinks with topological charge appear as edge vortices (see below). Spiral solutions with $m \neq \pm 1$ are unstable (Hagan, 1982). Single-charged spiral solutions are dynamically stable in certain regions of parameter space. The gray-coded image of a spiral and an edge vortex is shown in Fig. 11. For $b - c \to 0$, and also for $b, c \to \infty$, the asymptotic wave number of the spiral vanishes and the solution becomes the well-known vortex solution of the GLE and nonlinear Schrödinger equation, known in the context of superfluidity (Pitaevskii, 1961; Gross, 1963; Donnelly, 1991) and somewhat similar to that found in superconductivity in the London limit (Abrikosov, 1988; Blatter *et al.*, 1994). In periodic patterns, spirals and vortices become dislocations.

The asymptotic interaction is very different for the case $b = c$, where it is long range, decaying like r^{-1} with some corrections, whereas for $b - c \neq 0$ it is short range, decaying exponentially (see below). The interaction manifests itself in the motion of each spiral. The resulting velocity can have a radial (along the line connecting the spiral cores) and a tangential component.

[7] Spirals with zero topological charge $m = 0$ (targets) are unstable in the CGLE. However, inhomogeneities can stabilize the target. Hagan (1981) has found stable targets in the inhomogeneous CGLE in the limit of small c. Stationary and breathing targets over the wide parameter range of the CGLE were studied by Hendrey *et al.* (2000).

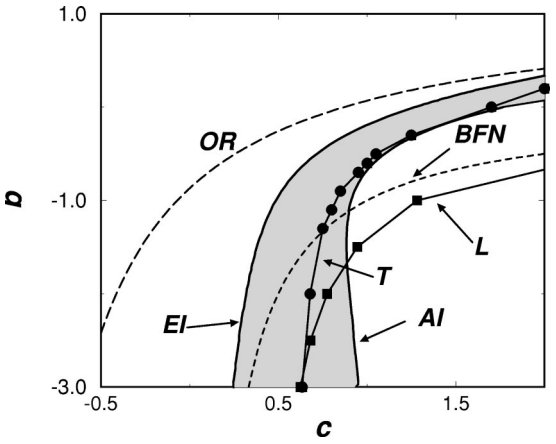

FIG. 12. Stability limits of a spiral wave solution. The boundary of convective (EI) and absolute instability (AI) for the waves emitted by the spiral are also shown (for an explanation see Sec. II.E and Aranson *et al.*, 1992). Bound states exist to the right of the OR line $(c-b)/(1+bc)=0.845$. BFN indicates the Benjamin-Feir-Newell limit $1+bc$, L shows the limit of 2D phase turbulence, and line T corresponds to the transition to defect turbulence for random initial conditions. From Chaté and Manneville (1996).

Spirals may form regular lattices and/or disordered quasistationary structures called vortex glass or the frozen state. When individual spirals become unstable (spiral breakup), the typical spatio-temporal behavior is chaotic.

B. Spiral stability

1. Outer stability

For spirals to be stable the wave number of the asymptotic plane wave has to be in the absolutely stable range (see Sec. II.E). In order to find this stability limit we have to evaluate condition (24) for the wave number Q emitted by the spiral (see Fig. 12). The existence of an absolutely stable spiral solution guarantees that small perturbations within the spiral will decay, but does not assure that it will evolve from generic initial conditions. For further discussion see Sec. IV.H.2.

2. Core instability

The spiral core may become unstable in a parameter range where diffusive effects are weak compared to dispersion (large b limit). Then it is convenient to rewrite the CGLE in the form

$$\partial_t A = A + (\varepsilon + i)\Delta A - (1+ic)|A|^2 A, \tag{46}$$

where $\varepsilon = 1/|b|$ and the length has been rescaled by $\sqrt{\varepsilon}$. This situation is typical in nonlinear optics (transversely extended lasers or passive nonlinear media). In this case a systematic derivation of the CGLE from the Maxwell-Bloch equations in the "good-cavity limit" for positive detuning between the cavity resonance and the atomic line leads to very small values of $\varepsilon > 0$ (Coullet, Gil, and Rocca, 1989; Oppo *et al.*, 1991; Newell and Moloney, 1992; Newell, 1995). Representative values are $\varepsilon \sim 10^{-3}$–10^{-2} (Coullet, Gil, and Rocca, 1989).

For $\varepsilon = 0$ one has the Galilean invariance mentioned in Sec. II.C (see van Saarloos and Hohenberg, 1992 for the 1D case); then, in addition to the stationary spiral, there exists a family of spirals moving with arbitrary constant velocity $\mathbf{v}$,

$$A(r,t) = F(r')\exp\left[i\left(-\omega' t + \theta + \psi(r') - \frac{\mathbf{r}'\cdot\mathbf{v}}{2}\right)\right], \tag{47}$$

where $\mathbf{r}' = \mathbf{r} + \mathbf{v}t$, $\omega' = \omega - v^2/4$, and the functions F, ψ are those of Eq. (45) (this invariance holds for any stationary solution). For $\varepsilon \neq 0$ the diffusion term $\sim \varepsilon \Delta A$ destroys the family and in fact leads to acceleration or deceleration of the spiral proportional to εv. The natural assumption is that one has deceleration so that the stationary spiral is stable (Coullet, Gil, and Rocca, 1989). In fact this is not the case. Stable spirals exist only above some critical value ε_c. Below ε_c stationary spirals are unstable to spontaneous acceleration (Aranson *et al.*, 1994).

For small values of ε one may expect the solution (47) to be slightly perturbed and have a slowly varying velocity $\mathbf{v}$ which obeys an equation of motion of the form $\partial_t \mathbf{v} + \varepsilon \hat{K}\mathbf{v} = 0$. Because of isotropy the elements of the tensor $\hat{K}$ must satisfy $K_{xx} = K_{yy}$ and $K_{xy} = -K_{yx}$, so the relation can also be written as

$$\partial_t \hat{v} + \varepsilon \kappa \hat{v} = 0, \tag{48}$$

where $\hat{v} = v_y + iv_x$ and $\kappa = K_{xx} - iK_{xy}$. Since in general the friction constant κ is complex, the spiral core moves on a (logarithmic) spiral trajectory.

The acceleration instability of the spiral core has a well-known counterpart in excitable media, where the spiral "tip" can perform a quasiperiodic motion leading to meandering (see, for example, Barkley, 1994). The main difference between the two cases can be understood by considering the nonlinear extension of Eq. (48) $\partial_t \hat{v} + \varepsilon \kappa \hat{v} = f(|\hat{v}|^2)\hat{v}$ with $f(0) = 0$. In excitable media one has $\mathrm{Re}\, f(|\hat{v}|^2) < 0$, which provides saturation of the instability. However, in the CGLE the sign of $\mathrm{Re}\, f(|\hat{v}|^2)$ is opposite and destabilizes the core according to simulations. This one has an alternative scenario of the meandering instability. The scenario appears to be generic and is not destroyed by small perturbations of the CGLE.

Now going to larger ε one finds that $\mathrm{Re}\,\kappa$ increases with ε and finally changes sign at a value ε_c. The result obtained from extensive numerical simulations is shown in Fig. 13.

The acceleration instability can also be interpreted as the destabilization of a localized core mode similar to the situation with the standing-hole solution in the 1D CGLE (Chaté and Manneville, 1992; Popp *et al.*, 1993; Sasa and Iwamoto, 1993; also see Sec. III).

The case of negative diffusion ($\varepsilon < 0, |\varepsilon| \ll 1$) is especially important for lasers with negative detuning (Oppo, 1991; Staliunas, 1993; Lega *et al.*, 1994). Then higher-order corrections to the diffusion (fourth deriva-

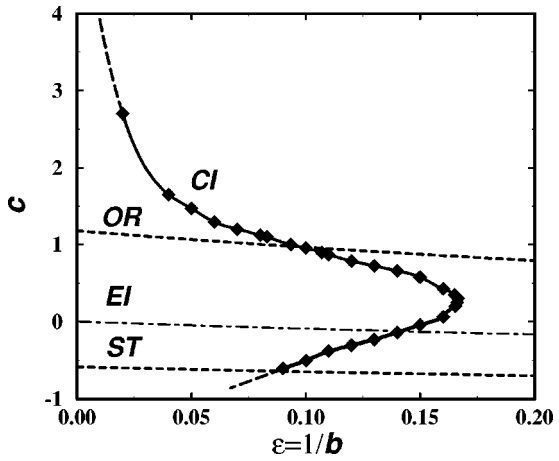

FIG. 13. Stability limits of a spiral wave in the large-b limit, $\varepsilon=1/b$. Here CI is the core-stability limit $\varepsilon=\varepsilon_c$ (unstable to the left), the area below EI is the Eckhaus unstable region, ST designates the transition line to strong turbulence (see text), and the area below OR is the oscillatory range. From Aranson *et al.* (1994).

tive) have to be included to stabilize the short-wave instability. The resulting complex Swift-Hohenberg equation is

$$\partial_t A = A + i\Delta A - \varepsilon(q_c^2+\Delta)^2 A - (1+ic)|A|^2 A. \quad (49)$$

This equation exhibits over some range of parameters ε, q_c a similar core instability. In a certain parameter range one has stable meandering of the spiral (Aranson and Tsimring, 1995; Aranson, Hochheiser, and Moloney, 1997)

C. Dynamics of vortices in the Ginzburg-Landau equation, in the nonlinear Schrödinger equation, and for $b=c$

1. Dynamics of vortices in the Ginzburg-Landau equation

In the GLE the spirals become vortices, i.e., in Eq. (45) one has $\omega=0$ and $\psi=0$. $F(r)$ is a monotonic function and $F\sim\alpha r$ for $r\to 0$, $F^2(r)\to 1-1/r^2$ for $r\to\infty$.

A more general isolated moving-vortex solution with wave vector $\mathbf{Q}$ away from the band center is described by

$$A = B(\mathbf{r}-\mathbf{v}t)\exp[i\mathbf{Q}\mathbf{r}], \quad (50)$$

where B fulfills the boundary conditions $|B|^2\to 1-Q^2$ for $r\to\infty$ with the appropriate phase jump of $\pm 2\pi$.[8]

For large systems such that $Rv\gg 1$, where R is the system size or the distance to another defect, the drift velocity v is perpendicular to the background wave number $\mathbf{Q}$, such that the free energy decreases. The speed v is given by the expression

$$\frac{1}{2}\mathbf{v}\ln(v_0/v) = \mathbf{U}\mathbf{Q}[1-0.35Q^2], \quad (51)$$

with the constant $v_0=3.29$ (see Bodenschatz, Pesch, and Kramer, 1988; Kramer *et al.*, 1990; Bodenschatz *et al.*, 1991). Here $\mathbf{U}$ is the $\pi/2$ rotation matrix

$$\mathbf{U}=\begin{pmatrix} 0 & 1 \\ -1 & 0 \end{pmatrix}.$$

The term in brackets on the right-hand side has been fitted to numerical results (see Bodenschatz *et al.*, 1991). The formula can be used throughout the stable range and is consistent with the experiments of Rasenat *et al.* (1990) on electroconvection in nematics. In small systems, $vR\ll 1, R\gg 1$, the velocity is given by $v=2Q/\ln(R/\xi_0)$ with $\xi_0=1.13$.

The above relations were rederived by Pismen and Rodriguez (1990), Rodriguez, Pismen, and Sirovich (1991), Ryskin and Kremenetsky (1991), and in part by Neu (1990a) using matching asymptotic techniques.

The result shows that for an isolated defect the limits of the system size going to infinity and wave number mismatch (or defect velocity) going to zero are not interchangeable. This is analogous to the 2D of Stokes law (drag of an infinite cylinder through an incompressible fluid), where one also has a logarithmic divergence of the mobility at vanishing velocities. The similarity was pointed out by Ryskin and Kremenetsky (1991). It is also useful to note that the force exerted on dislocations in a phase gradient, expressed by a wave vector $\mathbf{Q}$, is the analog of the well-known Peach-Koehler force on dislocations in crystals under stress.

In the following we consider linearly stable periodic states, in which $Q^2<Q_E^2$. All periodic states, except $Q=0$ (band center), are metastable. Evolution to the band center can occur by the motion of vortices, once they have been nucleated by finite fluctuations or disturbances (see Bodenschatz, Pesch, and Kramer, 1988 and Hernandez-Garcia *et al.*, 1993 for a discussion of the problem of homogeneous nucleation of vortices).

The asymptotic interaction between two vortices can be described approximately by Eq. (51) with the right-hand side replaced by the gradient of the resulting phase of another vortex at the center of the vortex. Since the gradient is perpendicular to the line connecting the vortex cores, the resulting force is directed along this line. As a result, oppositely charged vortices attract each other and eventually annihilate, whereas those with like charges repel each other.

Analysis of an isolated moving vortex shows that the deformation of the roll pattern decays in front exponentially over a distance $R\sim 1/v$, while behind the dislocation the decay is proportional to $R^{-1/2}$. Thus, if the background wave number is nonzero and two vortices with opposite topological charge are approaching each other, the velocity will be constant for $R\leqslant 2/v\sim 2/Q$. Subsequently the motion will accelerate and eventually

[8] It is important to mention that such a problem is not well defined for spiral waves ($b-c\neq 0$). Since the spiral waves are active sources, they cannot in general coexist with plane waves. Depending on the relation between the two frequencies, either the spiral would invade the entire plane or the plane wave would push the spiral away. For details see Sec. IV.F

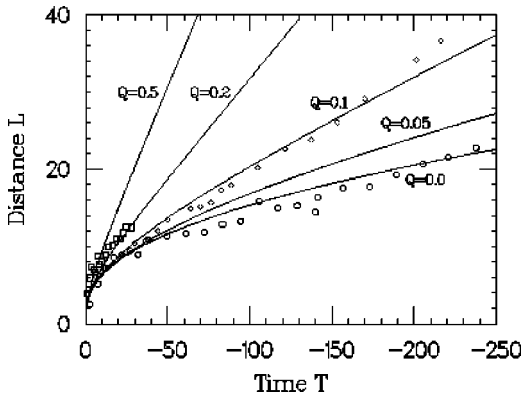

FIG. 14. The distance L between two defects of opposite polarity that approach each other on a straight line is plotted for different Q versus time T. From Bodenschatz *et al.* (1991). For comparison the experimental data of Braun and Steinberg (1991) are included. The different symbols denote different distances ε from the threshold: ○, $\varepsilon=0.02$; □, $\varepsilon=0.04$; ◇, $\varepsilon=0.005$.

the attraction will dominate over the Peach-Koehler force and lead to annihilation.[9] In experiments by Brawn and Steinberg (1991), the annihilation process was studied in detail near the band center ($Q\ll 1$) where accurate determination of Q is not possible. The quantitative comparison with theory is shown in Fig. 14, where the distance L between two vortices of opposite polarity approaching each other along a straight line versus time T is shown for different Q in scaled units (Bodenschatz *et al.*, 1991). At time $T=0$ the vortices annihilate. The solid line gives the numerical results, and the squares, circles, and diamonds are the experimental data.

The case $Q=0$, in which the Peach-Koehler force vanishes so that $v\to 0$ for $L\to\infty$, deserves special attention. The analysis of Bodenschatz, Pesch, and Kramer (1988) leads to $vL=2/C$, where $C\sim\ln(L/2.26)$ for $vL\ll 1$. Clearly for this to hold L needs to be exponentially large. Otherwise one is caught in the intermediate region $vL\sim 1$ where no accurate relation for C was found. For that reason the so-called self-consistent approximation was proposed by Pismen and Rodriguez (1990), Rodriguez, Pismen, and Sirovich (1991), and Pismen (1999):

$$\ln(v_0/v)=\exp(\pm vr/2)[K_0(vr/2)\pm K_1(vr/2)],$$
$$v_0=3.29, \tag{52}$$

where the + sign corresponds to a like-charged pair and the − sign to an oppositely charged one, and K_0 and K_1 are modified Bessel functions. The formula is not very accurate, as shown by comparison with full simulations (Weber *et al.*, 1991; Weber, 1992).

Allowing for a very small wave-vector displacement Q, one finds $v(L+1/Q)=2/C$. One can then get to the limit $vL\gg 1$ and then, for sufficiently large systems, $C=\ln(3.29/v)$.

For small distances, shortly before the annihilation of an oppositely charged pair, the gradient terms in the GLE become dominant and one may argue that the dynamics is governed by self-similar solutions of the diffusion equation so that $L\sim\sqrt{T}$, which appears consistent with the numeric results.

2. Dynamics of vortices in the nonlinear Schrödinger equation

Although the stationary vortex solution of the nonlinear Schrödinger equation coincides with that of the GLE, the dynamic behavior of vortices is very different. In the limit of small velocities, large separation, and properly quantized circulation the motion of vortices in the nonlinear Schrödinger equation is similar to the motion of point vortices in an ideal incompressible fluid (Lamb, 1932). The problem of vortex motion in the context of the nonlinear Schrödinger equation was first considered by Fetter (1966); since then many researchers have rederived this result more accurately (see, for example, Creswick and Morrison, 1980; Neu, 1990b; Lund, 1991; Pismen and Rubinstein, 1991; Rubinstein and Pismen, 1994).

Introducing the amplitude-phase representation $A=R\exp[i\theta]$ and the "superfluid density" $\rho=R^2$ as well as the superfluid velocity $\mathbf{V}=-2\nabla\theta$, one obtains from Eq. (6) a Euler equation,

$$\partial_t\mathbf{V}+(\mathbf{V}\cdot\boldsymbol{\nabla})\mathbf{V}=\boldsymbol{\nabla}P, \tag{53}$$

and the continuity equation for the "density" of a superfluid,

$$\partial_t\rho+\operatorname{div}\rho\mathbf{V}=0. \tag{54}$$

Here $P=2(-\nabla^2\sqrt{\rho}/\sqrt{\rho}+\rho-1)$ is the effective pressure, whereas the first term is called the "quantum pressure." The quantum pressure is irrelevant for large-scale perturbations of the density, i.e., $\nabla^2\rho\ll\rho$. In the Euler equation the incompressibility approximation $\rho=\rho_0=\text{const}\neq 0$ is reliable for velocities much smaller than the sound velocity $c_s=\sqrt{2\rho_0}$. One expects the analogy with classical incompressible vortex tubes in a liquid to hold for well-separated vortices moving with the velocity $v\ll c_s$. Thus, according to classical hydrodynamics (Lamb, 1932), the oppositely charged vortex pair drifts with the velocity $v=2/L$ normal to the line connecting the cores of the vortices, and the like-charged pair rotates around the center of the symmetry, where L is the distance between vortex centers. This result up to higher-order corrections holds for well-separated vortices ($L\gg 1$) in the nonlinear Schrödinger equation, as it was later rederived by Neu (1990b), Pismen and Rubinstein (1991), and Rubinstein and Pismen (1994), using a matching asymptotic technique. A numerical investigation of vortex dynamics in the nonlinear Schrödinger equation was also carried out by Nore *et al.* (1993),

[9] In this discussion we have tacitly considered the situation in which the Peach-Koehler force and the force due to interaction are parallel to each other. If this is not the case the vortices will move on curved trajectories.

Frisch *et al.* (1992), Abraham *et al.* (1995), and Josserand and Pomeau (1995).

For N well-separated vortices located at the points $\mathbf{R}_j=(X_j,Y_j)$ one has the more general formula

$$\mathbf{v_j}=2\sum_{j=1}^{N} n_j \frac{\mathbf{U}(\mathbf{R_j}-\mathbf{R_i})}{|\mathbf{R_i}-\mathbf{R_j}|^2}. \tag{55}$$

According to Eq. (55), obtained from the corresponding incompressible Euler equation, the vortex velocities diverge as the intervortex distances vanish. However, the above expression becomes incorrect when the intervortex distance d becomes of the order of the coherence length $d\sim O(1)$ (one in our scaling). For small separations the interaction of two like-charged vortices can be considered as a small perturbation of a double-charged vortex. Aranson and Steinberg (1995) have shown that for $d\to 0$ the velocity of vortices vanishes, and the frequency of rotation Ω for the like-charged vortex pair approaches a constant as $d\to 0$ [the "classical formula" (55) results in infinite frequency]. Similarly, for an oppositely charged pair the velocity remains finite for $d\to 0$.

An important problem in the context of the nonlinear Schrödinger equation is the nucleation (or generation) of vortices from zero-vorticity flow. Frisch, Pomeau, and Rica (1992) considered the stability of flow passing an obstacle and found nucleation of vortex pairs above some critical velocity. Yet another mechanism of vortex generation is related to the instability of quasi-1D dark solitons, predicted by Kuznetsov and Turitsyn (1988). Josserand and Pomeau (1995) studied the instability of dark solitons numerically and found that the nonlinear stage of this instability results in the creation of vortex pairs.

3. Dynamics of vortices for $b=c$

The general case $b=c$, including the nonlinear Schrödinger equation limit, can be related to the GLE limit by generalizing the ansatz (50) to

$$A=B(\mathbf{r}-\mathbf{v}t)\exp[i\mathbf{Q}\mathbf{r}-ibt]. \tag{56}$$

Equation (1) can be written as

$$-\frac{1}{1+b^2}\mathbf{v}\nabla B=\Delta B+2i\left(\mathbf{Q}+\frac{b}{2(1+b^2)}\mathbf{v}\right)\nabla B +(1-Q^2)B-|B|^2B. \tag{57}$$

After neglecting the higher-order term Q^2B, one observes that Eq. (57) coincides with the corresponding equation for $b=0$ if one replaces $\mathbf{Q}$ with $\mathbf{Q}+b/2(1+b^2)\,\mathbf{v}$.[10]

As a result we may extend Eq. (51) for arbitrary b leading to

$$\frac{1}{2}\mathbf{v}\ln[(1+b^2)v_0/v]=\mathbf{U}\left[(1+b^2)\mathbf{Q}+\frac{b}{2}\mathbf{v}\right]. \tag{58}$$

We obtain oblique motion with respect to $\mathbf{Q}$, with the angle depending on b and Q. In the nonlinear Schrödinger equation limit the motion becomes parallel to $\mathbf{Q}$. Concerning the interaction between vortices, we obtain oblique repulsion or attraction: for $b\neq 0$ two vortices never move along the line connecting their centers but instead spiral with respect to each other (Pismen, 1999).

D. Dynamics of spiral waves for $b\neq c$

1. General

As we mentioned above, in the generic case of $b\neq c$ the asymptotic interaction of topological defects (spirals) is very different from the corresponding dynamics of vortices in the GLE and the nonlinear Schrödinger equation. The problem of spiral wave interaction was considered by Biktashev (1989), Rica and Tirapegui (1990, 1991a, 1991b, 1992), Elphick and Meron (1991), Aranson *et al.* (1991a, 1991b, 1993a), and Pismen and Nepomnyashchii (1991a, 1991b). The approach of Rica and Tirapegui (1990, 1991a) and Elphick and Meron (1991) explored a type of global phase approximation that in essence gave a long-range interaction $\sim 1/r$ between the spirals, in analogy to the cases treated above. The results were in obvious disagreement with numerical simulations done by Aranson *et al.* (1991a, 1991b), revealing an exponentially weak interaction between the spirals.

A more adequate solution of the problem was later obtained by Aranson *et al.* (1991a, 1991b) and Pismen and Nepomnyashchii (1991a, 1991b) on the basis of the phase-diffusion equation (see also Biktashev, 1989). The results demonstrated an exponentially weak asymptotic interaction, although they failed to describe the numerically observed bound states of spiral waves. The above-mentioned approach is adequate for the case $|b-c|\ll 1$. Biktashev (1989) considered the very restrictive problem of spiral motion in an almost circular domain. Due to some unphysical boundary conditions, the results of Pismen and Nepomnyashchii (1991a, 1991b) were in conflict with the numerical simulations (Aranson *et al.*, 1993a).

In later papers Rica and Tirapegui (1991b, 1992) attempted to improve their interaction approach by combining it with that of Aranson *et al.* (1991a, 1991b). However, in our view, the results remain unsatisfactory because of an uncontrolled perturbation technique.

A consistent theory with quantitative predictions of asymptotic spiral wave interaction including bound-state formation was presented by Aranson *et al.* (1993a, 1993b) using the matching-perturbation method. The idea of the method is straightforward: in the full solutions for a spiral pair (or a spiral and a wall, or more complicated aggregates of spirals) the spirals move with certain velocities, and thus solutions exist only with the "correct" velocities. Such solutions may be constructed approximately by starting with isolated spirals, each one restricted to the region in space filled by its emitted waves and moving with (small) velocities to be deter-

[10]The calculations can be generalized to arbitrary Q.

mined. For a symmetric spiral pair one simply has two half planes. In a first step the corrections are assumed to be determined to sufficient accuracy by the linearized (perturbational) problem with boundary conditions that take into account the neighboring spiral (or wall, etc.). The velocity comes in as an inhomogeneity. The occurrence of bound states can already be seen from the behavior of stationary perturbations of the asymptotic plane waves emitted by the spirals, as given by Eq. (25). Bounds states occur in the oscillatory regime, outside the curves $(c-b)/(1+bc)=\pm c_{cr}, c_{cr}=0.845$ (one must choose the curves inside the Benjamin-Feir-Newell-stable region). The oscillatory range is plotted in Fig. 12 (curve OR). Also included in Fig. 12 is the convective Eckhaus-stability boundary (curve EI; see Sec. II.D) and the boundary of absolute stability (curve AI; see Sec. II.E) for the waves emitted by the spirals.

The inhomogeneities involve the velocity linearly, and as a consequence the solution for arbitrary (but not too small) distance can be expressed in terms of one inhomogeneous and one homogeneous solution. Once these are determined numerically and used to match the boundary conditions, the velocity versus distance relation comes out. For $b=0$ (for simplicity) the resulting velocities of the spiral at distance X from a plane boundary [or, equivalently, a pair of oppositely charged spirals at the points $(\pm X,0)$] are of the form

$$v_x=\mathrm{Im}\left(\frac{-Q\sqrt{1-Q^2}\exp(-pX)}{\delta C_y\sqrt{2\pi pX}}X^{-\mu}\right)\Big/\ \mathrm{Im}(C_x/C_y),$$

$$v_y=\mathrm{Re}\left(\frac{-Q\sqrt{1-Q^2}\exp(-pX)}{\delta C_y\sqrt{2\pi pX}}X^{-\mu}\right)-v_x\,\mathrm{Re}(C_x/C_y), \tag{59}$$

where Q is the spiral wave number, v_x is the component of the velocity along the line connecting spiral cores (radial velocity), and v_y is the velocity perpendicular to this line (the tangential velocity). The constants C_x and C_y are obtained numerically and the parameter μ is derived from the linearized problem (Aranson *et al.*, 1993a). The bound states correspond to the case of $v_x=0$. The bound state will drift with the velocity v_y. The equilibrium distance $2X_e$ between spirals is found from the equation

$$\mathrm{Im}\left(\frac{-Q\sqrt{1-Q^2}\exp(-pX_e)}{\delta C_y\sqrt{2\pi pX_e}}X_e^{-\mu}\right)=0. \tag{60}$$

Since only p and μ are complex, this gives

$$\mathrm{Im}[pX_e+\mu\ln X_e]=-\phi+\pi l, \tag{61}$$

where $l=1,2,3,\ldots$ and $\phi=-\arg[1/(\delta C_y p^{1/2})]$. Even values of l correspond to stable bound states, odd l to unstable ones. Usually the lowest bound state with $l=2$ is relevant. Approaching the boundary of the oscillatory range, the equilibrium distance diverges.

Generalization to arbitrary b can be done along the lines of the similarity transformation (16). The result is unchanged at leading order.[11]

Note that the symmetries $A(x,y)=A(-x,-y)$ (like charged) and $A(x,y)=A(-x,y)$ (oppositely charged) have nearly the same effect on the boundary conditions at $x=0$ for large spiral separation. Thus for large separation X the interaction of like-charged spirals is similar to the interaction of oppositely charged ones. The only difference is that for the like-charged case both components of the spirals' velocities have the opposite sign, whereas for the oppositely charged case the tangential components have the same sign. This causes the rotation of the spirals around the common center of the symmetry in the like-charged case.

Like-charged spirals may form more complicated bound states or aggregates. In contrast to the two-spiral bound states, which are simply rotating with constant velocity, each spiral in the aggregate performs a more complicated motion (possibly nonperiodic) on the background of a steady-state rotation, perhaps similar to the "dance" of spiral aggregates observed in a variant of the Belousov-Zhabotinsky reaction (Steinbock and Müller, 1993). Certain problems of interaction between spiral waves and hole solutions were considered by Bazhenov and Rabinovich (1993, 1994). The interaction of spirals with external periodic perturbation and response functions of the spiral core were studied by Biktasheva *et al.* (1998, 1999, 2000).

2. Comparison with results of numerical simulations

Bound states of spirals are shown in Fig. 15. In Fig. 16(a) the dependence of the velocities on the spiral separation $2X$ is plotted for $b=0, c=1$ and compared with results from full numerical simulations. There is reasonable agreement, particularly for the radial velocity v_x. The first two zeros of v_x at $2X_e\approx 11.5$ and 22.8 correspond to $l=1,2$ in Eq. (61). Here the velocities are already extremely small. From the simulations no other bound state could be resolved. The equilibrium distance obtained from the theory for the stable bound state [$l=2$ in Eq. (61)] is in very good agreement with the results of the simulations of the full CGLE [see Fig. 16(a)]. There is a discrepancy between the values of the tangential velocity v_y by a factor of about 1.5 [see Fig. 16(b)] although the functional dependencies on c are very similar. This discrepancy results from the fact that the shock is not described well by a linear treatment.

More accurate estimates can be obtained by treating the shock fully nonlinearly. Far away from the core the motion of the spiral can be neglected and one may consider the stationary shock produced by the waves emitted by the spirals. Thus one has to solve the stationary

[11]Note that the additional term $-ib\mathbf{v}\nabla A$ arising in the corresponding equations of motion for each spiral can be absorbed in the nonsingular part of the linear problem (Aranson and Pismen, 2000).

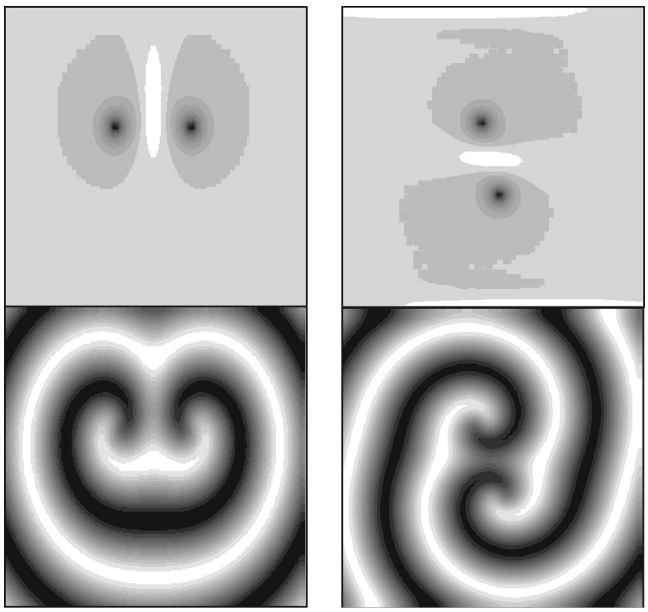

FIG. 15. The bound state of (a) oppositely charged spirals and (b) like-charged spirals for $b=0, c=1.5$ in a 100×100 domain. Images show $|A(x,y)|$ (top) and $\mathrm{Re}\,A(x,y)$ (bottom), respectively.

CGLE with boundary conditions $A\sim r\exp[i\theta]$ for $x\to X$, and $\partial_x A=0$ at $x\to0$. This is a rather complicated 2D problem. Numerically one could extract more accurate values of the constants $C_{1,2n}$, characterizing reflection at the shock [see Fig. 16(b)].

3. Interaction in the monotonic range

In the case $0<c<c_{cr}$ there exist two real positive roots of Eq. (25). Using the analogous numerical procedure one can also determine the constants $C_{x,y}$, but for small c it is technically very difficult in this form. The results can be simplified considerably for the case $c\to0$ and $|cQ|X\gg1$. Then one can neglect the coefficients C_{2n} because for $c\to0$ one has $0<p_1\approx-2cQ\ll1$, $p_2\approx\sqrt{2}$, $\mu_1\to0$, and $\delta_1\to-1/(2Q^2)$. One obtains $v_{x,y}\approx C_{x,y}^{-1}\exp(-2|cQ|X)/\sqrt{X}$, which explicitly exhibits the exponential decay of the interaction and reproduces the earlier analysis using a phase-diffusion equation (Biktashev, 1989; Aranson *et al.*, 1991a, 1991b; Pismen and Nepomnyashchii, 1991a, 1991b).

Numerical simulations for oppositely charged spirals for $b=0$ and $c=0.5$ indicate asymptotic repulsion (Aranson *et al.*, 1993a). This result can be inferred from the work of Biktashev (1989), who used a phase-diffusion equation and asymptotic matching to treat the interaction of spirals with a boundary. It appears to be in conflict with the work of Pismen and Nepomnyashchii (1991a, 1991b) in which matching with the internal solution was done analytically in the limit $c\to0$ and asymptotic attraction was found. The repulsive range is expected to move to larger X roughly as $|cQ|^{-1}$ for smaller c. In this way the crossover to the long-range attraction within the GLE is recovered. The interaction becomes attractive at smaller distances, leading to final annihilation of the spiral pair.

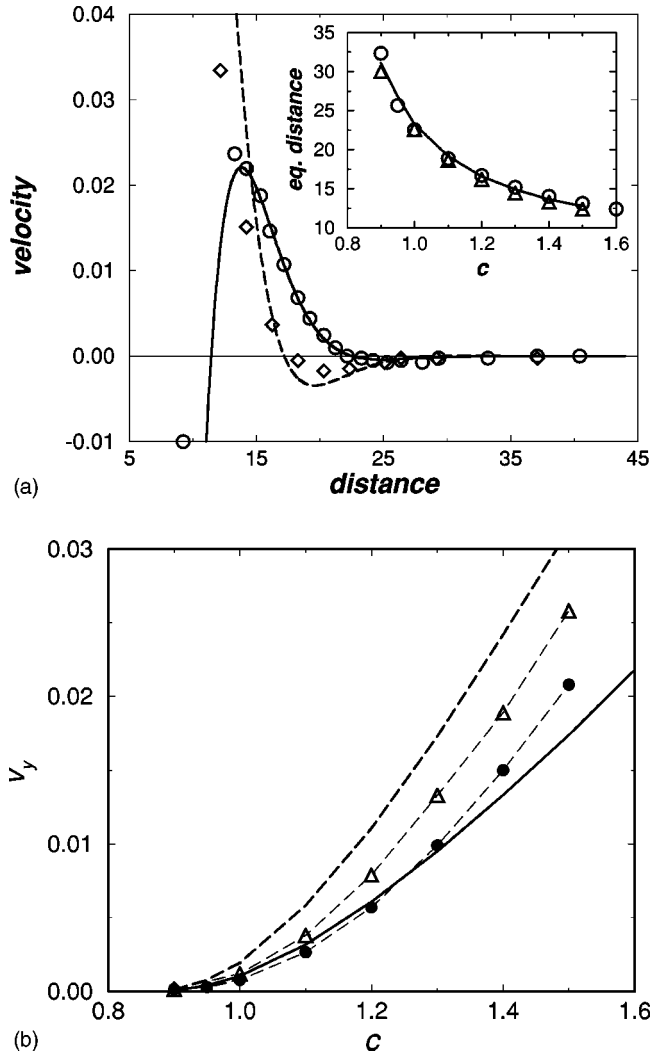

FIG. 16. Dependence of velocities on spiral separation $2X$: (a) Radial velocity (v_x) and tangential velocity (v_y) vs spiral separation $2X$ for $b=0, c=1$ for an oppositely charged pair. Solid and dashed lines show radial and tangential velocities obtained from solution of Eq. (59), respectively. Symbols (○ is radial and ◇ is tangential) for velocities are obtained from the simulations. Inset: Equilibrium distance $2X_e$ (solid line) given by Eq. (61) as a function of c for $b=0$; ○ and △ correspond to numerical results for oppositely charged and like-charged pairs, respectively. (b) Tangential velocity v_y at the equilibrium distance for $b=0$; ● and △ correspond to numerical results for oppositely charged and like-charged pairs, respectively. Solid and dashed lines show theoretical results obtained using nonlinear and linear treatments of the shock.

Like-charged spirals for $c<c_{cr}$ have repulsion at large distances (as in the oppositely charged case) and also at small distances. So it is quite clear that the interaction is repulsive everywhere.

E. Interaction of spirals with an inhomogeneity

Spirals may interact with inhomogeneities of the medium. This problem is particularly interesting in the con-

text of Bose-Einstein condensation as described by the nonlinear Schrödinger equations in a parabolic potential (for a review see Dalfovo *et al.*, 1999). Weak inhomogeneities are sometimes included in the CGLE in the form

$$\partial_t A = [1+\nu(\mathbf{r})]A + (1+ib)\Delta A - (1+ic)|A|^2 A, \quad (62)$$

with an appropriate function $\nu(\mathbf{r})$. An interesting problem is the drift of a spiral in the gradient created by a localized, radially symmetric inhomogeneity (see Staliunas, 1992; Gil *et al.*, 1992). The spiral may be trapped (pinned) by the inhomogeneity or perform a stationary rotation at some distance from it, as observed in optical systems (Arecchi, 1990, 1991; Brambilla *et al.*, 1991).

Using the method described above, one arrives at the following expression for the spiral velocity due to interaction with weak axisymmetric inhomogeneity (Aranson *et al.*, 1995):

$$\mathbf{v} = \mathbf{G}(\mathbf{r}), \quad (63)$$

where r is the distance from the inhomogeneity to the spiral core, v is the spiral core velocity, and the function G is obtained by a convolution of the inhomogeneity profile $\nu(r)$ with the corresponding solution of the linearized CGLE. Equation (63) is the analog to the motion of a "massless particle" in a radially symmetric field. Numerical simulations with the CGLE show that Eq. (63) describes the motion of the spiral fairly well for not too large values of $|b|$ [see Fig. 17(a)].

For large $|b|$ the complex trajectories of the spiral core are not captured by Eq. (63) [see Fig. 17(b)]. In order to describe the numerical simulations one has to include the effective "mass" term in the equation of motion:

$$\frac{d\mathbf{v}}{dt} + \varepsilon \hat{K}\mathbf{v} = \mathbf{G}, \quad (64)$$

where $\hat{K}$ is the friction tensor (or mobility tensor) and $\varepsilon = 1/b$ (see Sec. IV.B.2). Although these features were obtained in the stable range $\mathrm{Re}\,\kappa > 0$ ($\varepsilon > \varepsilon_c$), the external forces created by the inhomogeneity can excite the weakly damped core mode. This can explain the complex motion of the spiral core observed in the presence of obstacles (Sepulchre and Babloyantz, 1993).

Spiral motion in a slowly varying (on the scale of the coherence length) inhomogeneity was considered by Hendrey *et al.* (1999). In this situation additional simplifications are possible. A related problem is the motion of the spiral in the presence of small thermal noise. As was shown by Aranson, Chaté, and Tang (1998), the spiral core has finite mobility and exhibits Brownian motion.

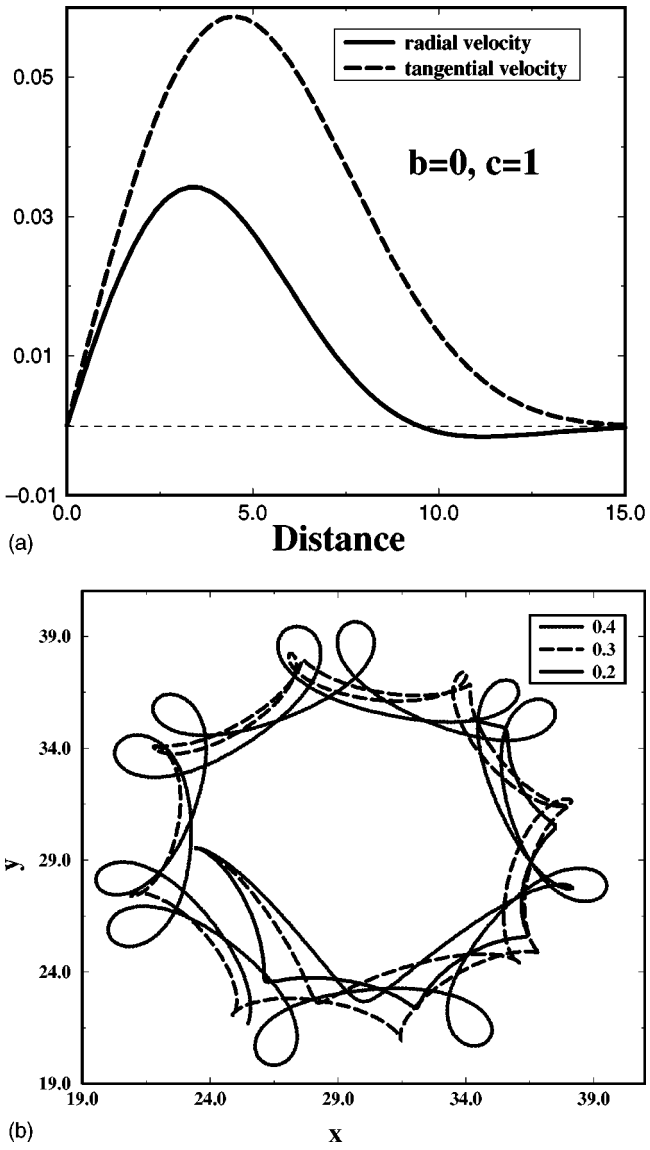

FIG. 17. (a) The tangential and radial velocities of a spiral versus the distance X from the inhomogeneity $\nu(r) = b_0 \exp(-X^2/\sigma)$ for $b=0, c=1$ and $b_0=0.3, \sigma=20$, see Eq. (63). From the numerical solution one finds the radius of the first stationary orbit $r_0 \approx 9.8$. (b) Numerical simulations with the CGLE. The limiting orbits of the spiral core for different values of inhomogeneity strength $b_0 = 0.1, 0.2, 0.3$ in the large-b limit for $\varepsilon = 1/b = 0.2, c=1, \sigma=20$.

F. Symmetry breaking

Symmetric bound states of spirals are not necessarily stable. There is numerical evidence that symmetric bound states, after a sufficiently long evolution, spontaneously break the symmetry such that one spiral begins to dominate, pushing away other spirals (Weber *et al.*, 1991; Weber, 1992; Aranson *et al.*, 1993b). Broken-symmetry states are often produced directly from random initial conditions (Aranson *et al.*, 1993b). To understand the symmetry-breaking instability one must consider the perturbation of the relative phase, or the frequency ω of the waves emitted by each spiral, caused by interaction with the other spiral. Indeed, from analysis of the CGLE it is known that the shock (or sink) where two waves with different frequencies ω_i collide moves in the direction of smaller frequency, due to conservation of phase. This means that after a sufficiently long time only the larger frequency [or equivalently the larger wave number $|Q|$, because of the dispersion relation $\omega = c(1-Q^2) + bQ^2$] dominates in a bounded

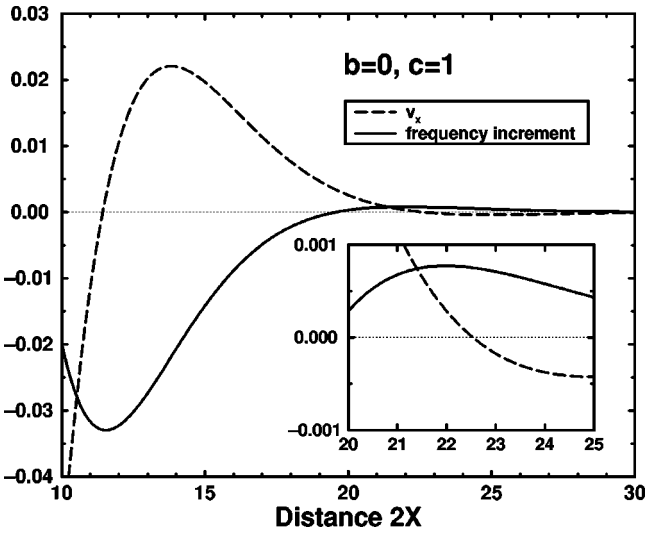

FIG. 18. The dependence of radial velocity (v_x) and the frequency increment $\zeta = d(\partial_t\varphi)/d\varphi$ at $\varphi = 0$ for $b = 0, c = 1$.

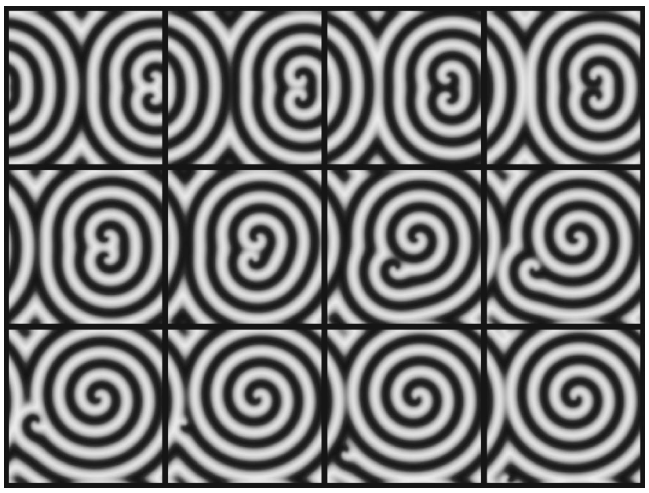

FIG. 19. Evolution of an unlike-charged spiral pair into a stable antisymmetric state, $b = 0, c = 1, L_x = L_y = 100$, time lapse between snapshots $= 50$.

system. The velocity of the motion is given by $v_f \sim (c-b)(Q_1+Q_2) = \frac{1}{2}(v_{g1}+v_{g2})$, where $v_g = d\omega/dQ$ is the group velocity of a plane-wave state. If due to the interaction the frequencies of the spirals become different, one can expect a drastic breaking of the symmetry of the system. This effect appears to be very important for the generic long-time evolution of large systems containing spirals (vortex glass).

The symmetry-breaking instability of spiral pairs can be understood from the dynamics of the relative phase of the spirals $\phi = \phi_1 - \phi_2$. Aranson *et al.* (1993b) derived an equation governing the phase difference between two spirals separated by the distance $2X$:

$$\partial_t\phi = 2\,\mathrm{Im}\left[\frac{-Q\sqrt{1-Q^2}\exp(-pX)}{\delta\sqrt{2\pi pX}}X^{-\mu}C_0^*\sinh\left(\frac{p\phi}{2Q}\right)\right] \Big/ \mathrm{Im}(C_{10}C_0^*) \sim \zeta\phi, \tag{65}$$

where C_{10}, C_0 are the constants obtained from the linearized CGLE. The last term represents the lowest-order term of an expansion in ϕ. The constant ζ determined numerically from Eq. (65) turns out to be positive for the (first) symmetric bound state (see Fig. 18), so that the state is unstable with respect to ϕ. According to Aranson *et al.* (1993b), bound states are unstable with respect to symmetry breaking over the whole oscillatory range. Due to the fact that ζ is very small, the symmetric bound state is rather long lived. As a result of symmetry breaking, only one "free" spiral will remain, whereas the other spiral is pushed away to the boundary. Depending on the boundary conditions, the second spiral will finally either annihilate at the boundary (nonflux boundary conditions, i.e., zero normal derivative on the boundary) or, with periodic boundary conditions, the defect will persist for topological reasons, but reduced to a sink and enslaved in the corner of the shock structure of the free spiral (edge vortex; see Fig. 19). This leads to an asymmetric lattice of topological defects, which appears to be stable in the oscillatory case.

The absence of symmetry breaking in the limit $|c-b| \to 0$ and $|(c-b)Q|X \gg 1$ can be inferred from the paper of Hagan (1982). From this work one finds that decreasing the radius increases the spiral wave number, which ultimately means stability of the shocks. The stability of symmetric states together with the repulsion of the spirals indicates the possible existence of symmetric (antiferromagnetic) lattices of spirals (or "Wigner crystal"), i.e., lattices made up of developed spirals with alternating topological charge. Such lattices were obtained in numerical simulations in this range by Aranson *et al.* (1993b). They appear to exist over the whole nonoscillatory range.[12]

Since for large separation X the properties of like-charged spirals are analogous to those of oppositely charged spirals, one expects the same mechanism of symmetry breaking. Indeed for $|b-c|$ above the critical value such a breaking was observed in numerical simulations.

Certain aspects of spiral pair dynamics were studied numerically by Komineas *et al.* (2001). It was shown that

[12] Aranson *et al.* (1993b) have found stable square lattices in rather small systems and for relatively small numbers of spiral (4×4). There is no guarantee that similar lattices are stable in arbitrarily large systems.

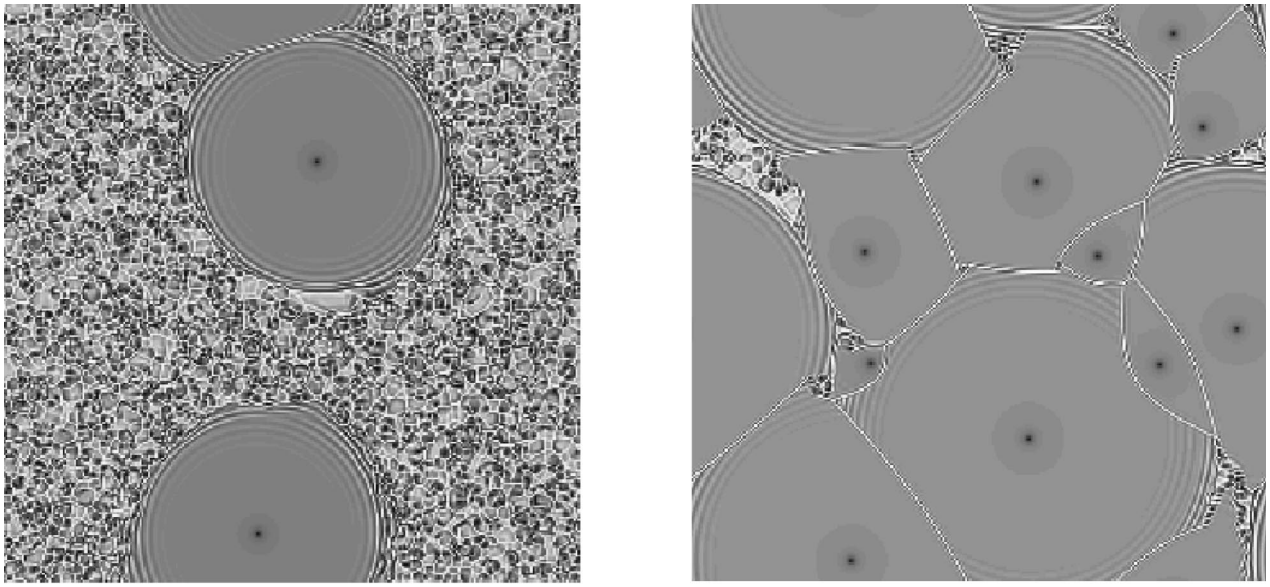

FIG. 20. Vortex glass in the convectively unstable range, 1024×1024 lattice, periodic boundary conditions (Chaté and Manneville, 1996): left side, large spirals nucleating in turbulent sea, $c=0.75, b=-2$ right-side, developed vortex glass for $c=0.7, b=-2$.

for $c>c_{cr}$ (the symmetry-breaking range) the spirals interchange partners and form new pairs. For $c<c_{cr}$ (the monotonic range) symmetric spiral states were found.

G. Vortex glass

A fascinating problem concerns the effect of symmetry breaking on the long-time behavior of large systems that evolve from random initial conditions in the parameter range where one has an oscillatory interaction and spirals. Numerical simulations, carried out by Huber *et al.* (1992) and Chaté and Manneville (1996), have shown a remarkable phenomenon: from an initially strongly turbulent state spirals with a developed far field eventually evolve. The spirals grow until the entire space is filled (see Fig. 20), each spiral occupying a certain domain. The domains have various sizes and typically have a four- or five-sided near-polygon structure. Locally each domain boundary, represented by a shock, is nearly hyperbolic. The shocks often contain "enslaved" or edge vortices. This state appears to persist indefinitely, although sometimes domain boundaries break and edge vortices annihilate. The state was called vortex glass by Huber *et al.* (1992). Some aspects of relaxation to the vortex glass state were considered by Braun and Feudel (1996) and Kevzekidis *et al.* (2002).

The existence of vortex glass is connected with the nonmonotonic dependence of the spiral frequency on the domain size. As can be seen from Fig. 21 the spiral frequency oscillates as the radius of the domain increases and approaches the asymptotic value for $r\to\infty$. (The computations were done for a radially symmetric domain, but we expect the result to be qualitatively correct for domains with arbitrary convex shape.) As a result, one has sets of domain radii r_i corresponding to the same frequency. Neighboring domains can only coexist without (further) symmetry breaking if they correspond to the same spiral frequency. Ultimately one can conceive of a network of fully synchronized domains of various shapes and sizes. These are likely the ingredients necessary to explain the variability in domain sizes observed in a quasistationary vortex glass. The vortex glass is presumably also a global attractor in the full convectively stable oscillatory range.

Bohr *et al.* (1996, 1997) considered the shapes of spiral domains in vortex glass. They found that they differ from Voronoi polygons and obtained the form of the domain boundaries from the condition of phase continuity across the shocks. In particular, far away from the center of an unperturbed spiral, the phase is given by $\phi_i=\pm\theta_i+Qr_i+C_i$, where r_i,θ_i are the polar coordinates measured from the center of the spiral and C_i is the phase constant of the spiral. If one assumes that the distance between two neighboring spirals is much larger

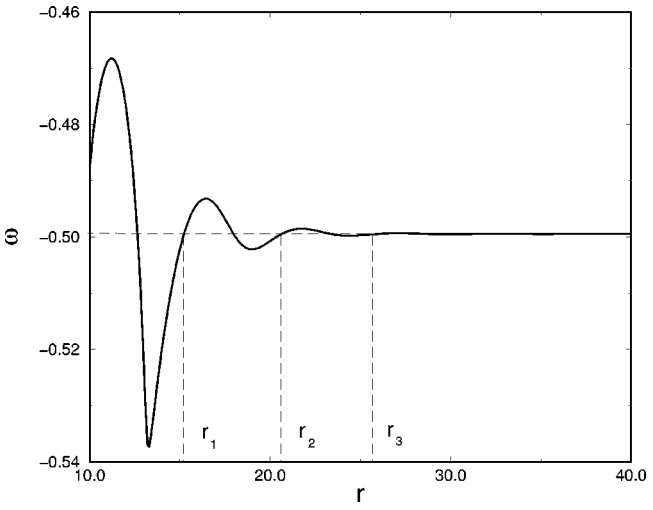

FIG. 21. The spiral's frequency ω as a function of the domain radius for $c=0.8, b=-1$.

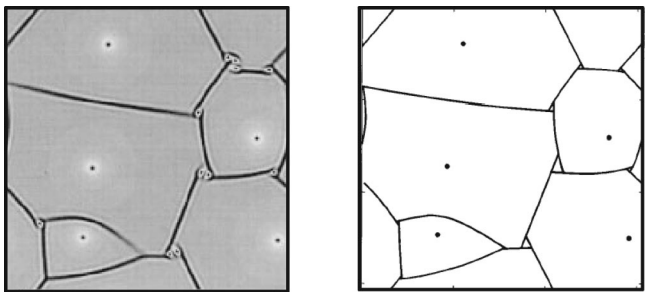

FIG. 22. Close-up of the shock structure (left). Reconstruction of the shock structure using the hyperbolic approximation (right). From Bohr *et al.* (1996).

than the wavelength $2\pi/Q$, one obtains a hyperbola describing the shock shape: $r_i - r_j = (C_j - C_i)/Q$. This simple formula reproduces the structure of the spiral domains with high accuracy (see Fig. 22).

H. Phase and defect turbulence in two dimensions

On a rough scale, two types of turbulent behaviors can be identified in two dimensions: phase and defect turbulence. Defect turbulence is characterized by persistent creation and annihilation of point defects. By contrast, in phase turbulence no defects occur. In a system with periodic boundary conditions the total phase gradient across the system, the *winding number*, is conserved. The simulations of Manneville and Chaté (1996) provide some evidence that phase turbulence breaks down in the infinite size, infinite time limit. However, it could be that the transition is characterized by a sharp bifurcation scenario similar to the situation in one dimension (see III.D.1).

1. Transition lines

The most detailed survey of various regimes occurring in two dimensions is that of Chaté and Manneville (1996) and Manneville and Chaté (1996). According to Chaté and Manneville (1996), the transition from vortex glass to defect turbulence starting from random initial conditions occurs at the numerically determined line T (see Fig. 12). The transition occurs somewhat prior to the absolute instability limit given from the linear stability analysis of plane waves emitted by spirals. However, by starting from carefully prepared initial conditions in the form of large spirals one can approach the absolute instability limit.

Before the line T one finds transient defect turbulence which finally exhibits spontaneous nucleation of spirals from the "turbulent sea." At line T the nucleation time presumably diverges. Before line T the entire space will finally be filled by large spirals separated by shocks, forming a vortex glass state.

As in one dimension, persistent phase turbulence also exists in two dimensions between the Benjamin-Feir-Newell line and the line L (Chaté and Manneville, 1996; Manneville and Chaté, 1996). The range is somewhat smaller than in one dimension. Beyond line L defects are created spontaneously, leading to defect chaos. Actually, in two dimensions, phase turbulence is always metastable with respect to defect turbulence or vortex glass.

2. Spiral breakup

Spiral breakup was observed in experiments on chemical oscillatory media by Ouyang and Flesselles (1996) and Zhou and Ouyang (2000), in simulations of the CGLE by Chaté and Manneville (1996), and in model reaction-diffusion systems by Bär and Or-Guil (1999). The instability likely originates from the outer region of the spiral and thus is expected to occur beyond line T. Quenching a large spiral to this domain will usually trigger a breakup scenario. However, a careful adiabatic procedure allows one, in principle, to avoid breakup and to preserve one large spiral up to the (linear) *absolute instability threshold*. (In the presence of noise, the convective instability actually imposes a maximal noise-dependent radius R_{noise}.) Not too far from the absolute instability limit one is left with a smaller spiral surrounded by strong chaos [Fig. 20(left)] whose well-defined radius R depends neither on system size nor on distance to the boundaries, but vanishes as one approaches the absolute instability threshold.

In the experiments and in some model systems, a spiral need not be introduced initially, as the chaotic phase is only metastable to the spontaneous nucleation of spirals whose radius grows up to R. Thus the asymptotic configuration over a long time scale is actually a quasi-frozen cellular state [Fig. 20(right)].

The above concept of spiral breakup in large systems is in contrast to arguments by Tobias and Knobloch (1998), who stated that spiral wave breakup occurs in the regime of absolute Eckhaus instability via "a globally unstable wall-mode confined to the outer boundary" whose front structure is at the origin of the stable "laminar" spirals immersed in a turbulent sea. Whereas a stationary front can indeed be associated with the absolute stability limit (see Sec. II.E), it can only give an upper limit to the existence of the convectively unstable state.

In the breakup scenario studied by Zhou and Ouyang (2000), spirals emitting modulated waves in the presence of stable meandering of the core were observed. This behavior can be understood in terms of the spatial amplification of periodic perturbations due to core meandering in the regime of convective instability of the background waves (Brusch, Bär, and Torcini, 2001). Although the saturated meandering does not occur in the framework of the CGLE, a properly perturbed CGLE may exhibit both saturated meandering and convective instability (see Aranson, Hochheiser, and Moloney, 1997).

3. Defect statistics

Defect turbulence is the most chaotic state in two dimensions. It is characterized by the exponential decay of correlations, with short correlation lengths and times.

The density of defects varies with b and c. However, it can be argued that, at least in the most studied region with b,c of order one, the defects do not play the role of particlelike excitations. Indeed, the defects in defect turbulence are very different from spiral waves, since they do not emit waves. They behave as passive objects and are merely advected by the surrounding chaotic fluctuations. According to Chaté and Manneville (1996), "amplitude turbulence" is a more appropriate name for such a spatio-temporally chaotic state.

One may argue that the stationary distribution for the number of defects is described by $p(n)\sim\exp[-(n-\overline{n})^2/\overline{n}]$, where $\overline{n}$ is the average number of defects. The formula follows in the limit $n\to\infty$ from treating defect pairs as statistically independent entities (Gil *et al.*, 1990). Note that this assumption is strictly valid only for large domains. Otherwise the statistics are influenced by defects entering/leaving the subsystem. When these processes dominate, the exponent acquires a factor $\frac{1}{2}$.

Egolf (1998) extracted the degrees of freedom associated with defects from those of phase fluctuations by using the concept of a finite-time Lyapunov dimension. He found that each defect "carries" from one to two degrees of freedom. Although one may argue that the number of defects can be a convenient characterization of some types of spatio-temporal chaos, the method of separation does not appear fully convincing because the relation between the finite-time dimension and the number of defects is not examined for different system sizes and duration intervals.

It is interesting to note that a similar analysis performed by Strain and Greenside (1998) for a reaction-diffusion system resulted in a much higher dimension per defect, namely, between 3 and 7.

Mazenko (2001) studied defect statistics in the CGLE in the "defect-coarsening regime," presumably the region of small b and c and mean distance between defects smaller than the screening length $1/(|b-c|Q)$, using an expression for the defect velocity similar to that of Rica and Tirapegui (1990, 1991a), which is not applicable for defects separated by more than the core size of O(1).

4. Core instability and spiral turbulence for large b

One expects that in the full core-unstable range $\varepsilon=1/b<\varepsilon_c$, a state with persistent defects should typically exhibit spatio-temporaly chaos.

In the monotonic range (Fig. 13, above curve OR), this turbulence is characterized by rapid motion of the defects and collisions which often do not result in annihilation, in contrast to the usual defect chaos discussed above. In Fig. 23, the number n of defects as a function of time is shown for a fairly large system (150×150). Apart from the rapid fluctuations due to creation and annihilation there is an extremely slow decrease of n. Crossing ε_c in the monotonic range, the disordered state appears to persist (or is at least very long lived). This indicates a hysteretic behavior, which is to be expected from the subcritical character of the core instability.

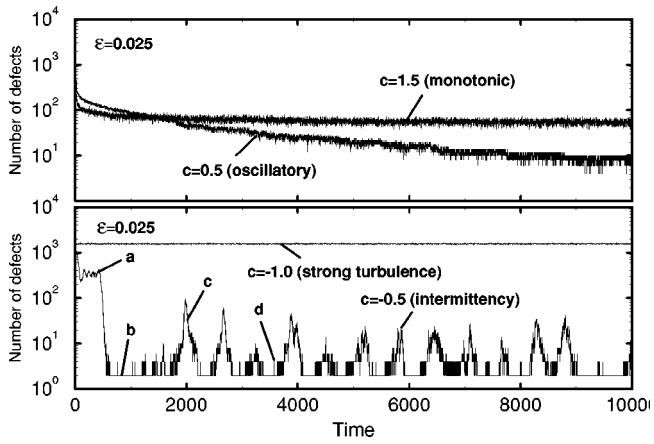

FIG. 23. The number of defects versus time for four different values of c and $\varepsilon=0.025$. Parameters of the simulations are as follows: domain of integration, 150×150; number of Fourier harmonics, 256×256; time step, 0.02.

In the oscillatory Eckhaus-stable range (Fig. 13, below curve OR), the behavior is drastically different. Starting from random initial conditions one first sees evolution towards a vortex glass as in the range $\varepsilon>\varepsilon_c$ (see Fig. 23 and Sec. IV.G; Aranson *et al.* 1993b). However, the spirals are unstable with respect to acceleration, resulting in continued dynamics of the spiral and shocks. Additional spirals are created very rarely. One might call this a "hot vortex glass."

When the Eckhaus instability sets in at the curve EI of Fig. 13, the perturbations produced by the accelerating core of the dominant spiral are amplified away from the core due to the convective character of the instability. When some critical level is exceeded, the state loses stability and many new defects are created throughout the

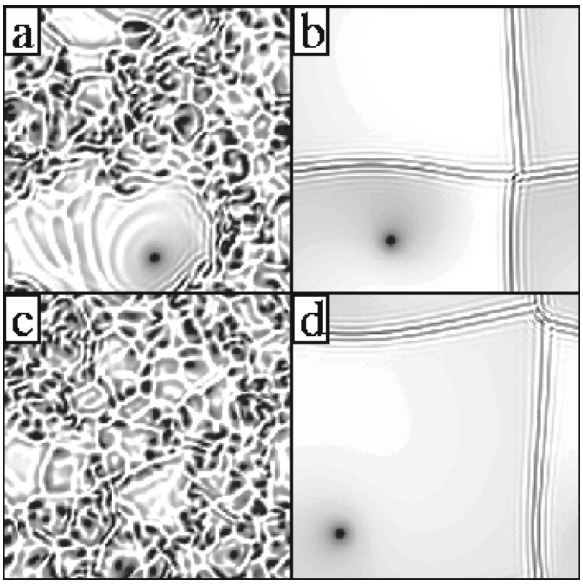

FIG. 24. Snapshots of $|A(x,y)|$ in the intermittency range for four consecutive times [$c=-0.5,\varepsilon=0.025$; black: $|A(x,y)|=0$, white: $|A(x,y)|=1$]. The times corresponding to (a)–(d) are indicated in Fig. 23.

cell. Then the process repeats (Figs. 23 and 24). Such phenomena are very similar to the spatio-temporal intermittency of holes observed in the 1D CGLE (Popp *et al.*, 1993; Chaté *et al.*, 1994; see also Sec. III.D.4) and might be called *defect-mediated intermittency*. In a large cell one expects to have such processes developing independently in different regions of the cell, so one has persistent chaotic bursts (or spots) on the background of growing spirals.

Below the curve ST in Fig. 13, which presumably is the continuation of the T curve in the range $\varepsilon > \varepsilon_c$ (Chaté and Manneville, 1996), the strong chaotic character of the intermittent bursts becomes persistent. The state is similar to the usual defect chaos. The curve ST lies somewhat above the limit of absolute instability, curve AI (see Sec. II.E). For $\varepsilon \to 0$ the AI curve tends to $c \approx -1.2$. The curve was determined by simulating Eq. (46) with the restricted class of functions (45) and boundary conditions $A(0)=0, \partial_r A(L)=0, L \gg 1$, which is effectively a 1D problem. The curve ST determined in this manner is consistent with 2D simulations (Aranson *et al.*, 1994).

V. DYNAMICS IN THREE DIMENSIONS

A. Introduction

The 3D analog of the 2D vortex or spiral wave is called a *vortex filament* or *scroll wave*. The point singularity of the phase of the complex function A at the center of the spiral becomes a line singularity in three dimensions. The filaments can be open (scrolls), closed (vortex loops and rings), knotted, or even interlinked, twisted, or entangled. Depending on the parameters of the CGLE the scroll wave can be stable or can develop some instabilities. Remarkably, 3D vortices can be highly unstable even in the range of parameters where their 2D analog is completely stable.

The CGLE has a stationary solution in the form of a straight vortex with a twist:

$$A(r,\theta,z) = F(r) \exp i[\omega t \pm \theta + \psi(r) + k_z z]. \tag{66}$$

Here the axial wave number k_z characterizes the twist. Curved vortex lines are nonstationary. In most cases vortices untwist, and the solution with $k_z = 0$ is the most stable one.

Scroll waves have been observed experimentally in slime mold (Siegert and Weijer, 1991), heart tissues (Gray and Jalife, 1996), and the gel-immobilized Belousov-Zhabotinskii reaction (Vinson *et al.*, 1997). Long-lived entangled vortex patterns in three-dimensional Belousov-Zhabotinskii reactions were observed by the group of Winfree using optical tomography techniques (Winfree *et al.*, 1995). Complex vortex configurations have also been observed in numerical simulations of reaction-diffusion equations (Winfree, 1995; Aranson and Mitkov, 1998; Biktashev, 1998; Fenton and Karma, 1998a, 1998b; Qu, Xie, and Garfinkel, 1999).

Theoretical investigation of scroll vortices in reaction-diffusion systems was pioneered by Keener and Tyson (1990, 1991) who derived the equation of motion for the filament axis. In particular, it was found that vortex rings typically shrink with a rate proportional to the local curvature of the filament, leading to collapse in finite time. The existence of nonvanishing vortex configurations and the expansion of vortex loops, also observed in numerical simulations of reaction-diffusion equations, was interpreted as "negative line tension" of the vortex filament (Biktashev, 1998).

In order to characterize the motion of vortex lines in three-dimensional space let us consider a curve C at any moment of time t in a parametric form $\mathbf{X}(s,t)$, where s is the arclength. At any point of the curve a local orthogonal coordinate basis can be defined (the Frenet trihedron), yielding the Frenet-Sorret equations (see, for example, Pismen, 1999),

$$\mathbf{X}_s = \mathbf{l}, \quad \mathbf{l}_s = \kappa \mathbf{n}, \quad \mathbf{n}_s = -\kappa \mathbf{l} + \tau \mathbf{b}, \quad \mathbf{b}_s = -\tau \mathbf{n}, \tag{67}$$

where $\mathbf{l}$, $\mathbf{n}$, and $\mathbf{b}$ are tangent, normal, and binormal unit vectors, and κ and τ are the curvature and torsion of the curve, respectively.

B. Vortex line motion in the nonlinear Schrödinger equation

As in two dimensions, the analysis of vortex motion in the 3D nonlinear Schrödinger equation is based on the analogy with the Euler equation for ideal fluids (see Batchelor, 1967; Pismen, 1999). Following the analogy with the vortex lines in an ideal fluid, the local "superfluid velocity" $\mathbf{v} = \nabla \phi, \phi = \arg A$ can be found from the Biot-Savart integral

$$\mathbf{v}(\mathbf{x}) = -\frac{\Gamma}{2} \oint_C \frac{\mathbf{R} \times d\mathbf{l}}{R^3}, \tag{68}$$

where $\oint \nabla \phi = 2\pi\Gamma$, $\Gamma = \pm 1$ is the vorticity of the line, $\mathbf{R} = \mathbf{x} - \mathbf{X}$, and $R = |\mathbf{R}|$. The Biot-Savart integral describes the velocity far away from the vortex line but does not allow one to compute the velocity of the line, since it diverges at the core. In order to get the velocity of the line motion one needs to match the vortex core field with the far field given by the Biot-Savart integral (Pismen and Rubinstein, 1991; Pismen, 1999). As a result of matching one obtains

$$\mathbf{v}_\perp = \mathbf{v}_\mathbf{s} + \Gamma \kappa \mathbf{b} \ln \frac{\lambda}{a_0}, \tag{69}$$

where $\mathbf{v}_\perp$ is the vortex drift velocity in the local normal plane, λ is a constant dependent on the geometry of the vortex, and $a_0 \approx 1.856$ for a single-charged vortex line. For a vortex ring of radius R one has $\lambda = 8R$. The last term expresses the drift along the binormal with the speed proportional to the curvature, and the first term $\mathbf{v}_\mathbf{s}$ accounts for a contribution from the nonlocal induction of the Biot-Savart integral. Neglecting the first term, one recovers the localized induction approximation, often used in hydrodynamics (for a review see Ricca, 1996).

The localized induction approximation is in fact a rather crude approximation of vortex motion in the nonlinear Schrödinger equation. It has been extensively used due to its mathematical elegance.

In the simplest case of a vortex ring of radius R, one finds from Eq. (69) that the ring drifts as a whole along the binormal, i.e., along the axis of symmetry, with the speed given by (Pismen, 1999)

$$v=\frac{1}{R}\ln(R/R_0), \tag{70}$$

where $R_0\approx 0.232$ is the constant obtained from matching with the vortex core. Clearly, a similar result can be obtained for classical vortices in an ideal fluid, with the difference that in the latter there is no well-defined core.

C. Collapse of vortex rings in the complex Ginzburg-Landau equation

In the GLE one finds that a vortex ring with radius R collapses. Indeed, substituting the ansatz

$$A(r,\theta,z,t)=A_0\left(r-\int_0^t v(t')dt',z\right) \tag{71}$$

(A_0 is the 2D stationary vortex solution; r, θ, and z are cylindrical coordinates) into the 3D GLE one derives

$$-v\,\partial_r A_0=A_0(1-|A_0|^2)+\partial_r^2 A_0+\partial_z^2 A_0+\frac{1}{r}\partial_r A_0. \tag{72}$$

Replacing the explicit r dependence in the last term by the radius of the ring, one obtains from the consistency condition that

$$v=\frac{dR}{dt}=-\frac{1}{R}. \tag{73}$$

Solving Eq. (73), one derives $R(t)=\sqrt{R_0^2-2t}$, i.e., the ring collapses in finite time. Surprisingly, in the case of the GLE the analog of the localized induction approximation produces the correct answer.

Gabbay *et al.* (1997, 1998a) generalized this result for the CGLE where the ansatz Eq. (71) has to be generalized to include the curvature-induced shift of the filament wave number. They showed that the ring collapses in finite time according to the evolution law

$$\frac{dR}{dt}=-\frac{1+b^2}{R}. \tag{74}$$

In addition, there is no overall drift (at least, at first order in $1/R$) of the vortex ring in the direction perpendicular to the motion of collapse. The collapse rate (often associated with the line tension) $\nu=1+b^2$ appears to be in reasonable agreement with simulations for not too large $|b|$. This corrects a previous erroneous estimate $\nu=1+bc$ (Frisch and Rica, 1992).

For the evolution of the local twist of a straight vortex one obtains the Burgers equation (Gabbay, Ott, and Guzdar, 1997, 1998b; Nam *et al.*, 1998)

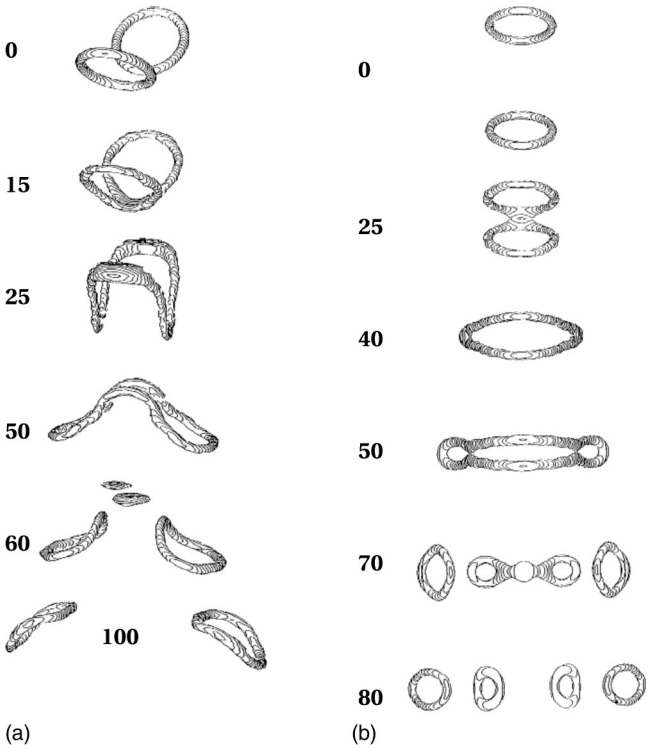

FIG. 25. Dynamics of vortex rings in the nonlinear Schrödinger equation: (a) in-plane collision of two rings at 90° incidence, seen from the side; (b) in-plane collision of two rings at 120° incidence, seen from above. From Koplik and Levine (1996).

$$\partial_t\phi=(b-c)(1-k_0^2)(\partial_z\phi_z)^2+[1+bc+(b-c)bk_0^2]\partial_{zz}\phi, \tag{75}$$

where $\partial_z\phi=k_z$ and k_0 is the asymptotic wave number of the 2D spiral solution. A more complicated equation was obtained for a twisted and curved vortex filament.

D. Vortex nucleation and reconnection

Vortex reconnection in nonlinear Schrödinger equation was studied in relation to turbulence in superfluid liquid helium. Large-scale computations were performed by Schwarz (1988) using the localized induction approximation. These computations give an impressive picture of vortex tangles. However, it remains unclear whether the particular features of the tangle are real or an artifact of the localized induction approximation.

Obviously, vortex reconnection must be described by the full nonlinear Schrödinger equation. Koplik and Levine (1993, 1996) find in full numerical simulations of the nonlinear Schrödinger equation that vortices reconnect when they approach to within a few core lengths. Depending on conditions, the vortex rings may subsequently scatter, merge, or break up (see Fig. 25).

Gabbay *et al.* (1998b) studied vortex reconnection in the CGLE. As a result of the interplay between two effects—motion of the filaments towards each other due to attraction (two-dimensional effect) and opposite mo-

tion due to curvature (three-dimensional effect)—a criterion for vortex reconnection was proposed.

In the GLE vortex rings ultimately shrink. However, with an additional phase gradient j parallel to the ring axis (e.g., due to rotation of a superfluid or supercurrent in superconductors) the vortex rings may expand. The additional force is the analog of the Peach-Koehler force on a 2D vortex in a background wave number $Q=j$. In this situation one has the following equation for the ring radius R:

$$\frac{dR}{dt}=-\frac{1}{R}+\sigma j, \tag{76}$$

where $\sigma\approx 2/\ln(v_0/2j)$ [see Eq. (51)]. Thus if $R>1/(\sigma j)$ the vortex ring will expand.

Expanding vortex rings in the GLE were obtained in simulations as a result of nucleation after a rapid thermal quench by Aranson, Kopnin, and Vinokur (1999). This problem was considered by Ruutu *et al.* (1996, 1998) in the context of experiments in superfluid liquid ^{3}He heated well above the transition temperature by absorption of neutrons. This experiment was designed to verify a fluctuation-dominated mechanism for the formation of topological defects in the early Universe, as suggested by Kibble (1976) and Zurek (1985) and elaborated in later work by Dziarmaga *et al.* (1999), and Antunes *et al.* (1999) mostly in one and two dimensions.

Selected results are shown in Fig. 26. One can see [Figs. 26(a)–(c)] that without fluctuations the vortex rings nucleate upon passage of the thermal front. Not all of the rings survive; the small ones collapse and only the big ones grow. Although the vortex lines are centered around the point of the quench, they exhibit a certain degree of entanglement. After a long transient period, most of the vortex rings reconnect and form an almost axisymmetric configuration.

It turns out that fluctuations have a strong effect at early stages: the vortices nucleate not only at the normal-superfluid interface, but also in the bulk of the supercooled region [Figs. 26(d) and (e)]. However, small vortex rings in the interior later collapse and only larger rings (primary vortices) survive and expand [Fig. 26(f)].

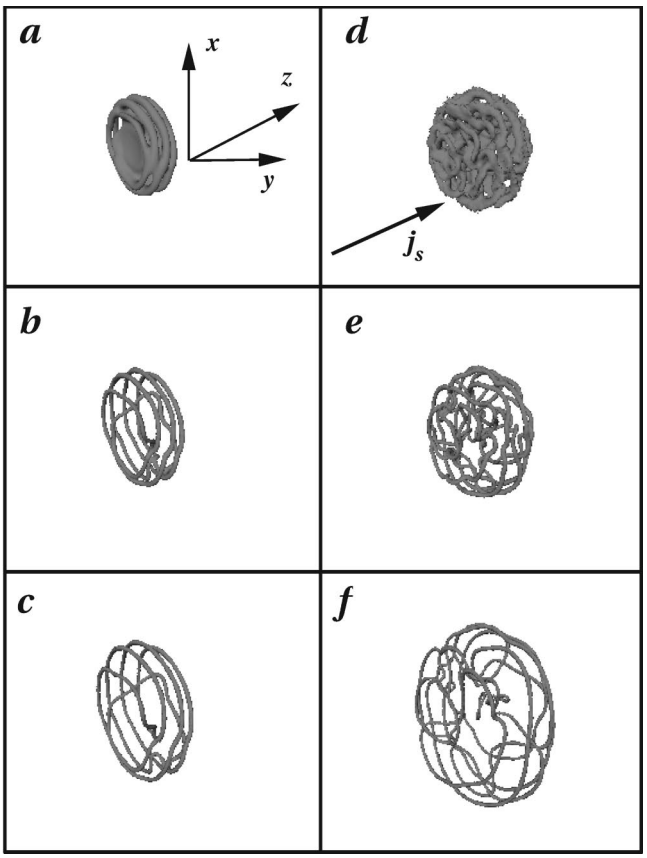

FIG. 26. Nucleation and expansion of vortices in the GLE with background $k=0.4$. The supercurrent j_s is given by $j_s=k(1-k^2)$. Shown are the 3D isosurfaces f $|A|=0.4$: (a)–(c) no thermal fluctuations, images are taken at times $t=36,48,80$; (d)–(f) amplitude of thermal fluctuations $T_f=0.002$,$t=24,48,80$. From Aranson, Kopnin, and Vinokur (1999).

E. Instability of weakly curved filaments in the large-*b* limit

Aranson and Bishop (1997) and Aranson, Bishop, and Kramer (1998) have shown that the simple relation for the collapse rate Eq. (74) is violated in the large-b limit, $b=1/\epsilon\gg 1$. As a result of an asymptotic expansion for $\epsilon\ll 1$ the equation of motion of the filament takes the form

$$\partial_t \mathbf{v}+\hat{K}[\epsilon\mathbf{v}-\kappa\mathbf{n}]=\mathbf{0}, \tag{77}$$

where $\mathbf{v}$ is the velocity of the filament and κ is the local curvature. The 2×2 matrix $\hat{K}$ corresponds to the "friction" matrix of 2D spiral waves (see Sec. IV.B.2).

Note that by dropping the acceleration term in Eq. (77) one recovers the result of Eq. (74) for $b\to\infty$, since for the ring $v_N=\partial_t R, \kappa=-1/R$. Restoring the original scaling $r\to r/\sqrt{b}$, one obtains $\partial_t R=-b^2/R$. However, since in three dimensions the local velocity in general varies along the vortex line, even a small acceleration may cause severe instability, because the local curvature becomes very large. Moreover, deviation of the local velocity from the direction of the normal will lead to stretching and bending of the vortex line. Thus the acceleration term, which formally can be considered as a higher-order correction to the equation of motion, plays a pivotal role in the dynamics of a vortex filament.

1. Perturbation around a straight vortex

An almost straight vortex parallel to the z axis can be parametrized by the position along the z coordinate: $[X_0(z),Y_0(z)]$. Since in this limit the arclength s is close to z, the curvature correction to the velocity $\kappa\mathbf{n}$ is simply $\kappa\mathbf{n}=(\partial_z^2 X_0,\partial_z^2 Y_0)=\partial_z^2\mathbf{r}$, where $\mathbf{r}=(X_0,Y_0)$. Using $\partial_t\mathbf{r}=\mathbf{v}$, Eq. (77) reduces to a linear equation,

$$\partial_t\mathbf{v}+\hat{K}[\epsilon\mathbf{v}-\partial_z^2\mathbf{r}]=0. \tag{78}$$

The solution can be written in the form $\mathbf{r}\sim\exp[ikz+\lambda(k)t]$, where λ is the growth rate. We immediately obtain the following relation for λ:

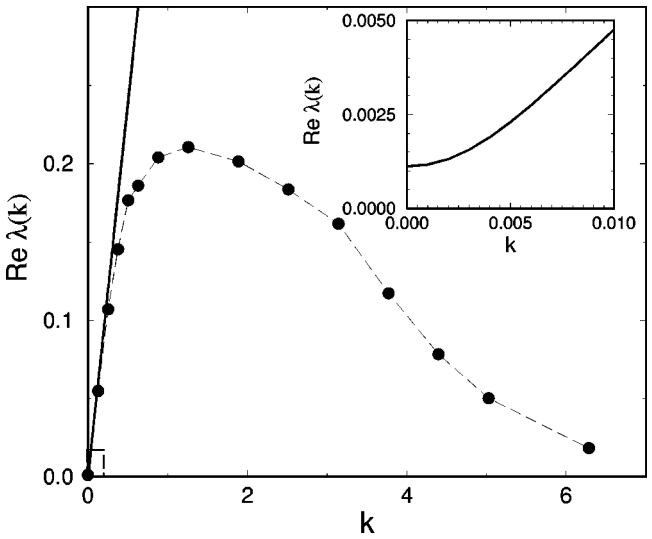

FIG. 27. The growth rate $\mathrm{Re}\,\lambda(k)$ as a function of k for $\epsilon=0.02, c=0.1$: solid line; theoretical result for $k \ll 1$; dashed line, result of numerical solution of 3D CGLE; inset, blowup of the small-k region. From Aranson and Bishop (1997).

$$\lambda^2+\chi(\epsilon\lambda+k^2)=0, \tag{79}$$

where $\chi=K_{xx}\pm iK_{xy}$ is the complex friction (compare Sec. IV.B.2). One may consider two cases: $k \ll \epsilon$ and $k \gg \epsilon$. For $k \ll \epsilon$, from Eq. (79) one obtains $\lambda=-\epsilon\chi+O(k^2)$, i.e., recovers the core instability of the 2D spiral. For $k \gg \epsilon$ one derives $\lambda \approx \pm\sqrt{-(K_{xx}\pm iK_{xy})}k$. There always exists a root with a large positive real part: $\lambda \sim k \gg \epsilon$. Therefore, for finite k, the growth rate $\lambda(k)$ may significantly exceed the growth rate of the acceleration instability in two dimensions (corresponding to $k=0$): $\mathrm{Re}\,\lambda=-\epsilon K_{xx}$. Hence the small-curvature approximation considered above can be valid only for finite time. The falloff of the growth rate λ at large k is not captured by the small-curvature approximation used here.

2. Numerical results

The theoretical results are compared with numerical simulations in Fig. 27. As an initial condition, a straight vortex line with small periodic modulation along the z axis was taken. As the figure shows, the growth rate indeed increases initially with k and then falls off for large k. The theoretical expression (79) shows reasonable agreement with the simulations for small enough k. The growth rate at the optimal wave number exceeds the corresponding growth rate of the acceleration instability ($k=0$) by more than two orders of magnitude.

The long-time evolution of a perturbed straight vortex is shown in Fig. 28. As can be seen from the figure, the length of the vortex line grows. The dynamics seems to be vary rapidly in time, and the line intersects itself many times, forming numerous vortex loops. The long-time dynamics shows, however, a saturation when a highly entangled vortex state is developed and the total length of the line cannot grow further due to a repulsive interaction between closely packed line segments. The

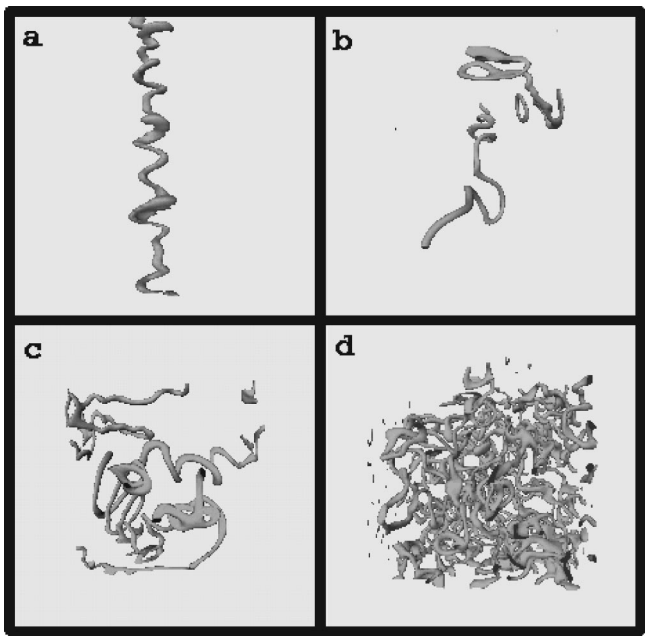

FIG. 28. Instability of a straight vortex filament. 3D isosurfaces of $|A(x,y,z)|=0.1$ for $\epsilon=0.02, c=-0.03$, shown at four times: (a) 50, (b) 150, (c) 250, (d) 500. A similar dynamics is also observed for a larger value of ϵ. From Aranson and Bishop (1997).

dependence of the line length on time is shown in Fig. 29. Two distinct stages of the dynamics can be identified, rapid growth of the length; second, oscillations of the line's length around some mean value.

For small enough ϵ, two distinct behaviors of the total vortex length depending on the value of c are observed. Above a critical value c_c corresponding approximately to the convective instability range of the 2D spiral ($c_c \to 0$ for $\epsilon \to 0$), the total length approaches some equilibrium value and does not exhibit significant fluctuations. In contrast, for $c<c_c$, the total length exhibits large

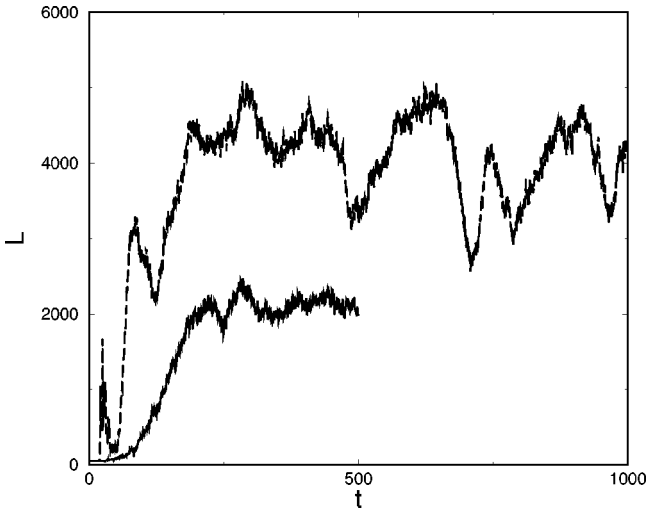

FIG. 29. The dependence of filament length L on time: solid line, $\epsilon=0.02, c=-0.03$; dashed line; $\epsilon=0.02, c=-0.5$.

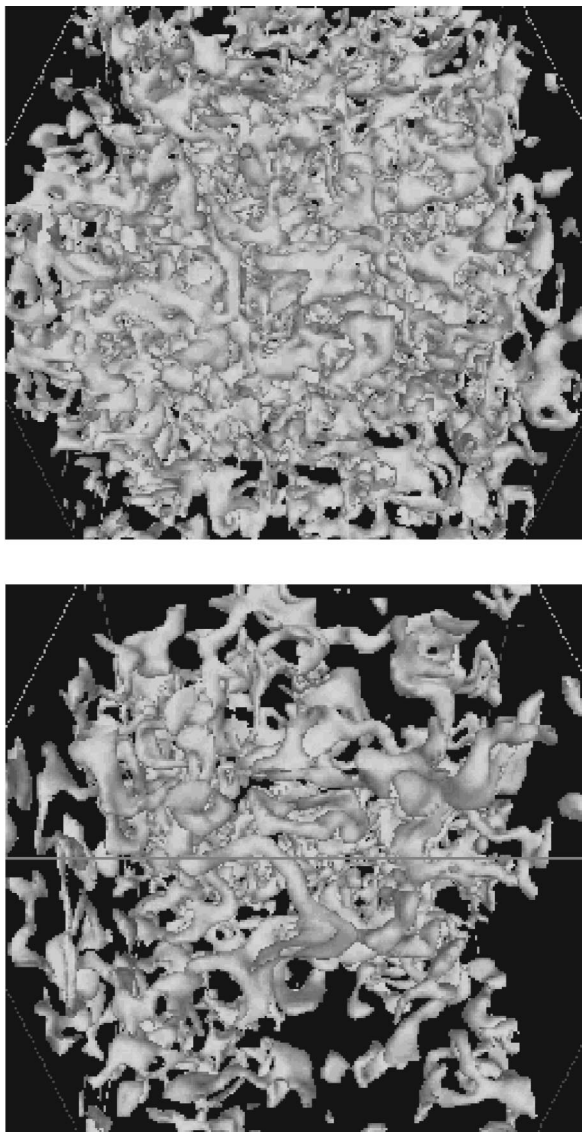

FIG. 30. Two snapshots of 3D isosurfaces of $|A|$ taken in the regime of spatio-temporal intermittency, $\epsilon=0.02, c=-0.5$: (a) $t\approx 620$ for Fig. 29; (b) $t\approx 740$. From Aranson, Bishop, and Kramer (1998).

nondecaying intermittent fluctuations around the mean value. Figure 30 presents snapshots illustrating the structure of the vortex field corresponding to maximum and minimum moments of the length. One can see that in this situation some segments of the vortex lines start to expand spontaneously, pushing away other vortex filaments and creating substantial vortex-free holes around them. The instability then takes over and destroys these almost-straight segments of filament, bringing the system back to a highly chaotic state. This dynamics can be considered a 3D spatio-temporal vortex intermittency, which is an extension of the spiral intermittency discussed in Sec. IV.H.4. For even smaller values, $c<-1$, one has the transition to a highly chaotic state, which is an analog of defect turbulence in the 2D CGLE. In this regime small vortex loops nucleate and annihilate spontaneously.

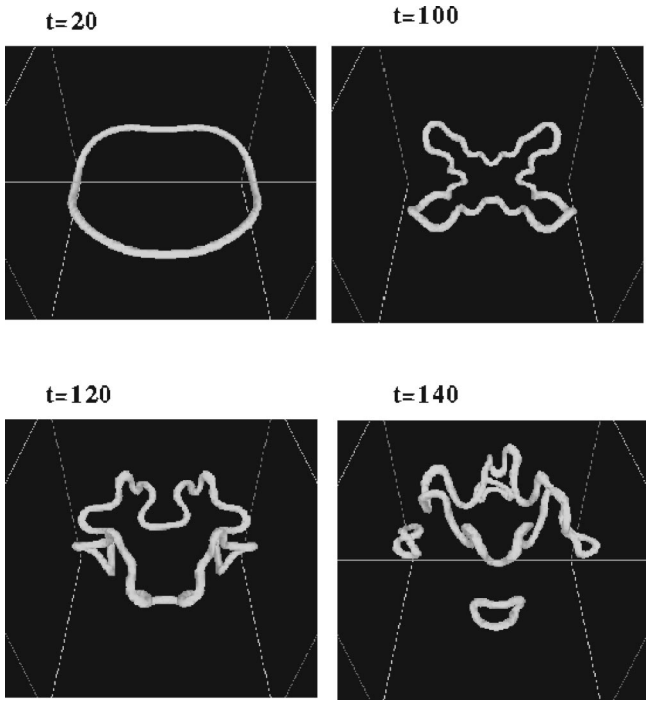

FIG. 31. Sequence of snapshots demonstrating the evolution of a vortex ring for $\epsilon=0.2$ and $c=0.2$.

The evolution of a closed vortex loop is shown in Fig. 31. The simulations show that the 3D instability may prevent the ring from collapse, causing stretching of the loop in the direction transvere to the motion of collapse. However, small rings typically collapse, since the instability described above does not have time to develop substantial distortions of the ring. Even in this situation the ring exhibits a few oscillations of the radius.

3. Limits of three-dimensional instability

The previous analysis indicates instability of vortex lines in the limit $\epsilon\to 0$ for all c. However, it cannot describe the boundary of the instability for increasing ϵ. In order to obtain the stability limit one needs to perform a full linear stability analysis of a straight vortex solution, not limited to small k and ϵ (Aranson, Bishop, and Kramer, 1998). The linear stability analysis shows that the 3D instability persists substantially beyond the 2D core instability. The results are shown in Fig. 32. Moreover, the typical growth rate in 3D is much higher than in 2D.

F. Helices, twisted vortices, and supercoiling instability

Close to the stability boundary of the 3D instability, the evolution of a straight vortex does not necessarily result in spatio-temporal chaos. In contrast, the simulations show that the instability saturates, resulting in a traveling-helix solution (Aranson, Bishop, and Kramer, 1998) or a superposition of two helices with opposite chirality (zigzag) (Rousseau *et al.*, 1998). Indeed, since the left and right rotating unstable modes of a straight vortex have the same growth rate, the resulting configu-

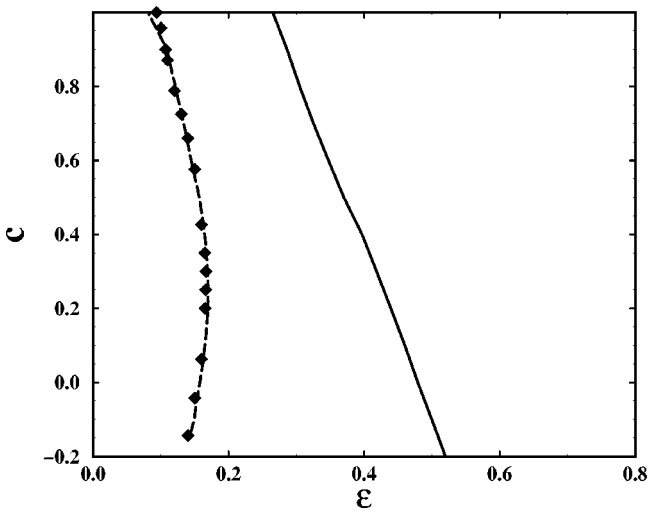

FIG. 32. Stability limits in three dimensions (solid line) and two dimensions (dashed line), obtained from linear stability analysis: ♦, limit of the two-dimensional instability, obtained by direct numerical simulation of the CGLE (Aranson, Kramer, and Weber, 1994). Vortex lines and two-dimensional spirals are stable to the right of the respective lines.

ration is determined by the cross-coupling coefficient between these modes, which is a function of the parameters b,c.

The symmetry between left and right rotating helices can be broken by applying an additional twist to the straight filament. Studies of twisted filaments were performed by Rousseau *et al.* (1998) and Nam *et al.* (1998). The simulations revealed stable helices and a secondary supercoiling instability.

Nam *et al.* (1998) performed linear stability analysis of a straight filament with twist. It was shown that the twist reduces the domain of stability for the straight filament.

The question arising in this context is how to prepare a vortex with twist. One way to proceed is to create an inhomogeneity close to the axis of the vortex filament. The inhomogeneity will locally change the frequency of the vortex and will result in persistent twist. This situation was realized experimentally in a reaction-diffusion system by Mironov *et al.* (1996).

VI. GENERALIZATIONS OF THE COMPLEX GINZBURG-LANDAU EQUATION

The CGLE is a minimal, universal model that cannot be further simplified. However, there are many ways to generalize it in order to include qualitatively new features (we are not concerned with additional terms that merely give quantitative corrections). The main trends of generalization can be associated with the different terms of the CGLE:

- generalization of the nonlinearity,
- generalization of the differential operator,
- generalization of the symmetry group.

A. Subcritical complex Ginzburg-Landau equation

1. Small-amplitude solutions in the weakly nonlinear case

In this subsection we consider the CGLE with a destabilizing nonlinearity,

$$\partial_t A = A + (1+ib)\Delta A - (-1+ic)|A|^2 A. \tag{80}$$

The CGLE was first derived in this form for a physical system by Stewartson and Stuart (1971) in the context of plane Poiseuille flow, where one has a (strongly) subcritical bifurcation.

Spatially homogeneous solutions of Eq. (80) with $A(t=0)=A_0$ diverge at finite time according the expression

$$|A| = \frac{|A_0|e^t}{[1+|A_0|^2(1-e^{2t})]^{1/2}}. \tag{81}$$

Also, for $c\neq 0$ the rate of phase winding diverges. When $|A|$ is a function of x, however, its behavior is more subtle.

At first sight one expects a blowup of the solutions, which can be avoided by adding a fifth-order stabilizing term. It was suggested by Hocking and Stewartson (1972) and Hocking *et al.* (1972) that for generic initial conditions the blowup does not occur in a considerable region of the parameter space (b,c). By considering the evolution of pulselike solutions, the region in the (b,c) plane was found where the solution remains bounded. Since $|c|$, which is the ratio of nonlinear dispersion over nonlinear growth, has to be sufficiently large, this may be called the weakly subcritical case.

These results were then apparently forgotten and were addressed again (independently) by Bretherton and Spiegel (1983) (in the limit $c\to\infty$) and by Schöpf and Kramer (1991). They reproduced many of the results of Hocking and Stewartson (1972) and found stable periodic solutions of Eq. (80). The analytic work was supported by detailed simulations. The work was continued by Powell and Jakobsen (1993), Kaplan *et al.* (1994a, 1994b), Kramer *et al.* (1995), and Popp *et al.* (1998). Weakly subcritical Hopf bifurcations are found in convection in binary fluids (see Heinrichs *et al.*, 1987; Moses *et al.*, 1987; Kolodner *et al.*, 1988, 1995, 1999) and presumably in nonlinear optics (Powell and Jakobsen, 1993; Kramer *et al.*, 1995).

Hocking and Stewartson (1972), Bretherton and Spiegel (1983), and Schöpf and Kramer (1991) have found bursts of two types depending on the relative signs of b,c (by analogy with the nonlinear Schrödinger equation the case of $bc\geqslant 0$ will be called the focusing case and the others called defocusing).

Kaplan *et al.* (1994a, 1994b) and Kramer *et al.* (1995) proposed a simple physical mechanism, called the *phase gradient mechanism*, which arrests collapse in Eq. (80) if $|c|$ is sufficiently large and $|b|$ is not too large. The phase-gradient effect manifests itself as a fast differential phase rotation resulting from an explosive burst amplitude increase. To understand this effect it is convenient to rewrite Eq. (80) in the variables $A=\sqrt{R}\exp[i\theta]$ [see Eqs. (10)]. For the sake of simplicity

let us consider the limit $b \ll 1$. Introducing the local wave number $k = \partial_x \theta$, we find that Eqs. (10) reduce to

$$\partial_t R = (1+R^2)R + \partial_x^2 R - k^2 R,$$
$$\partial_t k = c\,\partial_x R^2 + \partial_x \left(\frac{\partial_x (R^2 k)}{R^2} \right). \quad (82)$$

From the second equation one sees that a gradient in R drives the growth of $|k|$, which in turn saturates R via the last term in the first equation. If $|c|$ is sufficiently large, this effect overcomes the explosive growth manifest in the first term on the right-hand side of the first equation. Specifically, consider an initial pulse having a small, broad, constant plateau and decaying away at the edges. Let $k=0$ initially. At the linear stage of the instability and then in the subsequent blowup regime, the amplitude will remain approximately constant inside the plateau region. At the boundaries sharp gradients of R will be formed. These gradients will act as sources for the generation of the phase gradient, i.e., k, in narrow regions. There the large value of k will saturate the blowup. The net result will be two counterpropagating fronts representing the moving plateau boundaries. The front propagation speed will not be constant but it will grow at the blowup stage. Thus, if $|c|$ is sufficiently large, the pulse will be "eaten" by these fronts moving from the edges to the center.

2. Strongly subcritical case

The solutions considered above bifurcate from the trivial state supercritically (in the range of b,c where they remain bounded), in spite of the fact that the sign of the real part of the nonlinear term signals a subcritical bifurcation. Thus in that parameter range, but below threshold, the trivial state is the global attractor. The scenario is not changed qualitatively by the addition of stabilizing higher-order terms. Outside this parameter range one needs (at least) quintic terms to saturate the explosive instability provided by the cubic term. The equation can be written in the form

$$\partial_t A = \epsilon A + (1+ib)\Delta A - (-1+ic)|A|^2 A - (1+id)|A|^4 A. \quad (83)$$

The finite-amplitude solutions persist stably with respect to amplitude fluctuations below threshold $\epsilon < 0$ in a certain parameter range, where they coexist with the linearly stable trivial solution. There exist moving fronts and—surprisingly—stable localized pulses over a finite interval of parameters (Thual and Fauve, 1988). This clearly is a result of the nonvariational nature of Eq. (83). A study of the existence, stability, and selection of various solutions is given by van Saarloos and Hohenberg (1992). Localized perturbations around the trivial state can either decay (small ϵ), evolve into pulses (intermediate $\epsilon < 0$), or develop into fronts that invade a plane-wave state. In certain cases their velocity is selected by a nonlinear marginal stability criterion below some positive value of ϵ and by linear marginal stability, as in the supercritical cubic CGLE, for larger ϵ. In a parameter range with sufficiently small nonlinear dispersion there exists a class of fronts that can be expressed in the form (polynomial fronts)

$$k = k_N + e_0 (R^2 - R_N^2), \quad R' = e_1 R (R^2 - R_N^2). \quad (84)$$

Very recently steady fronts that cannot be expressed in this form have been found (Coullet and Kramer, 2001). They exist in particular in a parameter range where there are no polynomial fronts. Whereas the polynomial fronts are sources in their rest frame, the new fronts are sinks. They move in a direction that generates the trivial state even for positive values of ϵ, which can be understood from the phase-gradient mechanism discussed above. They play a significant role in the dynamics of spatio-temporal chaotic states and in the formation of localized structures.

Deissler and Brand (1994, 1995) and Akhmediev *et al.* (2001) have studied periodic, quasiperiodic, and chaotic pulses of Eq. (83) and its generalization. The interaction of these solutions in the framework of two coupled equations [Eq. (83)] shows that the result depends sensitively on the initial conditions. Convective and absolute instabilities in the subcritical CGLE are investigated by Colet *et al.* (1999).

Deissler and Brand (1991) found in two dimensions localized particlelike solutions of Eq. (83). Moreover, one expects localized solutions possessing a topological charge coexisting with extended (conventional) spirals known for CGLE (Malomed and Rudenko, 1988). Recently the properties of spiral waves and other localized solutions in the cubic-quintic CGLE were studied by Crasovan *et al.* (2001).

B. Complex Swift-Hohenberg equation

The complex Swift-Hohenberg equation in the form

$$\partial_t A = rA - (1+ic)|A|^2 A + ia\Delta A - (\Omega + \Delta)^2 A, \quad (85)$$

where $r \ll 1$ is the control parameter and a characterizes the diffraction properties of the active media, was derived asymptotically in the context of large-aperture lasers (class A and B) with small detuning Ω between the atomic and cavity frequencies (see Staliunas, 1993; Lega, Moloney, and Newell, 1994, 1995). This equation is also believed to be relevant for oscillatory convection in binary fluids; however, it cannot be derived asymptotically from appropriate Navier-Stokes equations. Equation (85) is a generic equation in the vicinity of a codimension-2 bifurcation where the coefficient in front of the diffusive term is allowed to change sign (see, for example, Coullet and Repaux, 1987).

Clearly one should distinguish between the real Swift-Hohenberg equation (see, for example, Cross and Hohenberg, 1993) and Eq. (85). The Swift-Hohenberg equation is a phenomenological model and cannot be

rigorously derived from the original equations.[13] In contrast, the complex Swift-Hohenberg equation in the form of Eq. (85) is derived asymptotically and is rigorous in the limit of $\Omega \to 0$, i.e., in the long-wavelength limit. In this limit the differential nonlinearities have formally higher order and therefore can be dropped. In this case the wave-number-selecting term $(\Omega+\Delta)^2 A$ is just a small correction to the diffraction term $ia\Delta A$. Thus the complex Swift-Hohenberg equation can be treated as a perturbed CGLE. In contrast to the real Swift-Hohenberg equation, Eq. (85) has two independent wave-number selection mechanisms: the first is related to the $(\Omega+\Delta)^2$ term, providing maximal amplification for the plane wave $\exp[i(\omega t+kx)]$ with the optimal wave number $k=\sqrt{\Omega}$; the second mechanism is related to the selection of wave number by topological defects (e.g., spirals, holes) in the CGLE and relies on the diffraction $ia\Delta A$. For this case the last term in Eq. (85) slightly changes the wave number selected by the defects (Aranson, Hochheiser, and Moloney, 1997).

The stability of plane waves in Eq. (85) was studied in detail by Lega *et al.* (1994). A new feature is the zigzag (transversal) instability of plane waves for wave numbers away from the band center.

In two dimensions Eq. (85) possesses, as does the CGLE, topological defects in the form of spiral waves. Aranson, Hochheiser, and Moloney (1997) show that in the limit of small r these spiral waves undergo a core instability, leading to stable meandering. Another feature of Eq. (85) in two dimensions is the existence of domain boundaries between traveling waves with different orientation, usually called *zipper states*. Furthermore, in two dimensions, the question of wave-number selection can be transformed into one of wave-vector selection, since the domain wall can adjust the direction of ingoing or outgoing waves. The domain wall itself may no longer be stationary, but may move in a certain direction if there is no reflection symmetry of the wave pattern with respect to the domain-wall axis. The second spatial dimension (along the domain wall) opens the possibility for additional instabilities of the wall, as was observed experimentally in convection in a binary mixture by Moses *et al.* (1987) and La Porta and Surko (1997). Aranson and Tsimring (1995) have shown that near threshold the active (emitting waves) zipper states are alway unstable with respect to transverse undulation. The nonlinear stage of this instability leads to the creation of a chain of topological point defects (spirals), which themselves are unstable. The latter appears to be analogous to the famous Kelvin-Helmholtz instability of a tangential discontinuity of shear flows. Passive (absorbing) zipper states turn out to be stable.

[13]The Swift-Hohenberg equation is obtained by keeping only one nonlinear term. However, nonlinear terms also involving derivatives have formally the same order and, strictly speaking, cannot be neglected.

C. The complex Ginzburg-Landau equation with broken gauge invariance

It is interesting to break the global gauge invariance of the CGLE. This corresponds in particular to a situation in which a system undergoing a Hopf bifurcation with the frequency ω_c is parametrically forced (modulated) at a frequency near $\omega_c/2$. This leads to

$$\partial_t A = A(\epsilon + i\omega) + (1+ib)\Delta A - (1+ic)|A|^2 A + \gamma A^*. \tag{86}$$

Obviously, instead of global gauge invariance $A \to A e^{i\Phi}$ one is left with the discrete symmetry $A \to -A$. Here ω is the detuning, $\gamma > 0$ is the forcing amplitude, and ϵ describes the distance from the threshold of instability.

1. From oscillations to bistability ($\epsilon > 0$)

For $\epsilon > 0$,[14] depending on the values of the other parameters, Eq. (86) describes an oscillatory or bistable situation. In the latter case the system is in general (i.e., for $b, c, \omega \neq 0$) of an excitable nature. In the context of ferromagnets in a static magnetic field it describes domain walls separating two stable states (domains with opposite spins). The domain walls exhibit a transition involving a spontaneous breaking of chirality (in ferromagnets Ising walls become Bloch walls as the strength of crystal anisotropy is reduced; Lajzerowicz and Niez, 1978, 1979). In such an equilibrium situation the imaginary coefficients in Eq. (86) vanish and Eq. (86) can be cast in variational form:

$$\partial_t A = -\frac{\delta F}{\delta A^*}, \tag{87}$$

where the free-energy functional is of the form

$$F = \int \left(-\epsilon|A|^2 + \frac{|A|^4}{2} + |\nabla A|^2 - \frac{\gamma}{2}[(A^*)^2 + A^2] \right) dx\,dy. \tag{88}$$

Equation (87) possesses stationary kinklike solutions connecting stable homogeneous equilibria $A = \pm\sqrt{1+\gamma}$ for $\epsilon = 1$:

$$A_I = \pm\sqrt{1+\gamma}\tanh(\sqrt{1+\gamma}x), \tag{89}$$

$$A_B = \pm\sqrt{1+\gamma}\tanh(\sqrt{2\gamma}x) \pm i\frac{\sqrt{1-3\gamma}}{\cosh(\sqrt{2\gamma}x)}. \tag{90}$$

The first solution, called by Coullet *et al.* (1990) an *Ising wall*, is stable when $\gamma > \gamma_c = 1/3$; the second solution, which is stable for $\gamma < \gamma_c$ and breaks chirality, is called a *Bloch wall*. The order parameter A vanishes at the core of the Ising wall but not at the core of the Bloch wall. For $\gamma = 1/3$ an exchange of stability (pitchfork bifurcation) occurs between these two solutions.

Coullet *et al.* (1990) investigated the behavior of Ising and Bloch walls in nonequilibrium conditions, when at

[14]Note that for $\epsilon > 0$, by rescaling $t, \mathbf{r}, \omega, \gamma, A$ in Eq. (86), ϵ can be replaced by 1.

least one of the coefficients b, c, or ω is nonzero. They found that nonpotential effects in general lead to motion of the Bloch walls and not of the Ising walls (see also Coullet and Emilson, 1992; Sakaguchi, 1992; Mizuguchi and Sasa, 1993; Chaté *et al.*, 1999). Coullet *et al.* (1991) applied this concept to the description of the Ising-Bloch transition in ferromagnets in a rotating magnetic field.

Frisch *et al.* (1994) have studied Eq. (86) in two dimensions in the context of a homeotropically aligned nematic liquid crystal in a rotating magnetic field in the vicinity of the electric Fredericks transition. They have found that Bloch walls containing a defect separating the two variants assume the form of rotating spiral waves. Those spiral waves were also studied experimentally by Migler and Meyer (1994). Frisch *et al.*, (1994) have shown that spiral waves in Eq. (86) combine the properties of spirals in oscillatory media (as in the CGLE) and of excitable spirals (as in reaction-diffusion systems; Tyson and Keener, 1988). The problem of the spiral's frequency selection was solved by Aranson (1995) for small ω and $b=c=0$. In particular, it was shown that the frequency is selected by the local curvature of the moving Bloch wall. For $\gamma,\omega \ll 1$ the spiral wave solution can be described in the phase approximation by the overdamped sine-Gordon equation ($\phi = \arg A$),

$$\partial_t \phi = \omega - \gamma \sin(2\phi) + \Delta\phi. \tag{91}$$

Korzinov *et al.* (1992) have studied Eq. (86) in the context of periodically forced convection. Hanusse and Gomez-Gesteira (1994) considered it in the context of chemical systems.

Frisch and Gilli (1995) as well as Coullet and Plaza (1994) considered the more general equation

$$\partial_t A = A(1+i\omega) + (1+ib)\Delta A - (1+ic)|A|^2 A + \gamma A^* + \gamma_0. \tag{92}$$

The term γ_0 is responsible for the effect of a tilted magnetic field. In contrast to Eq. (86) the spiral waves in the framework of Eq. (92) exhibit a diverse variety of behaviors from rigid rotation to meandering and even hypermeandering. The Ginzburg-Landau equation with more complicated forcing terms was studied by Gilli and Gil (1994).

2. Parametric excitation of waves in the Ginzburg-Landau equation

Equation (86) for $\epsilon < 0$ is a phenomenological model of parametric excitation of surface waves in fluids (Gollub and Langer, 1999). In the absence of parametric driving γA^* the system always relaxes towards the trivial state $A=0$. However, if the parametric driving exceeds the critical value $\gamma_c = (\omega - \epsilon b)/\sqrt{1+b^2}$, the trivial state $A=0$ becomes unstable with respect to standing waves with wave vector $k_c^2 = (b\omega + \epsilon)/(1+b^2)$ of arbitrary orientation. In this sense Eq. (86) is reminiscent of the Swift-Hohenberg equation (Cross and Hohenberg, 1993).

In two dimensions a variety of nontrivial static and dynamic states are possible. Theoretical studies of spatio-temporal chaos in Eq. (86) in the context of surface waves in fluids were conducted by Zhang and Viñals (1995). Spiral waves were studied experimentally and theoretically by Kiyashko *et al.* (1996).

Tsimring and Aranson (1997) and Aranson, Tsimring, and Vinokur (1999) used Eq. (86) coupled to an additional field to describe pattern formation in a thin layer of vibrated granular materials in connection with experimental studies (Melo *et al.*, 1994, 1995; Umbanhowar *et al.*, 1996). In this case the parameters γ and ω can be associated with the amplitude and the frequency of external periodic driving. Depending on the values of γ and ω, a variety of stable solutions were found ranging from localized oscillons and interfaces separating domains of opposite polarity to periodic stripes, squares, and hexagons. The topology of the transition lines between different types of solutions turns out to be in agreement with the experiments.

D. Anisotropic complex Ginzburg-Landau equation in two dimensions

In many physically relevant situations the 2D CGLE is essentially anisotropic (see Sec. I.A class iii), i.e., it is of the form

$$\partial_t A = A + (1+ib_1)\partial_x^2 A + (1+ib_2)\partial_y^2 A - (1+ic)|A|^2 A, \tag{93}$$

with $b_1 \neq b_2$. The equation in this form was studied by Weber *et al.* (1991), Brown *et al.* (1993), and Roberts *et al.* (1996). The stability of plane waves depends on the orientation of the wave vector, in particular, the situation in which the wave is stable in only one direction. Under such a condition Weber *et al.* (1991) found stable lattices of defects.

New features of phase and defect chaos in the 2D anisotropic CGLE were found by Faller and Kramer (1998, 1999). The phase-chaotic states exist over a broader parameter range than in the isotropic case, often even broader than in one dimension. They may represent the global attractor of the system. There exist two variants of phase chaos: a quasi-one-dimensional and a two-dimensional solution. The transition to defect chaos is of the intermittent type.

E. Coupled Ginzburg-Landau equations

When both the critical wave number q_c and the critical frequency ω_c are nonzero at the bifurcation (class iii) with reflection symmetry (see Sec. I.A), the primary modes are traveling waves that in one dimension or in the presence of anisotropy are described by two coupled complex Ginzburg-Landau equations. The physical fields in the weakly nonlinear regime are of the form

$$\sim A_R \exp[-i(\omega_c t - q_c x)] + A_L \exp[-i(\omega_c t + q_c x)] + \text{c.c.},$$

where A_R and A_L are the complex amplitudes of right- or left-traveling waves. In one dimension the coupled CGLE's are given by

$$\partial_t A_R + s\partial_x A_R = A_R + (1+ib)\partial_x^2 A_R - [(1+ic)|A_R|^2 + (1+id)g|A_L|^2]A_R,$$
$$\partial_t A_L - s\partial_x A_L = A_L + (1+ib)\partial_x^2 A_L - [(1+ic)|A_L|^2 + (1+id)g|A_R|^2]A_L, \quad (94)$$

where s is the linear group velocity and $(1+id)g$ is the complex coupling coefficient between the two modes (Cross and Hohenberg, 1993).

In addition to the usual CGLE parameters b and c one has here three relevant parameters s, d, and g. Careful surveys of the various regimes occurring in Eqs. (94) are given by van Hecke *et al.* (1999) and Riecke and Kramer (2000); see also Amengual *et al.* (1996, 1997) and Neufeld *et al.* (1996).

The case of strong suppression corresponds to $g>1$. In this situation dual-wave solutions with $A_R = A_L \neq 0$ are unstable. In contrast, single-wave solutions with $A_R \neq 0, A_L = 0$ or vice versa can be stable. For $g>1$ a variety of source and sink solutions in counterpropagating waves were analyzed by Malomed (1994), Alvarez *et al.* (1997), and van Hecke *et al.* (1999).

F. Complex defects in the vector Ginzburg-Landau equation

The vector CGLE can be viewed as a particular case of Eq. (94) for $s=0$:

$$\partial_t A_\pm = A_\pm + (1+ib)\nabla^2 A_\pm - (1+ic)[|A_\pm|^2 + (1+id)g|A_\mp|^2]A_\pm. \quad (95)$$

The problem of nonlinear dynamics of a complex vector field arises most naturally in the context of nonlinear optics, where the order parameter is the electric-field envelope in the plane normal to the direction of propagation; the fields $A_\pm$ can be identified with the two circularly polarized waves of opposite sense (Gil, 1993; Haelterman and Sheppard, 1994; Pismen, 1994a, 1994b, 1999; San Miguel, 1995; Buryak *et al.*, 1999; Hernandez-Garcia *et al.*, 1999; Hoyuelos *et al.*, 1999).

A distinguishing feature of the vector GLE is the possibility of a transition between two phases, which can be characterized by either mixing or separation of two superfluids. Defects (vortices) can exist in both superfluids, and transitions between alternative core structures are possible (Pismen, 1994a, 1994b, 1999); in this sense the real case (vector GLE) could be viewed as a toy model for the nine-component description of superfluid ^{3}He, dressed down to two components. Pismen (1994a, 1994b) introduced the notation of vector and scalar defects in the vector GLE. Vector defects have a topological charge (and therefore zeros of $A_\pm$) in both fields, whereas scalar defects have a nonzero charge in only one of the fields $A_\pm$.

Simulations of the vector CGLE by Hernández-García *et al.* (1999, 2000) have shown spiral wave patterns with an exceptionally rich structure in which both separated (but closely packed) scalar defects in the two fields and vector defects with a common core could be seen.

A particularly intriguing possibility, suggested by Pismen (1994a), is the formation of a bound pair of defects in the two fields, i.e., a vortex "molecule" with dipole structure. Aranson and Pismen (2000) have shown that such a molecule requires complex coefficients. Analytical calculations were conducted in the limit of small coupling g between two complex fields. As was shown, the interaction between a well-separated pair of defects in two different fields is always long range (powerlike), in contrast to the interaction between defects in the same field, which falls off exponentially as in a single CGLE (Aranson, Kramer, and Weber, 1993a). In a certain region of parameters of the vector CGLE, stable rotating bound states of two defects—a vortex molecule—are found.

G. Complex oscillatory media

Two-dimensional oscillatory media exhibit a wide variety of wave phenomena, including spiral waves, phase and defect turbulence, etc. The CGLE describes the dynamics of oscillatory media in the vicinity of a primary Hopf bifurcation. Brunnet *et al.* (1994) and Goryachev and Kapral (1996) have shown that spiral waves may also exist in systems with more complex local dynamics, e.g., period-doubling bifurcations or chaos. In this situation the rotational symmetry of spiral waves may be broken by line synchronization defects.

Goryachev *et al.* (1999) studied transitions to line-defect turbulence in complex oscillatory media supporting spiral waves. Several types of line-defect turbulence were found in a system in which the local dynamics is described by a chaotic Rössler oscillator. Such complex periodic spirals and line-defect turbulence were observed experimentally in chemical systems by Park and Lee (1999).

VII. CONCLUDING REMARKS

In this work we have attempted to overview a wide variety of dynamic phenomena described by the CGLE in one, two, and three dimensions. The CGLE exhibits in many respects similar behavior in all dimensions, e.g., active and passive defects, distinct chaotic states, convective and absolute instabilities, etc. Surprisingly, quantitative aspects of instabilities and transitions are different. In particular, the core (acceleration) instability of 1D Nozaki-Bekki holes, 2D spirals, and 3D vortex filaments has different manifestations: Nozaki-Bekki holes undergo a stationary instability, spirals exhibit unsaturated Hopf bifurcations, and 3D vortex filaments show a supercritical Hopf bifurcation. One observes a general trend in the region of occurrence: 1D defects have the smallest stability domain, 2D spirals are stable over a

much wider range of parameters, and the stability domain again decreases for 3D vortex filaments.

The unique combination of all of these features in one equation stimulates continuous interest in this topic in a broad scientific community. The insights obtained from the CGLE over the last decades have had an enormous impact on the physics of nonequilibrium systems, pattern formation, biophysics, etc. and will be useful for further progress in the physics of complex systems.

Let us discuss briefly some open problems in the world of the CGLE.

- Description of turbulent states in all dimensions. Although considerable work has been done to identify the stability limits and transition lines between various turbulent states in the CGLE, surprisingly little is known about the statistical properties of these states. The main obstacle is the lack of appropriate analytical tools, since the traditional methods of statistical physics are not suitable for a description of spatio-temporal chaos.
- The structure and statistical properties of vortex glass. The "glassy" properties of this state (such as power-like decay of correlations and a hierarchy of relaxation times) are not yet adequately explained.
- The dynamics of the 3D CGLE. The revolutionary development in computers will make possible a detailed investigation of this area.

Hopefully the last two questions will be elaborated on during the next decade. However, the problems of spatio-temporal chaos and turbulence may require considerable time and effort.

ACKNOWLEDGMENTS

We would like to thank all our colleagues who have assisted us in preparing this review over a number of years: Alex Abrikosov, Markus Bär, Alan Bishop, Eberhard Bodenschatz, Thomas Bohr, Helmut Brand, Lutz Brusch, Hugues Chaće, Pierre Coullet, Michael Cross, Jerry Gollub, Pierre Hohenberg, David Kessler, Nikolay Kopnin, Herbert Levine, Maxi Sam Miguel, Igor Mitkov, Alan Newell, Werner Pesch, Len Pismen, Antonio Politi, Yves Pomeau, Mikhail Rabinovich, Hermann Riecke, Victor Steinberg, Harry Swinney, Alessandro Torcini, Lev Tsimring, Martin van Hecke, Wim van Saarloos, Valerii Vinokur, Andreas Weber, Walter Zimmermann, and many others. This work was supported by the U.S. Department of Energy at Argonne National Laboratory under Contract No. W-31-109-ENG-38.

REFERENCES

Abraham, M., I. S. Aranson, and B. Galanti, 1995, Phys. Rev. B **52**, R7018.

Abrikosov, A. A., 1988, *Fundamentals of the Theory of Metals* (North-Holland, Amsterdam).

Afanasjev, V. V., N. N. Akhmediev, and J. M. Soto-Crespo, 1996, Phys. Rev. E **53**, 1931.

Akhmediev, N. N., and V. V. Afanasjev, 1995, Phys. Rev. Lett. **75**, 2320.

Akhmediev, N. N., V. V. Afanasjev, and J. M. Soto-Crespo, 1996, Phys. Rev. E **53**, 1190.

Akhmediev, N., J. M. Soto-Crespo, and G. Town, 2001, Phys. Rev. E **63**, 056602.

Alvarez, R., L. M. van Hecke, and W. van Saarloos, 1997, Phys. Rev. E **56**, R1306.

Amengual, A., E. Hernandez-Garcia, R. Montagne, and M. San Miguel, 1997, Phys. Rev. Lett. **78**, 4379.

Amengual, A., D. Walgraef, M. San Miguel, and E. Hernandez-Garcia, 1996, Phys. Rev. Lett. **76**, 1956.

Antunes, N. D., L. M. A. Bettencourt, and W. H. Zurek, 1999, Phys. Rev. Lett. **82**, 2824.

Aranson, I. S., 1995, Phys. Rev. E **51**, R3827.

Aranson, I., L. Aranson, L. Kramer, and A. Weber, 1992, Phys. Rev. A **46**, R2992.

Aranson, I. S., and A. R. Bishop, 1997, Phys. Rev. Lett. **79**, 4174.

Aranson, I. S., A. R. Bishop, and L. Kramer, 1998, Phys. Rev. E **57**, 5276.

Aranson, I. S., H. Chaté, and L.-H. Tang, 1998, Phys. Rev. Lett. **80**, 2646.

Aranson, I. S., A. V. Gaponov-Grekhov, and M. I. Rabinovich, 1985, Zh. Eksp. Teor. Fiz. **89**, 92 [Sov. Phys. JETP **62**, 52 (1985)].

Aranson, I. S., D. Hochheiser, and J. V. Moloney, 1997, Phys. Rev. A **55**, 3173.

Aranson, I. S., N. B. Kopnin, and V. M. Vinokur, 1999, Phys. Rev. Lett. **83**, 2600.

Aranson, I. S., L. Kramer, and A. Weber, 1991a, Physica D **53**, 376.

Aranson, I. S., L. Kramer, and A. Weber, 1991b, Phys. Rev. Lett. **67**, 404.

Aranson, I. S., L. Kramer, and A. Weber, 1993a, Phys. Rev. E **47**, 3231.

Aranson, I., L. Kramer, and A. Weber, 1993b, Phys. Rev. E **48**, R9.

Aranson, I., L. Kramer, and A. Weber, 1994, Phys. Rev. Lett. **72**, 2316.

Aranson, I., L. Kramer, and A. Weber, 1995, "The Theory of Motion of Spiral Waves in Oscillatory Media," in *Proceedings of the NATO Advanced Research Workshop on Spatio-Temporal Patterns in Nonequilibrium Complex Systems*, Santa Fe, 1993 (Addison-Wesley, Reading, MA), p. 479.

Aranson, I. S., and I. Mitkov, 1998, Phys. Rev. E **58**, 4556.

Aranson, I. S., and L. M. Pismen, 2000, Phys. Rev. Lett. **84**, 634.

Aranson, I. S., and V. Steinberg, 1995, Phys. Rev. B **53**, 75.

Aranson, I. S., and L. S. Tsimring, 1995, Phys. Rev. Lett. **75**, 3273.

Aranson, I. S., L. S. Tsimring, and V. M. Vinokur, 1999, Phys. Rev. E **59**, R1327.

Arecchi, F. T., G. Giacomelli, P. L. Ramazza, and S. Residori, 1990, Phys. Rev. Lett. **65**, 2531.

Arecchi, F. T., G. Giacomelli, P. L. Ramazza, and S. Residori, 1991, Phys. Rev. Lett. **67**, 3749.

Babcock, K. L., G. Ahlers, and D. S. Cannell, 1991, Phys. Rev. Lett. **67**, 3388.

Bar, D. E., and A. A. Nepomnyashchy, 1995, Physica D **86**, 586.

Bär, M., and M. Or-Guil, 1999, Phys. Rev. Lett. **82**, 1160.

Barkley, D., 1994, Phys. Rev. Lett. **72**, 164.

Batchelor, G. K., 1967, *An Introduction to Fluid Dynamics* (Cambridge University Press, Cambridge), p. 615.
Bazhenov, M., and M. Rabinovich, 1993, Phys. Lett. A **179**, 191.
Bazhenov, M., and M. Rabinovich, 1994, Physica D **73**, 318.
Bazhenov, M. V., M. I. Rabinovich, and A. L. Fabrikant, 1992, Phys. Lett. A **163**, 87.
Bensimon, D., B. I. Shraiman, and V. Croquette, 1988, Phys. Rev. A **38**, 5461.
Biktashev, V. N., 1989, "Drift of reverberator in active media due to interaction with boundaries," in *Nonlinear Waves II*, edited by A. V. Gaponov-Grekhov and M. I. Rabinovich, Research Reports in Physics (Springer, Heidelberg), p. 87.
Biktashev, V. N., 1998, Int. J. Bifurcation Chaos Appl. Sci. Eng. **8**, 677.
Biktasheva, I. V., 2000, Phys. Rev. E **62**, 8800.
Biktasheva, I. V., Yu. E. Elkin, and V. N. Biktashev, 1998, Phys. Rev. E **57**, 2656.
Biktasheva, I. V., Y. E. Elkin, and V. N. Biktashev, 1999, J. Biol. Phys. **25**, 115.
Blatter, G., M. V. Feigelman, V. B. Geshkenbein, A. I. Larkin, and V. M. Vinokur, 1994, Rev. Mod. Phys. **66**, 1125.
Bodenschatz, E., M. Kaiser, L. Kramer, W. Pesch, A. Weber, and W. Zimmermann, 1990, in *New Trends in Nonlinear Dynamics and Pattern-Forming Phenomena: The Geometry of Nonequilibrium*, edited by P. Coullet and P. Huerre, *NATO Advanced Study Institute, Series B: Physics* (Plenum, New York), p. 111.
Bodenschatz, E., W. Pesch, and L. Kramer, 1988, Physica D **32**, 135.
Bodenschatz, E., A. Weber, and L. Kramer, 1991a, in *Nonlinear Wave Processes in Excitable Media*, edited by A. V. Holden, M. Markus, and H. G. Othmer, *NATO Advanced Study Institute, Series B: Physics* (Plenum, New York), Vol. 244, p. 383.
Bodenschatz, E., A. Weber, and L. Kramer, 1991b, J. Stat. Phys. **64**, 1007.
Bodenschatz, E., W. Zimmermann, and L. Kramer, 1988, J. Phys. (Paris) **49**, 1875.
Börzsönyi, T., A. Buka, A. P. Krekhov, O. A. Scaldin, and L. Kramer, 2000, Phys. Rev. Lett. **84**, 1934.
Bogoliubov, N. N., and I. U. A. Mitropolskii, 1961, *Asymptotic Methods in the Theory of Nonlinear Oscillations* (Hindustan, Delhi) [stamped: New York, Gordon and Breach].
Bohr, T., G. Huber, and E. Ott, 1996, Europhys. Lett. **33**, 589.
Bohr, T., G. Huber, and E. Ott, 1997, Physica D **106**, 95.
Bohr, T., M. H. Jensen, G. Paladin, and A. Vulpiani, 1998, *Dynamical Systems Approach to Turbulence* (Cambridge University, New York).
Brambilla, M., F. Battipede, L. A. Lugiato, V. Penna, and C. O. Weiss, 1991, Phys. Rev. A **43**, 5090.
Braun, E., and V. Steinberg, 1991, Europhys. Lett. **15**, 167.
Braun, R., and F. Feudel, 1996, Phys. Rev. E **53**, 6562.
Bretherton, C. S., and E. A. Spiegel, 1983, Phys. Lett. A **96A**, 152.
Brevdo, L., and T. J. Bridges, 1996, Philos. Trans. R. Soc. London, Ser. A **354**, 1027.
Brown, R., A. L. Fabrikant, and M. I. Rabinovich, 1993, Phys. Rev. E **47**, 4141.
Brunnet, L., H. Chaté, and P. Manneville, 1994, Physica D **78**, 141.
Brusch, L., M. Bär, and A. Torcini, 2001, unpublished.
Brusch, L., A. Torcini, M. van Hecke, M. G. Zimmermann, and M. Bär, 2001, Physica D **160**, 127.
Brusch, L., M. Zimmermann, M. van Hecke, M. Bär, and A. Torcini, 2000, Phys. Rev. Lett. **85**, 86.
Buka, A., and L. Kramer, 1996, Eds., *Pattern Formation in Liquid Crystals* (Springer-Verlag, New York).
Burguette, J., H. Chaté, F. Daviaud, and N. Mukolobwiez, 1999, Phys. Rev. Lett. **82**, 3252.
Buryak, A. V., Yu. S. Kivshar, Shih Ming-Feng, and M. Segev, 1999, Phys. Rev. Lett. **82**, 81.
Busse, F. H., 1978, Rep. Prog. Phys. **41**, 1929.
Chaté, H., 1994, Nonlinearity **7**, 185.
Chaté, H., 1995, "Disordered regimes of the one-dimensional complex Ginzburg-Landau equation," in *Spatiotemporal Patterns in Nonequilibrium Complex Systems*, Santa Fe Institute Series in the Sciences of Complexity (Addison-Wesley, Reading, MA), p. 33.
Chaté, H., and P. Manneville, 1992, Phys. Lett. A **171**, 183.
Chaté, H., and P. Manneville, 1996, Physica A **224**, 348.
Chaté, H., A. Pikovsky, and O. Rudzick, 1999, Physica D **131**, 17.
Colet, P., D. Walgraef, and M. San Miguel, 1999, Eur. Phys. J. B **11**, 517.
Coullet, P., and K. Emilsson, 1992, Physica D **61**, 119.
Coullet, P., L. Gil, and J. Lega, 1989, Phys. Rev. Lett. **62**, 1619.
Coullet, P., L. Gil, and F. Rocca, 1989, Opt. Commun. **73**, 403.
Coullet, P., and L. Kramer, 2001, unpublished.
Coullet, P., J. Lega, B. Houchmanzadeh, and J. Lajzerowicz, 1990, Phys. Rev. Lett. **65**, 1352.
Coulett, P., J. Lega, and Y. Pomeau, 1991, Europhys. Lett. **15**, 221.
Coullet, P., and F. Plaza, 1994, Int. J. Bifurcation Chaos Appl. Sci. Eng. **4**, 1173.
Coullet, P., and D. Repaux, 1987, Europhys. Lett. **3**, 573.
Crasovan, L.-C., B. A. Malomed, and D. Mihalache, 2001, Phys. Rev. E **63**, 016605.
Creswick, T., and N. Morrison, 1980, Phys. Lett. A **76**, 267.
Cross, M. C., and P. C. Hohenberg, 1993, Rev. Mod. Phys. **65**, 851.
Dalfovo, F., S. Giorgini, L. P. Pitaevskii, and S. Stringari, 1999, Rev. Mod. Phys. **71**, 463.
Dangelmayr, G., and L. Kramer, 1998, "Mathematical Approaches to Pattern Formation," in *Evolution of Spontaneous Structures in Dissipative Continuous Systems*, edited by F. H. Busse and S. C. Müller (Springer, New York), p. 1.
Daniels, K. E., B. B. Plapp, and E. Bodenschatz, 2000, Phys. Rev. Lett. **84**, 5320.
Deissler, R. J., and H. R. Brand, 1991, Phys. Rev. A **44**, R3411.
Deissler, R. J., and H. R. Brand, 1994, Phys. Rev. Lett. **72**, 478.
Deissler, R. J., and H. R. Brand, 1995, Phys. Rev. Lett. **74**, 4847.
Deissler, R. J., and H. R. Brand, 1998, Phys. Rev. Lett. **81**, 3856.
Deo, P. S., V. A. Schweigert, F. M. Peeters, and A. K. Geim, 1997, Phys. Rev. Lett. **79**, 4653.
de Wit, A., 1999, Adv. Chem. Phys. **109**, 435.
Di Prima, R. C., W. Eckhaus, and L. A. Segel, 1971, J. Fluid Mech. **49**, 705.
Dias, F., and Ch. Kharif, 1999, Annu. Rev. Fluid Mech. **31**, 301.
Doelman, A., 1995, Physica D **97**, 398.
Doering, C. R., J. D. Gibbon, D. D. Holm, and B. Nicolaenko, 1987, Phys. Rev. Lett. **59**, 2911.

Doering, C. R., J. D. Gibbon, D. D. Holm, and B. Nicolaenko, 1988, Nonlinearity **1**, 279.
Donnelly, R. J., 1991, *Quantized Vortices in Heliuum II* (Cambridge University, Cambridge, England/New York).
Dubois-Violette, E., E. Guazelli, and J. Prost, 1983, Philos. Mag. A **48**, 727.
Dziarmaga, J., P. Laguna, and W. H. Zurek, 1999, Phys. Rev. Lett. **82**, 4749.
Egolf, D., 1998, Phys. Rev. Lett. **81**, 4120.
Egolf, D. A., and H. S. Greenside, 1995, Phys. Rev. Lett. **74**, 1751.
Elphick, C., and E. Meron, 1991, Physica D **53**, 385.
Eltayeb, I. A., 1971, Proc. R. Soc. London, Ser. A **326**, 229.
Faller, F., and L. Kramer, 1998, Phys. Rev. E **57**, R6249.
Faller, R., and L. Kramer, 1999, Chaos, Solitons Fractals **10**, 745.
Fenton, F., and A. Karma, 1998a, Chaos **8**, 20.
Fenton, F., and A. Karma, 1998b, Phys. Rev. Lett. **81**, 481.
Fetter, A., 1966, Phys. Rev. **151**, 100.
Flesselles, J.-M., V. Croquette, and S. Jicquois, 1994, Phys. Rev. Lett. **72**, 2871.
Frisch, T., L. Gil, and J. M. Gilli, 1993, Phys. Rev. E **48**, R4199.
Frisch, T., and J. M. Gilli, 1995, J. Phys. II **5**, 561.
Frisch, T., Y. Pomeau, and S. Rica, 1992, Phys. Rev. Lett. **69**, 1644.
Frisch, T., and S. Rica, 1992, Physica D **61**, 155.
Frisch, T., S. Rica, P. Coullet, and J. M. Gilli, 1994, Phys. Rev. Lett. **72**, 1471.
Frisch, U., Z. S. She, and O. Thual, 1986, J. Fluid Mech. **168**, 221.
Gabbay, M., E. Ott, and P. N. Guzdar, 1997, Phys. Rev. Lett. **78**, 2012.
Gabbay, M., E. Ott, and P. N. Guzdar, 1998a, Physica D **118**, 371.
Gabbay, M., E. Ott, and P. N. Guzdar, 1998b, Phys. Rev. E **58**, 2576.
Geim, A. K., S. V. Dubonos, J. G. S. Lok, M. Henini, and J. C. Maan, 1998, Nature (London) **396**, 144.
Gil, L., 1993, Phys. Rev. Lett. **70**, 162.
Gil, L., K. Emilsson, and G.-L. Oppo, 1992, Phys. Rev. A **45**, R567.
Gil, L., J. Lega, and J. L. Meunier, 1990, Phys. Rev. A **41**, 1138.
Gilli, J. M., and L. Gil, 1994, Liq. Cryst. **17**, 1.
Ginzburg, V. L., and L. D. Landau, 1950, Sov. Phys. JETP **20**, 1064.
Gollub, J. P., and J. S. Langer, 1999, Rev. Mod. Phys. **71**, S396.
Gorkov, L. P., 1957, Sov. Phys. JETP **6**, 311.
Gorkov, L. P., and G. M. Eliashberg, 1968, Sov. Phys. JETP **27**, 338.
Goryachev, A., H. Chaté, and R. Kapral, 1999, Phys. Rev. Lett. **83**, 1878.
Goryachev, A., and R. Kapral, 1996, Phys. Rev. Lett. **76**, 1619.
Gray, R. A., and J. Jalife, 1996, Int. J. Bifurcation Chaos Appl. Sci. Eng. **6**, 415.
Gross, E. P., 1963, J. Math. Phys. **4**, 195.
Haelterman, M., and A. P. Sheppard, 1994, Phys. Rev. E **49**, 3389.
Hagan, P. S., 1981, Adv. Appl. Math. **2**, 400.
Hagan, P. S., 1982, SIAM (Soc. Ind. Appl. Math.) J. Appl. Math. **42**, 762.
Hager, G., 1996, Diploma thesis (University of Bayreuth, Germany).
Hanusse, P., and M. Gomez-Gesteira, 1996, Phys. Scr. **67T**, 117.
Heinrichs, R., G. Ahlers, and D. S. Cannell, 1987, Phys. Rev. A **35**, 2761.
Hendrey, M., K. Nam, P. Guzdar, and E. Ott, 2000, Phys. Rev. E **62**, 7627.
Hendrey, M., E. Ott, and T. M. Antonsen, Jr., 1999, Phys. Rev. Lett. **82**, 859.
Hernandez-Garcia, E., M. Hoyuelos, P. Colet, R. Montagne, and M. San Miguel, 1999, Int. J. Bifurcation Chaos Appl. Sci. Eng. **9**, 2257.
Hernandez-Garcia, E., M. Hoyuelos, P. Colet, and M. San Miguel, 2000, Phys. Rev. Lett. **85**, 744.
Hernandez-Garcia, E., J. Vinals, R. Toral, and M. San Miguel, 1993, Phys. Rev. Lett. **70**, 3576.
Hocking, L. M., and K. Stewartson, 1972, Proc. R. Soc. London, Ser. A **326**, 289.
Hocking, L. M., K. Stewartson, J. T. Stuart, and S. N. Brown, 1972, J. Fluid Mech. **51**, 705.
Hohenberg, P. C., and B. Halperin, 1977, Rev. Mod. Phys. **49**, 435.
Hoyuelos, M., E. Hernandez-Garcia, P. Colet, and M. San Miguel, 1999, Comput. Phys. Commun. **121-122**, 414.
Huber, G., P. Alstrøm, and T. Bohr, 1992, Phys. Rev. Lett. **69**, 2380.
Huerre, P., and P. A. Monkewitz, 1990, Annu. Rev. Fluid Mech. **22**, 473.
Hynne, F., P. G. Sørenson, and T. Møller, 1993, J. Chem. Phys. **98**, 219.
Ipsen, M., and M. van Hecke, 2001, Physica D **160**, 103.
Janiaud, B., A. Pumir, D. Bensimon, V. Croquette, H. Richter, and L. Kramer, 1992, Physica D **55**, 269.
Josserand, C., and Y. Pomeau, 1995, Europhys. Lett. **30**, 43.
Kapitula, T., and J. Rubin, 2000, Nonlinearity **13**, 77.
Kaplan, E., E. Kuznetsov, and V. Steinberg, 1994a, Europhys. Lett. **28**, 237.
Kaplan, E., E. Kuznetsov, and V. Steinberg, 1994b, Phys. Rev. E **50**, 3712.
Keener, J. P., and J. J. Tyson, 1990, Physica D **44**, 191.
Keener, J. P., and J. J. Tyson, 1991, Physica D **53**, 151.
Kevrekidis, P. G., A. R. Bishop, and K. O. Rasmussen, 2002, Phys. Rev. E **65**, 016122.
Kibble, T. W. B., 1976, J. Phys. A **9**, 1387.
Kiyashko, S. V., L. N. Korzinov, M. I. Rabinovich, and L. S. Tsimring, 1996, Phys. Rev. E **54**, 5037.
Kolodner, P., D. Bensimon, and C. M. Surko, 1988, Phys. Rev. Lett. **60**, 1723.
Kolodner, P., G. Flatgen, and I. G. Kevrekidis, 1999, Phys. Rev. Lett. **83**, 730.
Kolodner, P., S. Slimani, N. Aubry, and R. Lima, 1995, Physica D **85**, 165.
Komineas, S., F. Heilmann, and L. Kramer, 2001, Phys. Rev. E **63**, 011103.
Koplik, J., and H. Levine, 1993, Phys. Rev. Lett. **71**, 1375.
Koplik, J., and H. Levine, 1996, Phys. Rev. Lett. **76**, 4745.
Korzinov, L., M. I. Rabinovich, and L. S. Tsimring, 1992, Phys. Rev. A **46**, 7601.
Kramer, L., E. Bodenschatz, and W. Pesch, 1990, Phys. Rev. Lett. **64**, 2588.
Kramer, L., E. Bodenschatz, W. Pesch, W. Thom, and W. Zimmermann, 1989, Liq. Cryst. **5**, 699.
Kramer, L., and W. Pesch, 1995, Annu. Rev. Fluid Mech. **27**, 515.

Kramer, L., S. Popp, E. A. Kuznetsov, and S. K. Turitsyn, 1995, Pis'ma Zh. Eksp. Teor. Fiz., **61**, 887 [JETP Lett. **61**, 904 (1995)].
Kramer, L., and W. Zimmermann, 1985, Physica D **16**, 221.
Krekhov, A., and L. Kramer, 1996, Phys. Rev. E **53**, 4925.
Kuramoto, Y., 1984, *Chemical Oscillations, Waves and Turbulence*, Springer Series in Synergetics (Springer, Berlin).
Kuramoto, Y., and T. Tsuzuki, 1976, Prog. Theor. Phys. **55**, 356.
Kuznetsov, E. A., and S. K. Turitsyn, 1988, Zh. Eksp. Teor. Fiz. **94**, 119 [Sov. Phys. JETP **67**, 1583].
La Porta, A., and C. M. Surko, 1997, Phys. Rev. E **56**, 5351.
Lajzerowicz, J., and J. J. Niez, 1978, "Structure and stability of domain walls-phase transition," in *Solitons and Condensed Matter Physics*, edited by A. R. Bishop and T. Schneider (Springer-Verlag, Berlin/New York), p. 195.
Lajzerowicz, J., and J. J. Niez, 1979, J. Phys. (France) Lett. **40**, L165.
Lamb, H., 1932, *Hydrodynamics* (Cambridge University, Cambridge, England).
Landau, L. D., 1937a, "On the theory of phase transitions," in *Collected Papers of L. D. Landau* (Gordon and Breach, New York), p. 193.
Landau, L. D., 1937b, "X-ray scattering by crystals in the neighbourhood of the Curie point," in *Collected Papers of L. D. Landau* (Gordon and Breach, New York), p. 193.
Landau, L. D., 1944, "On the problem of turbulence," in *Collected Papers of L. D. Landau* (Gordon and Breach, New York), p. 387.
Landau, L. D., and E. M. Lifshitz, 1959, *Fluid Mechanics* (Pergamon, London/Addison-Wesley, Reading, MA).
Lega, J., 1991, Eur. J. Mech. B/Fluids **10** (suppl.), 145.
Lega, J., 2001, Physica D **152-153**, 269.
Lega, J., and S. Fauve, 1997, Physica D **102**, 234.
Lega, J., B. Janiaud, S. Jucquois, and V. Croquette, 1992, Phys. Rev. A **45**, 5596.
Lega, J., J. V. Moloney, and A. C. Newell, 1994, Phys. Rev. Lett. **73**, 2978.
Lega, J., J. V. Moloney, and A. C. Newell, 1995, Physica D **83**, 478.
Levermore, C. D., and D. R. Stark, 1997, Phys. Lett. A **234**, 269.
Leweke, T., and M. Provansal, 1994, Phys. Rev. Lett. **72**, 3174.
Leweke, T., and M. Provansal, 1995, J. Fluid Mech. **288**, 265.
Lücke, M., W. Barten, and M. Kamps, 1992, Physica D **61**, 183.
Lund, F., 1991, Phys. Lett. A **159**, 245.
Malkus, W. V. R., and G. Veronis, 1958, J. Fluid Mech. **4**, 225.
Malomed, B. A., 1983, Physica D **8**, 353.
Malomed, B. A., 1994, Phys. Rev. E **50**, R3310.
Malomed, B. A., and A. N. Rudenko, 1988, Izv. Vyssh. Uchebn. Zavede. Radiofiz. **31**, 288 [Sov. Radiophys. **31**, 209 (1988)].
Manneville, P., 1990, *Dissipative Structures and Weak Turbulence* (Academic, San Diego).
Manneville, P., and H. Chaté, 1996, Physica D **96**, 30.
Mazenko, G., 2001, Phys. Rev. E **63**, 016110.
Melbourne, I., 1998, J. Nonlinear Sci. **8**, 1.
Melo, F., P. Umbanhowar, and H. L. Swinney, 1994, Phys. Rev. Lett. **72**, 172.
Melo, F., P. B. Umbanhowar, and H. L. Swinney, 1995, Phys. Rev. Lett. **75**, 3838.
Mermin, N. D., 1979, Rev. Mod. Phys. **51**, 591.
Mielke, A., 1998, Physica D **117**, 106.
Mielke, A., and G. Schneider, 1996, in *Lectures in Applied Mathematics*, edited by P. Deift, C. D. Levermore, and C. E. Wayne (American Mathematics Society, Providence, RI), Vol. 31, p. 191.
Migler, K. B., and R. B. Meyer, 1994, Physica D **71**, 412.
Mironov, S., M. Vinson, S. Mulvey, and A. Pertsov, 1996, J. Phys. Chem. **100**, 1975.
Mizuguchi, T., and S. Sasa, 1993, Prog. Theor. Phys. **89**, 599.
Montagne, R., E. Hernandéz-Garcia, A. Amengual, and M. San Miguel, 1997, Phys. Rev. E **56**, 151.
Montagne, R., E. Hernandéz-Garcia, and M. San Miguel, 1996, Phys. Rev. Lett. **77**, 267.
Morse, P. M., and H. Feshbach, 1953, *Methods of Theoretical Physics* (McGraw-Hill, New York).
Moses, E., J. Fineberg, and V. Steinberg, 1987, Phys. Rev. A **35**, 2757.
Nam, K., E. Ott, P. N. Guzdar, and M. Gabbay, 1998, Phys. Rev. E **58**, 2580.
Nepomnyashchy, A. A., 1995a, Physica D **86**, 90.
Nepomnyashchy, A. A., 1995b, Europhys. Lett. **31**, 437.
Neu, J. C., 1990a, Physica D **43**, 385.
Neu, J. C., 1990b, Physica D **43**, 407.
Neufeld, M., D. Walgraef, and M. San Miguel, 1996, Phys. Rev. E **54**, 6344.
Newell, A. C., 1974, Lect. Appl. Math. **15**, 157.
Newell, A. C., 1995, "Patterns in Nonlinear Optics: A Paradigm," in *Proceedings of the NATO Advanced Research Workshop on Spatio-Temporal Patterns in Nonequilibrium Complex Systems*, Santa Fe, 1993 (Addison-Wesley, Reading, MA), p. 3.
Newell A. C., and J. V. Moloney, 1992, *Nonlinear Optics* (Addison-Wesley, Redwood City, CA).
Newell, A. C., T. Passot, and J. Lega, 1993, Annu. Rev. Fluid Mech. **25**, 399.
Newell, A. C., and J. A. Whitehead, 1969, J. Fluid Mech. **38**, 279.
Newell, A. C., and J. A. Whitehead, 1971, "Review of the finite bandwidth concept," in *Instability of Continuous Systems*, edited by H. H. E. Leipholz (Springer-Verlag, Berlin), p. 284.
Nicolis, G., 1995, *Introduction to Nonlinear Science* (Cambridge University, Cambridge, England/New York).
Nore, C., M. E. Brachet, and S. Fauve, 1993, Physica D **65**, 154.
Nozaki, K., and N. Bekki, 1984, J. Phys. Soc. Jpn. **53**, 1581.
Oppo, G.-L., G. D'Alessandro, and W. Firth, 1991, Phys. Rev. A **44**, 4712.
Ouyang, Q., and J. M. Flesselles, 1996, Nature (London) **379**, 143.
Park, J.-S., and K. J. Lee, 1999, Phys. Rev. Lett. **83**, 5393.
Passot, T., and A. C. Newell, 1994, Physica D **74**, 301.
Perraud, J.-J., A. De Witt, E. Dulos, P. De Kepper, G. Dewel, and P. Borckmans, 1993, Phys. Rev. Lett. **71**, 1272.
Pesch, W., and L. Kramer, 1986, Z. Phys. B: Condens. Matter **63**, 121.
Pismen, L. M., 1994a, Physica D **73**, 244.
Pismen, L. M., 1994b, Phys. Rev. Lett. **72**, 2557.
Pismen, L. M., 1999, *Vortices in Nonlinear Fields* (Oxford University/Clarendon Press, Oxford/New York).
Pismen, L. M., and A. A. Nepomnyashchii, 1991a Physica D **54**, 183.
Pismen, L. M., and A. A. Nepomnyashchii, 1991b, Phys. Rev. A **44**, R2243.
Pismen, L. M., and A. A. Nepomnyashchii, 1993, Physica D **69**, 163.

Pismen, L. M., and J. D. Rodriguez, 1990, Phys. Rev. A **42**, 2471.
Pismen, L. M., and J. Rubinstein, 1991, Physica D **47**, 353.
Pitaevskii, L., 1959, Sov. Phys. JETP **8**, 888.
Pitaevskii, L., 1961, Sov. Phys. JETP **13**, 451.
Pocheau, A., and V. Croquette, 1984, J. Phys. (Paris) **45**, 35.
Pomeau, Y., 1984, "Non-adiabatic phenomena in cellular structures," in *Cellular Structures in Instabilities*, edited by J. E. Wesfreid and S. Zalesky (Springer-Verlag, New York), p. 207.
Popp, S., O. Stiller, I. Aranson, and L. Kramer, 1995, Physica D **84**, 398.
Popp, S., O. Stiller, I. Aranson, A. Weber, and L. Kramer, 1993 Phys. Rev. Lett. **70**, 3880.
Popp, S., O. Stiller, E. Kuznetsov, and L. Kramer, 1998 Physica D **114**, 81.
Powell, J. A., and P. K. Jakobsen, 1993, Physica D **64**, 132.
Proceedings of Conference on The Nonlinear Schrödinger Equation, Chernogolovka, Russia, 1994, Physica D **87**, 1 (1995).
Qu, Z., F. Xie, and A. Garfinkel, 1999, Phys. Rev. Lett. **83**, 2668.
Rasenat, S., E. Braun, and V. Steinberg, 1991, Phys. Rev. A **43**, 5728.
Rica, S., and E. Tirapegui, 1990, Phys. Rev. Lett. **64**, 878.
Rica, S., and E. Tirapegui, 1991a, Physica D **48**, 396.
Rica, S., and E. Tirapegui, 1991b, Phys. Lett. A **161**, 53.
Rica, S., and E. Tirapegui, 1992, Physica D **61**, 246.
Ricca, R. L., 1996, Fluid Dyn. Res. **18**, 245.
Riecke, H., and L. Kramer, 2000, Physica D **137**, 124.
Roberts, B. W., E. Bodenschatz, and J. P. Sethna, 1996, Physica D **99**, 252.
Robinson, P. A., 1997, Rev. Mod. Phys. **69**, 507.
Rodriguez, J. D., L. M. Pismen, and L. Sirovich, 1991, Phys. Rev. A **44**, 7980.
Rousseau, G., H. Chaté, and R. Kapral, 1998, Phys. Rev. Lett. **80**, 5671.
Roussopoulos, K., and P. A. Monkewitz, 1996, Physica D **97**, 264.
Rovinsky, A. B., and M. Menzinger, 1992, Phys. Rev. Lett. **69**, 1193.
Rovinsky, A. B., and M. Menzinger, 1993, Phys. Rev. Lett. **70**, 778.
Rubinstein, B. Y., and L. M. Pismen, 1994, Physica D **78**, 1.
Ruutu, V. M. H., V. B. Eltsov, A. J. Gill, T. W. B. Kibble, M. Krusius, Yu. G. Makhlin, B. Placais, and G. E. Volovik, and W. Xu, 1996, Nature (London) **382**, 334.
Ruutu, V. M., V. B. Eltsov, M. Krusius, Yu. G. Makhlin, B. Placais, and G. E. Volovik, 1998, Phys. Rev. Lett. **80**, 1465.
Ryskin, G., and M. Kremenetsky, 1991, Phys. Rev. Lett. **67**, 1574.
Sakaguchi, H., 1989, Prog. Theor. Phys. **82**, 7.
Sakaguchi, H., 1990, Prog. Theor. Phys. **84**, 792.
Sakaguchi, H., 1991a, Prog. Theor. Phys. **85**, 417.
Sakaguchi, H., 1991b, Prog. Theor. Phys. **86**, 7.
Sakaguchi, H., 1992, Prog. Theor. Phys. **88**, 593.
Sakaguchi, H., 1993, Prog. Theor. Phys. **89**, 1123.
San Miguel, M., 1995, Phys. Rev. Lett. **75**, 425.
Sasa, S., and T. Iwamoto, 1993, Phys. Lett. A **175**, 289.
Schmid, A., 1968, Z. Phys. **215**, 210.
Schneider, G., 1994, Commun. Math. Phys. **164**, 157.
Schopf, W., and L. Kramer, 1991, Phys. Rev. Lett. **66**, 2316.
Schopf, W., and W. Zimmermann, 1990, Phys. Rev. A **41**, 1145.
Schwarz, K. W., 1985, Phys. Rev. B **31**, 5782.
Schwarz, K. W., 1988, Phys. Rev. B **38**, 2398.
Segel, L. A., 1969, J. Fluid Mech. **38**, 203.
Sepulchre, J. A., and A. Babloyantz, 1993, Phys. Rev. E **48**, 187.
Shraiman, B. I., A. Pumir, W. van Saarloos, P. C. Hohenberg, H. Chatè, and M. Holen, 1992, Physica D **57**, 241.
Siegert, F., and C. J. Weijer, 1991, Physica D **49**, 224.
Siggi, E., and A. Zippelius, 1981, Phys. Rev. A **24**, 1036.
Staliunas, K., 1992, Opt. Commun. **90**, 123.
Staliunas, K., 1993, Phys. Rev. A **48**, 1573.
Steinbock, O., and S. C. Muller, 1993, Int. J. Bifurcation Chaos Appl. Sci. Eng. **3**, 437.
Stewartson, K., and J. T. Stuart, 1971, J. Fluid Mech. **48**, 529.
Strain, M. C., and H. S. Greenside, 1998, Phys. Rev. Lett. **80**, 2306.
Stuart, J. T., 1960, J. Fluid Mech. **9**, 353.
Stuart, J. T., 1971, Annu. Rev. Fluid Mech. **3**, 347.
Stuart, J. T., and R. C. DiPrima, 1980, Proc. R. Soc. London, Ser. A **372**, 357.
Stiller, O., S. Popp, I. Aranson, and L. Kramer, 1995, Physica D **87**, 361.
Stiller, O., S. Popp, and L. Kramer, 1995, Physica D **84**, 424.
Thual, O., and S. Fauve, 1988, J. Phys. (Paris) **49**, 1829.
Tobias, S. M., and E. Knobloch, 1998, Phys. Rev. Lett. **80**, 4811.
Tobias, S. M., M. R. E. Proctor, and E. Knobloch, 1998, Physica D **113**, 43.
Torcini, A., 1996, Phys. Rev. Lett. **77**, 1047.
Torcini, A., H. Frauenkron, and P. Grassberger, 1997, Phys. Rev. E **55**, 5073.
Treiber, M., and L. Kramer, 1998, Phys. Rev. E **58**, 1973.
Tsameret, A., and V. Steinberg, 1994, Phys. Rev. E **49**, 4077.
Tsimring, L. S., and I. S. Aranson, 1997, Phys. Rev. Lett. **79**, 213.
Tu, Y., and M. C. Cross, 1992, Phys. Rev. Lett. **69**, 2515.
Tuckerma, L. S., and D. Barkley, 1990, Physica D **46**, 57.
Tyson, J. J., and J. P. Keener, 1988, Physica D **32**, 327.
Umbanhowar, P. B., F. Melo, and H. L. Swinney, 1996, Nature (London) **382**, 793.
van Harten, A., 1991, J. Nonlinear Sci. **1**, 397.
van Hecke, M., 1998, Phys. Rev. Lett. **80**, 1896.
van Hecke, M., P. C. Hohenberg, and W. van Saarloos, 1994, in *Fundamental Problems in Statistical Mechanics VIII*, edited by H. van Beijren and M. H. Ernst (North-Holland, Amsterdam), p. 245.
van Hecke, M., and M. Howard, 2001, Phys. Rev. Lett. **86**, 2018.
van Hecke, M., C. Storm, and W. van Saarloos, 1999, Physica D **134**, 1.
van Hecke, M., and W. van Saarloos, 1997, Phys. Rev. E **55**, R1259.
van Saarloos, W., 1988, Phys. Rev. A **37**, 211.
van Saarloos, W., 1995, in *Spatiotemporal Patterns in Nonequilibrium Complex Systems*, Santa Fe Institute Series in the Sciences of Complexity (Addison-Wesley, Reading, MA), p. 19.
van Saarloos, W., and P. C. Hohenberg, 1992, Physica D **56**, 303.
Vinson, M., S. Mironov, S. Mulvey, and A. Pertsov, 1997, Nature (London) **386**, 477.
Walgraaf, D., 1997, *Spatio-Temporal Pattern Formation* (Springer-Verlag, New York).
Weber, A., 1992, Ph.D. thesis (University of Bayreuth, Germany).

Weber, A., E. Bodenschatz, and L. Kramer, 1991, Adv. Mater. **3**, 191.
Weber, A., L. Kramer, I. S. Aranson, and L. B. Aranson, 1992, Physica D **61**, 279.
Winfree, A. T., 1995, Physica D **84**, 126.
Winfree, A. T., S. Caudle, G. Chen, P. McGuire, and Z. Szilagyi, 1995, Chaos **6**, 617.
Yuanming, L., and R. E. Ecke, 1999, Phys. Rev. E **59**, 4091.
Zakharov, V. E., 1984, in *Handbook of Plasma Physics*, edited by M. N. Rosenbluth, R. Z. Sagdeev, A. A. Galeev, and R. N. Sudan (North-Holland, Amsterdam), Vol. 2, p. 81.
Zakharov, V. E., and A. B. Shabat, 1971, Zh. Eksp. Teor. Fiz. **61**, 118 [Sov. Phys. JETP **34**, 62 (1972)].
Zhang, W., and J. Vinals, 1995, Phys. Rev. Lett. **74**, 690.
Zhou, L. Q., and Q. Ouyang, 2000, Phys. Rev. Lett. **85**, 1650.
Zurek, W. H., 1985, Nature (London) **317**, 505.